DEVELOPMENT OF A HEAT-BALANCE MODEL FOR THE CHARACTERIZATION OF WAX BLOCKAGE IN FLOWLINES

A Thesis

by

EBIAYE VALERIE OMBU

Submitted to the Office of Graduate Studies of
Texas A&M University
in partial fulfillment of the requirements for the degree of

MASTER OF SCIENCE

December 2004

Major Subject: Petroleum Engineering

DEVELOPMENT OF A HEAT-BALANCE MODEL FOR THE CHARACTERIZATION OF WAX BLOCKAGE IN FLOWLINES

A Thesis

by

EBIAYE VALERIE OMBU

Submitted to Texas A&M University
in partial fulfillment of the requirements
for the degree of

MASTER OF SCIENCE

Approval as to style and content by:

Stuart Scott (Chair of Committee)	Thomas Blasingame (Member)
Yassin Hassan (Member)	Stephen Holditch (Head of Department)

December 2004

Major Subject: Petroleum Engineering

ABSTRACT

Development of a Heat-Balance Model for the Characterization of Wax Blockage in Flowlines. (December 2004)

Ebiaye Valerie Ombu, B.S., Kwame Nkrumah University of Science and Technology

Chair of Advisory Committee: Dr. Stuart Scott

The presence of a blockage in a pipeline will alter the fluid dynamics of a flowing system in terms of the heat, mass and velocity characteristics. The analysis of the fluid dynamics is based on balances taken on the overall system to qualitatively and quantitatively assess the effects of the blockage. Pioneer work in the area of mass and momentum effects of blockages led to the development of blockage type curves useful in characterizing blockages from limited information. This work is an extension of previous work and is based on the application of a simplistic energy balance approach to characterize blockages in pipelines. The resulting heat models for the case of both a partially and fully-blocked flowline correctly predict the effect of wax deposition. Dimensionless temperature-based blockage maps developed here can be used in modeling unique cases where only two of the three necessary conditions are given. The heat model matches results from commercial software within a limited range of restricted flow conditions.

DEDICATION

This work is dedicated to all from whom I continue to learn kindness, wisdom and strength.

ACKNOWLEDGEMENTS

I wish to acknowledge first and foremost my Lord and Personal Savior, Jesus Christ, without whom, I am nothing.

I would also like to acknowledge my parents, Emmanuel and Viola Ombu, whose love and support have been unfailing.

Finally, I would like to acknowledge members of my committee: my advisor, Dr. Stuart Scott, thank you for everything; Dr. Tom Blasingame, I will never forget all your kindness to me; Dr. Yassin Hassan, thank you for your warmth and willingness to be on my committee and Dr. Malcolm Andrews; thank you for giving me a solid foundation in heat transfer and stepping in for my defense at the last minute.

TABLE OF CONTENTS

Page

Page

LIST OF FIGURES

FIGURE Page

FIGURE Page

FIGURE Page

LIST OF TABLES

INTRODUCTION

The exploitation of hydrocarbon resources is shifting more and more towards the development of offshore deepwater fields where flow assurance concerns increase exponentially and are critical to the economic viability of these projects. This shift has spurred growth in the area of flow assurance, resulting in significant technological advancements (multiphase pumps and meters) and increasingly sophisticated production techniques that have enhanced the economic attractiveness of offshore fields.

The term "flow assurance" has almost become a catch phrase in the oil industry in recent years. By no means a recent practice, flow assurance, a term thought to have been coined by Petrobras in the early 1990s as "garantia de fluxo" has been in existence from the commencement of commercial production of crude. It is exactly, as its name implies, the successful management of the vast array of issues involved in the production and transportation of crude, including the monitoring of the thermal and hydraulic behavior, PVT properties, and rheology of the crude; the prevention and control of blockages and leaks; and the maintenance of the mechanical integrity and stability of the entire production and processing facility. Flow assurance encompasses such issues as multiphase flow, blockage and leak prevention and control, slugging, system operability optimization, insulation, and corrosion.

This thesis follows the style and format of the *Journal of Petroleum Technology*.

One such critical issue, which serves as the focus of this research, is that of blockages. The majority of blockages or obstructions in flowlines can be traced to the deposition or precipitation of wax, asphaltenes, hydrates, scale, sand, or some combination of all these substances. One of the difficulties in dealing with blockages from more than one source is that each source (wax, asphaltenes, hydrate, sand, and scale) has unique properties such as phase envelopes, thermal conductivities and heat capacities and thus unique control techniques that sometimes conflict with one another and thus require some kind of trade-off. **Fig. 1** illustrates an arterial blockage from wax in a flowline.

Fig. 1–Illustration of a flowline plugged with wax.

Extensive research work on the actual mechanisms of blockage precipitation and deposition for wax is reviewed in the literature survey but does not serve as the focus of this study. The deposition models, which are developed from these theoretical

mechanisms, are often incorporated into simulation software and used for prediction purposes under actual conditions.

The traditional approaches to dealing with blockages have been both remedial with such intervention techniques as mechanical pigging, and preventive, using chemical inhibition schemes. These approaches, though the most viable options for handling blockages have significant drawbacks: Chemical inhibition is expensive and mechanical pigging involves considerable risk in the form of the constant threat of a stuck pig and the resulting tremendous cost of downtime to rectify the problem, or in the worst-case scenario, of losing the pipe entirely.

The problem of blockages does not have a unique panacea, rather a suite of tools, which collectively can be applied to the prevention, control, and remediation/removal of blockages. Analytical techniques that have been developed to characterize blockages serve as one such valuable tool. These include volume-based (mass) and friction-based (momentum) techniques developed by Scott and Satterwhite.[1] Their pioneer work including the application of the backpressure technique for blockage detection and the development of type curves are reviewed in the literature study. This study is an extension of their work but from a completely different perspective, the heat balance approach. It develops energy-based (heat) techniques for blockage characterization and presents a heat model quantifying the effects of a blockage on an overall energy balance from the original ideas set forth in the work of Chen et al.[2]

FOCUS OF RESEARCH

Wax deposition is a complex phenomenon requiring two basic models for its complete description; one model predicting the solid/liquid/vapor equilibria behind wax precipitation and the other, predicting the heat loss rate which controls the rate of wax deposition. This research is focused on developing a model for predicting the heat loss rate from flowlines in the presence of blockages.

Wellbore Heat Transfer vs. Flowline Heat Transfer

Heat Transfer from wellbore to formation is composed of heat transfer within the tubing and fluid-filled annulus; which is by convection and heat transfer through the tubing, casing walls and the formation; which is by conduction.[3] Heat transfer into the formation is transient and was originally modeled by Ramey[4] and improved for early times by Hasan and Kabir.[5]

Flowline heat transfer, which is the focus of this research, is composed primarily of convection from the flowline to the environment, though there is some conduction through the materials of the pipe wall and wax layer. Flowline heat transfer is being considered under steady-state conditions in this work.

BACKGROUND

The issue of blockages is critical in all installations but more so in offshore locations with installations of greater complexity, typically subsea completions tied back to existing platforms via flowlines of extensive lengths; and where accessibility is often limited. Among the serious economic consequences of blockages in pipelines is the obvious loss of revenue when production is deferred as the restriction reduces the flow capacity of the pipe. The problem of increased pumping pressure requirements as a result of the blockage, further compounded during startup as the waxy crude gels, leads to additional operational expenses.[6] Wax deposition also reduces the capacity of process equipment and interferes with valve operation and instrumentation, causing system upsets and reducing the overall system operability efficiency.[7] Undetected blockages can eventually plug the pipeline so severely that mechanical pigging is no longer an option and the entire pipe is lost. The loss of an offshore pipeline is disastrous, often leading to losses running into hundreds of millions of dollars.

Obviously, prevention, prediction, and early detection are the preferred options when dealing with blockages. Simulation software packages such as OLGA 2000[8] and PIPESIM[9] have built-in wax deposition modules based on thermodynamic models, which are able to estimate the degree of wax deposition. However, as with all simulation software, their application is limited by the inherent uncertainties. The prediction models upon which the simulation software are built, are still not considered to be very accurate, but they are believed to provide reasonable estimates of the rate of wax deposition and

thus provide a basis for assessing the needs for wax control.[10] There is a clear need for as many predictive, analytical, diagnostic and remediation tools as possible for handling blockages thus forming the basis of this research. A review of the tools used in the handling of blockages is presented here under five categories:

1. Prediction,
2. Detection,
3. Prevention,
4. Remediation,
5. Analysis.

PREDICTION

The predictive tools are essentially models that incorporate the physical phenomena behind the formation and deposition of wax. The complete description of the mechanism of wax deposition encompasses both equilibrium models, which deal with the solid/liquid/vapor phase equilibria behind the wax precipitation, and heat models, which deal with the actual rate of deposition of the precipitated wax. These models form the basis of such simulation software as OLGA 2000 and PIPESIM.

Equilibrium Models

The equilibrium models developed are based on the process of wax precipitation and deposition. This necessitates a brief description of waxes and the chemistry behind their precipitation.

Waxes

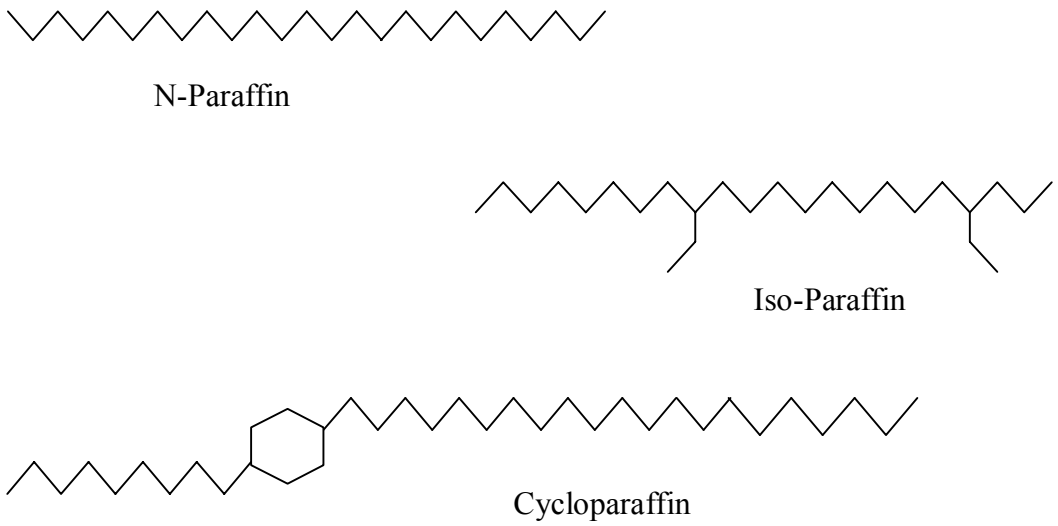

Fig. 2–Structure of the various forms of wax.

Waxes/paraffins are high molecular weight, high carbon number (30 to 75) hydrocarbon compounds. Crude oil with a wax content greater than 10% is considered waxy and causes severe problems in the oil industry including clogging pipelines and forming arterial blockages that restrict flow, causing equipment deterioration, production slowdown and economic losses.

Waxes are characterized by two properties:

a) Wax Appearance Temperature/Wax Crystallization Temperature/Cloud Point: This is the temperature at which wax crystals begin to crystallize and precipitate out of solution.
b) Pour Point: This is the temperature below which the crude ceases to flow. It is usually about 10-20 ^{o}F below the cloud point.[6]

Numerous equilibrium models have been proposed to describe the phase equilibria for wax deposition. The typical approach involves the application of two equilibrium models: a liquid/solid model and a vapor/liquid model. The equations that form the basis of any equilibrium are presented below.

The chemical potential of component *i* at temperature *T* in a liquid and solid phase, is:

$$\frac{\mu_i^{\,L}}{RT} = \frac{\mu_i^{\,O}}{RT} + \ln\left(x_i \gamma_i^{\,L}\right) \quad \text{..... (1)}$$

$$\frac{\mu_i^{\,w}}{RT} = \frac{\mu_i^{\,O}}{RT} + \ln\left(w_i \gamma_i^{\,w}\right) - \Delta H_i^{\,f}\left(\frac{1-\left(T/T_i^{\,f}\right)}{RT}\right) \text{..... (2)}$$

where μ^o = Chemical potential at standard state,

γ = Activity coefficient,

ΔH_f = Heat of fusion,

T_i^f = Fusion temperature,

x = Mole fraction in the liquid phase, and

w = Mole fraction in the wax phase.

For wax to be formed at a given temperature, the Gibbs free energy change (ΔG) for all possible wax compositions must be greater than zero as given by: [12]

$$\Delta G = \sum n_i^{\,w} \mu_i^{\,w} + \sum n_i^{\,L} \mu_i^{\,L} - \sum n_i^{\,F} \mu_i^{\,F} > 0 \quad \text{..... (3)}$$

where n_i is the number of moles of component i.

For thermodynamic equilibrium to be established between the liquid and wax phases, Eq. (4) must be satisfied.

$$\frac{w_i}{x_i} = \frac{\gamma_i^{\,L}}{\gamma_i^{\,W}} \exp \Delta H_i^{\,f} \left(\frac{1 - \left(T / T_i^{\,f} \right)}{RT} \right) \quad \text{..... (4)}$$

Won[11] developed a model from the fundamental equations above, which overestimated the cloud points.[12] Hansen *et al.*[13–15] proposed polymer solution theory for the liquid

phase and treating the solid phase as an ideal mixture to improve the estimation and Pedersen *et al*. used solution theory for both the liquid and solid phases.[14]

Another model by Erbar[15] applied by Majeed, Bringedal, and Overa[16] to North Sea oils is presented here:

$$\frac{w_i}{x_i} = \left(\frac{\gamma_i^{\,L}}{\gamma_i^{\,w}}\right) \exp\left[\frac{\Delta H_i^{\,f}}{RT}\left(1 - \frac{T}{T_i^{\,f}}\right) + \frac{\Delta C_p}{R}\left(1 - \frac{T_i^{\,f}}{T} + \ln\frac{T_i^{\,f}}{T}\right) + \int_0^P \frac{\Delta V}{RT}\,dP\right] \quad .. (5)$$

where ΔC_p = Heat capacity change in fusion, and

ΔV = Volume change of fusion.

The vapor/liquid equilibrium is based on the traditional application of cubic equations of state such as the Soave-Redlich-Kwong equation.

There are three critical considerations with equilibrium models:

1. The determination of the potentially wax forming components and subsequent characterization of the heavy fraction into pseudocomponents,
2. The calculation of the equilibrium coefficients (*K*-values),
3. and the satisfaction of the material balance constraints.

The models are solved to satisfy all material balance constraints while providing equilibrium concentrations of the components in all three phases at varying temperatures. This variation in concentration with temperature *dC/dT* serves as input to the diffusion models (*see Molecular Diffusion in the section to follow*).

These models are incorporated into PVTSim; and PIPESIM as a separate wax deposition module.

Heat Models

Generally, wax deposition occurs when changes in the equilibrium condition of the flowing fluid reduce solubility. These changes could be changes in composition, temperature reduction below the wax appearance temperature (WAT), pressure drop resulting in loss of lighter ends and saturation of the crude, or the presence of nucleation sites.[6] The rate of deposition is largely controlled by the amount of wax components dissolved in the crude and the rate of heat loss to the surroundings.

The physical phenomena describing wax deposition include molecular diffusion and shear dispersion. Molecular diffusion dominates at higher temperatures and heat fluxes while shear dispersion dominates at lower temperatures and heat fluxes.

Molecular Diffusion

This mechanism transports dissolved wax in solution across a temperature and concentration gradient. The bulk fluid ambient temperature difference forms the temperature gradient, which must be greater than zero for a net positive heat flux.[14,15] The transported wax is precipitated as a solid on the colder pipe wall and forms an immobile layer, which in turn creates a concentration gradient causing additional diffusion of the dissolved wax to the pipe wall. The concentration gradient is obtained from a thermodynamic calculation of the solid/liquid/vapor phase behavior.[16] Molecular diffusion is the most significant contributor to wax deposition and is described mathematically by Fick's law. [16-18]

$$n = \rho D_m \frac{dC}{dr} = \rho D \frac{dC}{dT}\frac{dT}{dr} \quad \text{..... (6)}$$

$$D_m = \frac{B}{\mu} \quad \text{..... (7)}$$

where n = Mass flux,

ρ = Density of solid wax,

D_m = Molecular diffusion coefficient,

dC/dT = Concentration gradient (from equilibrium model),

dT/dr = Temperature gradient (from heat transfer analysis),

B = Constant for a particular crude, and

μ = Dynamic viscosity of the crude.

Shear Dispersion

Solid/particulate wax such as wax crystals, which normally travel with the mean speed and direction of the surrounding fluid, are transported from the turbulent core laterally to the pipe wall as a result of shearing of the fluid close to the pipe wall.[16] This mechanism is controlled by the wall shear rate, the amount of wax out of solution, and the size and shape of particles. It becomes important when the precipitated wax content is high. The shear dispersion coefficient (D_s) is given by:

$$D_s = \frac{a^2 \gamma C_w^*}{10} \quad \text{.....(8)}$$

where a = Particle diameter,

γ = Shear rate of oil at the wall, and

C_w^* = Volume fraction concentration of wax out of solution at the wall.

(Note: The shear dispersion coefficient, D_s is added to the molecular diffusion coefficient when significant.)

Brownian motion and gravity settling are other wax deposition mechanisms but will not be discussed because their contribution is largely insignificant at the flowing conditions encountered in wells and pipelines.[19]

DETECTION

Unlike leaks that can in some cases be visually detected offshore with remotely operated vehicles, blockages are internal and thus pose a greater challenge to detect. The knowledge of the type of crude and its wax deposition potential, as determined from sampling and laboratory testing, is critical information that answers questions such as, Will wax form? Under what conditions? How much wax do we expect? Armed with this knowledge, production engineers can anticipate and design for the onset of wax deposition. The actual clues indicating the commencement of wax deposition/presence of blockages are wax crystals in produced crudes and wireline equipment, and unusual drop in production rate, wellhead pressure, or temperature due to Joule-Thompson effect.[6]

PREVENTION/CONTROL

A number of preventive methods currently used will be discussed in this section.

Chemical Control

This involves the use of wax inhibitors which come in two forms: wax crystal modifiers, which are polymers that inhibit or alter wax crystal growth thereby decreasing their pour point; and dispersants, which coat individual wax particles thereby preventing their agglomeration and subsequent deposition. Inhibitors also act to decrease the wax appearance temperature, increasing the non wax-forming operational envelope.

Needless to say, chemical control is costly. Monthly expenditures on chemical injection are estimated to run as high as $800,000, which when added to the value of deferred production (due to the blockage) could result in annual losses up to $25 to 30 million for a single oil well.[20]

Thermal Methods

They serve a dual purpose of prevention and remediation of blockages. Insulation and active heating are the primary options used to maintain the bulk fluid temperature above the wax appearance temperature. Procedures such as steaming the flowlines, installing bottomhole heaters, and hot oil/water circulation are implemented to melt the paraffin deposit.[21] Obvious drawbacks to these procedures include the considerable cost of energy for heating and the difficulty/impracticality of heating in hostile environments.[22]

A chemical process known as the Nitrogen Generating System (SGN) created by Petrobras (also available by Baker-Hughes) which is based on strongly exothermic reactions of salt solution mixtures is used to melt paraffin deposits.[23]

Production/Completion Techniques

These involve the use of plastic and coated pipes, application of backpressures, and the use of improved handling facilities.[6] The pressure boost provided by multiphase pumping, an emerging technology, is also thought to have an additional advantage of shifting flowing/production conditions out of the hydrate- and wax-forming operational envelope and also controlling pipeline slugging.[24]

Distributed Temperature Sensors[25] which are basically fibreoptic sensors are employed by companies such as Schlumberger to provide accurate, real-time temperature measurements necessary for a proactive approach to flow assurance. They provide critical information that aid in signaling the onset of leak and blockage detection, optimize energy requirements for flowline heating and reduce chemical injection.[25] This ultimately aids decision-making leading to prompt and effective remedial action as well as substantial cost savings.

Other commercially available tools for dispersion are magnetic and ultrasonic techniques. Magnetic techniques are based on the creation of a magnetic field that alters the chemical, mechanical, and electrical properties of the crude reducing the kinetics of

deposition and altering the cloud point mechanism. These flow-conditioning tools are in large-scale operation in China[26] and were the subject of investigation by Petrobras.[23]

Ultrasonic techniques involve the use of a movable source of electromagnetic radiation, such as in an electromagnetic pig. As the pig moves, the plug absorbs intense electromagnetic radiation, heats up and melts. Effective melting of the dielectric plug is achieved with the source moving along the pipeline as the solid–liquid interface propagates.[27]

Mechanical Techniques

The main mechanical techniques are pigging, wireline cutting, and through flowline cutting, which are all variations of the same concept of running a scraper through a pipeline.

Pigging

The most common method for removing accumulated wax deposits, the pig is sent down the line, carried along by the flow of crude, and mechanically scrapes off the wax, re-dispersing it in the bulk oil in front of the pig. This operation can be a successful, cost-effective method for managing paraffin deposits in flowlines and pipelines provided that a regularly scheduled pigging program is initiated upon commissioning.[28]

The numerous pig designs range from simple spheres, to foam pigs, to bristle pigs, to very aggressive pigs used for cleaning out severe deposits. The basic breeds of pigs are the poly pig, which is equipped with soft foam used often for gauging an unknown environment inside of a pipeline; the jet pig, armed with steel brushes used to scrape off solid, heavy deposits; and the super pig, which can be equipped with a variety of attachments, from brushes and cups to bi-directional disks.[26] There are also intelligent/ smart pigs known as Inline Inspection Tools (ILI),[29] which are equipped with a computer and battery pack and are used more for inspection to ensure pipeline integrity than for actual paraffin remediation.

Generally, in the early phase and design evaluation, a maximum wax layer thickness of 2 to 3 mm is used as the criterion for pipeline pigging.[10]

Wireline Cutting/Through-Flowline Cutting (TFL)

These operations involve pumping a cutting tool down the flowline and into the wellbore to cut wax deposits. Though TFL is not yet a common practice, it has the advantage of being able to remediate subsea flowlines and wellbores from a distant platform. It was used in the Pompano Paraffin Calibration Field Trials to clear of wax deposits before well testing.[28] A drawback of wireline cutting is its costliness.

Microbial-Based Techniques

These are commercially available microbial formulations used to treat paraffin deposition in the oil field. They have been successfully tested in fields in China[26] and are considered cheaper than most of the methods outlined above when readily available.

The bottom line is that there is no unique panacea to paraffin prevention and remediation; but rather the successful and unique combination of the solutions listed above must be determined on a case-by-case basis and, unfortunately, sometimes by trial and error to solve wax problems.

ANALYSIS TECHNIQUES

By analytical methods, we mean the various "simplistic" methods that have been developed from readily available pressure and volume data. The idea behind these analysis techniques is that they provide vital information that helps in decision making, such as the optimal amount of chemicals to be used; they also aid in the determining the risk of pigging and the type of pig to be run.[31]

The three basic analyses are mass, momentum and energy balance approaches. The common thread in all approaches is the qualitative and quantitative assessment of the deviation of the response when partially or fully-blocked from the baseline response.

Mass/Volume-Balance Approach

The mass/volume balance method, developed by the onshore industry, is one of the most accurate methods. It is based on a blockage factor defined as the ratio of the volume of a partially blocked pipe of radial geometry relative to its unblocked volume. This ratio is obtained experimentally by bleed-off tests at the time the pipe is commissioned and after the blockage occurs. It requires accurate metering of inlet and outlet flow rates, which is often a limitation due to difficulties in obtaining precise measurements of inlet flow rates. The blockage factor as defined for a pipe of radial geometry is:

$$F_{VB} = \frac{V_B}{V_P} = 1 - \frac{L_B}{L_P}\left[1 - \left(\frac{d_B}{d}\right)2\right] = 1 - L_{BD}\left(1 - d_{BD}{}^2\right) \quad \text{..... (9)}$$

where L_{BD} is the dimensionless blockage length, and d_{BD} the dimensionless blockage diameter.

The volumes of the blocked and unblocked pipeline are obtained from the basic definition of isothermal compressibility:

$$C_t = -\frac{1}{V_p}\left(\frac{\partial V_p}{\partial P}\right)_T \quad \text{..... (10)}$$

$$C_t = C_p + C_L\left(\frac{V_L}{V_P}\right) + C_B\left(\frac{V_B}{V_P}\right) \quad \text{..... (11)}$$

where C_p, C_L and C_B are the pipeline, liquid, and blockage compressibilities which can be estimated within the pressure range of interest.

The slope (dV_p/dP) can be obtained from volume bleed-off tests conducted at baseline conditions when the pipe is unblocked and at later times when the pipe is blocked. The blockage factor then becomes:

$$F_{VB} = \frac{V_B}{V_p} = \frac{\frac{1}{C_t}\left(\frac{\partial V_p}{\partial P}\right)\text{blocked}}{\frac{1}{C_t}\left(\frac{\partial V_p}{\partial P}\right)\text{baseline}} \quad \text{..... (12)}$$

Momentum-Balance Approach

The momentum-balance approach is based on the fact that a blockage reduces the hydraulic diameter of a pipe and increases the frictional pressure losses. The basic equations are:

$$\frac{dP}{dx} = \frac{2f\rho v^2}{d} \quad \text{..... (13)}$$

and

$$\Delta P_f = 4f\frac{L}{d}\frac{\rho}{2}\left(\frac{4Q_{flow}}{\pi d^2}\right)^2 \quad \text{..... (14)}$$

Substituting the expression for friction factor and further manipulation yields:

$$\left(d_i - 2\partial_w\right)^{5-n} = \frac{2c\rho L}{\Delta P_f}\left(\frac{\mu}{\rho}\right)\left(\frac{4Q_{flow}}{\pi}\right)^{2-n} \quad \text{..... (15)}$$

where δ_w is the wax thickness.

This method, originally reported by Weingarten and Euchner,[32] has been used successfully in experimental work by several investigators to determine wax thickness and wax appearance temperature.

From Eq. 14, Scott and Satterwhite[1] developed the backpressure technique of monitoring partial blockages in pipelines.

The backpressure equation for a single-phase liquid is given by:

$$Q = J\left(P_1 - P_3\right)^n \quad \text{..... (16)}$$

For a partially blocked pipe, the expression becomes:

$$Q = JF_{FB}\,(P_1 - P_3)^{\,n}, \quad \text{..... (17)}$$

where the constant J and the exponent n have different expressions for fully rough flow and smooth pipe.

They defined the friction-based factor (F_{FB}) by writing out Eq. 14 for both the partially blocked and unblocked sections of a pipeline. Eq. 18 gives the expression for F_{FB} for fully rough flow and Eq. 19 for smooth pipe;

$$F_{FB} = \frac{1}{\sqrt{\left(\frac{f_B}{f}\right)\left(\frac{L_B}{L_p}\right)\left(\frac{d}{d_B}\right)^5 + 1 - \left(\frac{L_B}{L_p}\right)}} \quad \text{..... (18)}$$

$$F_{FB} = \frac{1}{\sqrt{\left(\frac{L_B}{L_p}\right)\left(\frac{d}{d_B}\right)^{4.8} + 1 - \left(\frac{L_B}{L_p}\right)}} \quad \text{..... (19)}$$

This blockage factor (F_{FB}) represents the effect of the blockage evidenced by a very subtle deviation of the backpressure plot from the characteristic linear baseline response. Multirate tests are used to determine the baseline values of J and n to be able to separate out the friction-based factor as blockages develop.

The volume- and momentum-balance approaches can each be used to detect blockages in pipelines, but the actual characterization of the blockage requires the simultaneous solution of the volume- and friction-based factor equations (Eqs. 12 and 18 or 19) for blockage length (L_B) and diameter (d_B).

Energy-Balance Approach

The third approach, which is the focus of this research, is based on a heat balance. This is a novel approach that has been explored by such investigators as Kaminsky to interpret preliminary test data from the Wax Joint Industry Project currently underway at the University of Tulsa.[2]

The heat-balance approach is based on the concept that blockage resulting from the deposition of a wax layer contributes an additional layer of resistance to heat flow. This wax layer has an insulating effect that can be detected in the observed temperature drop from the inlet to the outlet of the pipeline. This insulating effect, quantified by the deviation of the observed temperature drop from the expected temperature drop, is directly related to the thickness and thermal conductivity of the wax deposited.

The original model,[2] which serves as the building block of this research, is shown below:

$$\frac{T_m - T_e}{q_o} = \frac{1}{h_i}\frac{r_o}{r_i - \partial_w} + \frac{r_o}{k_w}\ln\frac{r_i}{r_i - \partial_w} + \frac{r_o}{k_p}\ln\frac{r_o}{r_i} + \frac{1}{h_o}, \quad \text{..... (20)}$$

where q_o = Heat lost to the surroundings,

h_i = Internal film heat transfer coefficient,

h_o = Outside film heat transfer coefficient,

k_p = Thermal conductivity of the pipe,

k_w = Thermal conductivity of wax layer, and

δ_w = Wax thickness.

THE HEAT-BALANCE MODEL FOR A FULLY-BLOCKED PIPELINE

The base relations are summarized below (see Appendix A for details of development of the model).

1) Fundamental Heat-Balance equation

$$\Delta Q = Q_{in} - Q_{out} = 0 \quad \text{..... (21)}$$

where ΔQ = Change in heat energy,

Q_{in} = Heat energy entering the pipe, and

Q_{out} = Heat energy leaving the pipe.

2) Heat Loss Components

$$Q_{out} = Q = Q_1 = Q_2 = Q_3 = Q_4 \quad \text{..... (22)}$$

where Q_1 = Internal convection (from the fluid),

Q_2 = Conduction through the wax layer,

Q_3 = Conduction through the pipe wall, and

Q_4 = External convection (to the ambient air).

3) Heat Loss Expression

$$Q = UA\,\Delta T = \frac{T_{amb} - T_{mi}}{\frac{1}{h_i A_i} + \frac{\ln\left(r_i / r_i - \partial_w\right)}{2\pi L k_w} + \frac{\ln\left(r_o / r_i\right)}{2\pi L k_p} + \frac{1}{h_o A_o}} \quad \text{.. (23)}$$

4) Heat Input (Q_{in})

$$Q_{in} = q = \dot{m} C_p dT_m \quad \text{..... (24)}$$

5) Intermediate Heat-Balance Expression

$$\dot{m} C_p dT_m = q'' A = UA\Delta T = U(Pdx)\Delta T \text{ , ... (25)}$$

where P is the perimeter of the pipe.

6) Intermediate Heat-Balance Expression (after integration)

$$Q = \dot{m}C_p\left(\Delta T_o - \Delta T_i\right) = \left[\frac{-2\pi r_o L_p\left(\frac{\left(T_{\text{amb}} - T_{mo}\right) - \left(T_{\text{amb}} - T_{mi}\right)}{\ln\frac{T_{\text{amb}} - T_{mo}}{T_{\text{amb}} - T_{mi}}}\right)}{\frac{r_o}{h_i(r_i - \partial_w)} + \frac{r_o}{k_w}\ln\frac{r_i}{r_i - \partial_w} + \frac{r_o}{k_p}\ln\frac{r_o}{r_i} + \frac{1}{h_o}}\right] \quad \text{.... (26)}$$

7) Mass Flow Rate Expression

$$\dot{m} = \rho Q_{\text{flow}} \quad \text{..... (27)}$$

8) Heat-Balance Model

$$\frac{T_{\text{amb}} - T_{mo}}{T_{\text{amb}} - T_{mi}} = \exp\left\{\frac{-\overline{U}A_o}{Q_{\text{flow}}\rho C_p}\right\} \quad \text{..... (28)}$$

where;

$$\overline{U} = \frac{1}{\frac{r_o}{h_i\left(r_i - \partial_w\right)} + \frac{r_o}{k_w}\ln\frac{r_i}{r_i - \partial_w} + \frac{r_o}{k_p}\ln\frac{r_o}{r_i} + \frac{1}{h_o}} \quad \text{,..... (29)}$$

9) Final Heat-Balance Model for a Fully-Blocked Pipeline (expressed as a temperature drop)

$$T_{mi} - T_{mo} = T_{amb}\left[\exp\left\{\frac{-\overline{U}A_o}{Q_{\text{flow}}\rho C_p}\right\} - 1\right] + T_{mi}\left[1 - \exp\left\{\frac{-\overline{U}A_o}{Q_{\text{flow}}\rho C_p}\right\}\right] \quad \text{..... (30)}$$

With this model, given a certain wax thickness and other pipe and ambient properties, the temperature drop of the fluid from inlet to outlet can be estimated.

TEMPERATURE SKIN FACTOR FOR A FULLY-BLOCKED FLOWLINE

The concept of skin from the reservoir has been extended to pipe flow, in which case skin refers to any blockage that obstructs pipe flow. From a pressure drop analysis, the skin consists of an additional pressure drop term that increases the overall pressure drop in the pipe. Similarly, a skin factor can be derived from a temperature drop analysis, where the skin in this case would account for the insulating effect of the wax layer. The skin term would directly affect the overall heat transfer coefficient ($\overline{U}$) and in this case, would have an inverse relationship to the observed temperature drop from pipe inlet to pipe outlet. The skin term can be extracted from a comparison of the overall heat transfer coefficient expression written for an unblocked and blocked pipeline.

The heat transfer expressions for a blocked and unblocked pipe are given by Eqs. 31 and 32 respectively.

$$\overline{U} = \frac{1}{\frac{r_o}{h_i(r_i - \partial_w)} + \frac{r_o}{k_w}\ln\frac{r_i}{r_i - \partial_w} + \frac{r_o}{k_p}\ln\frac{r_o}{r_i} + \frac{1}{h_o}} \quad \text{..... (31)}$$

For an unblocked pipe, where $\delta_\omega = 0$,

$$\overline{U} = \frac{1}{\frac{r_o}{h_i r_i} + \frac{r_o}{k_p}\ln\frac{r_o}{r_i} + \frac{1}{h_o}} \quad \text{..... (32)}$$

Comparing the two equations, we can extract a skin factor from the denominator of the expression for the blocked pipe as;

$$S = \frac{r_o}{h_i(r_i - \partial_w)} + \frac{r_o}{k_w}\ln\frac{r_i}{r_i - \partial_w} - \frac{r_o}{h_i r_i} \quad \text{..... (33)}$$

The general expression for the heat transfer coefficient including the skin factor is:

$$\overline{U} = \frac{1}{\frac{r_o}{h_i r_i} + \frac{r_o}{k_p}\ln\frac{r_o}{r_i} + \frac{1}{h_o} + S} \quad \text{..... (34)}$$

The unit of this skin factor is m^2K/W. There is a direct relationship between the size of blockage (δ_w) and the skin factor. The greater the blockage, the greater the skin factor and the lower the temperature drop, as can be seen from the general expression for the blocked pipe.

GRAPHICAL REPRESENTATION OF HEAT-BALANCE MODEL FOR A FULLY-BLOCKED PIPELINE

Flowline and Fluid Properties

These relationships can be illustrated graphically for an actual pipeline. The pipeline is assumed to be 'fully-blocked', i.e. there is a blockage of uniform circumferential and longitudinal thickness that extends along the entire pipeline length. The characteristics of a North Sea pipeline selected from the work of Labes-Carrier[10] are summarized in **Table 1**.

Table 1–Characteristics of North Sea Pipeline Selected

Parameter	Value
Pipe Length	43 km
Pipe ID	0.38 m
Pipe OD	0.4054 m
Material	Stainless Steel

Arbitrary, but realistic values selected for the fluid properties (oil and air) are summarized in **Table 2**.

Table 2–Fluid Properties

Property	Oil	Ambient Air
Density (ρ), kg/m^3	875.32	1.271
Viscosity (μ), cp	1.0603	0.01748
Specific Heat Capacity (C_p), J/kgK	1890	1005
Thermal Conductivity (k), W/mK	0.18	0.02465

The thermal conductivity of the wax (k_w) is assumed to be equal to 0.25 W/mK.

Convective Heat Transfer Coefficients

Internal Convective Coefficient (h_i): It is estimated from the Dittus-Boelter correlation.[31]

$$N_{NU} = 0.023\, N_{RE}^{4/5} N_{PR}^{\ n} \quad \text{..... (35)}$$

$$N_{NU} = \frac{h_i D_i}{k} \quad \text{..... (36)}$$

$$N_{RE} = \frac{4\dot{m}}{\pi D \mu} \quad \text{..... (37)}$$

$$N_{PR} = \frac{C_p \mu}{k} \quad \text{..... (38)}$$

where n = 0.3 for cooling and 0.4 for heating (cooling is assumed; i.e., $T_s < T_m$), N_{NU} is the Nusselt number, N_{PR} the Prandtl number, and N_{RE} the Reynolds number. The Dittus-Boelter[33] correlation is applicable within the specified ranges below:

$$0.7 \le N_{PR} \le 160$$
$$N_{RE} \ge 10{,}000$$
$$\frac{L}{D} \ge 10$$

External Convective Coefficient (h_o): The simplest case scenario is considered here with the pipeline elevated 1 m above ground level and standing in ambient air of velocity less than 0.5 m/s. In this case, natural convection dominates and the recommended PIPESIM value for h_o of 4 $Wm^{-2}K^{-1}$ is used.[9]

The ambient air temperature was taken as 0°C and the pipe wall surface temperature as 32°C. The bulk fluid temperature at the inlet (T_{mi}) was taken as 35°C and all fluid thermodynamic properties were evaluated at this temperature with the assumption that the variation from pipe inlet to outlet is small.

The graphical results for variations in skin factor and flow rate are presented in **Figs. 3 to 6.**

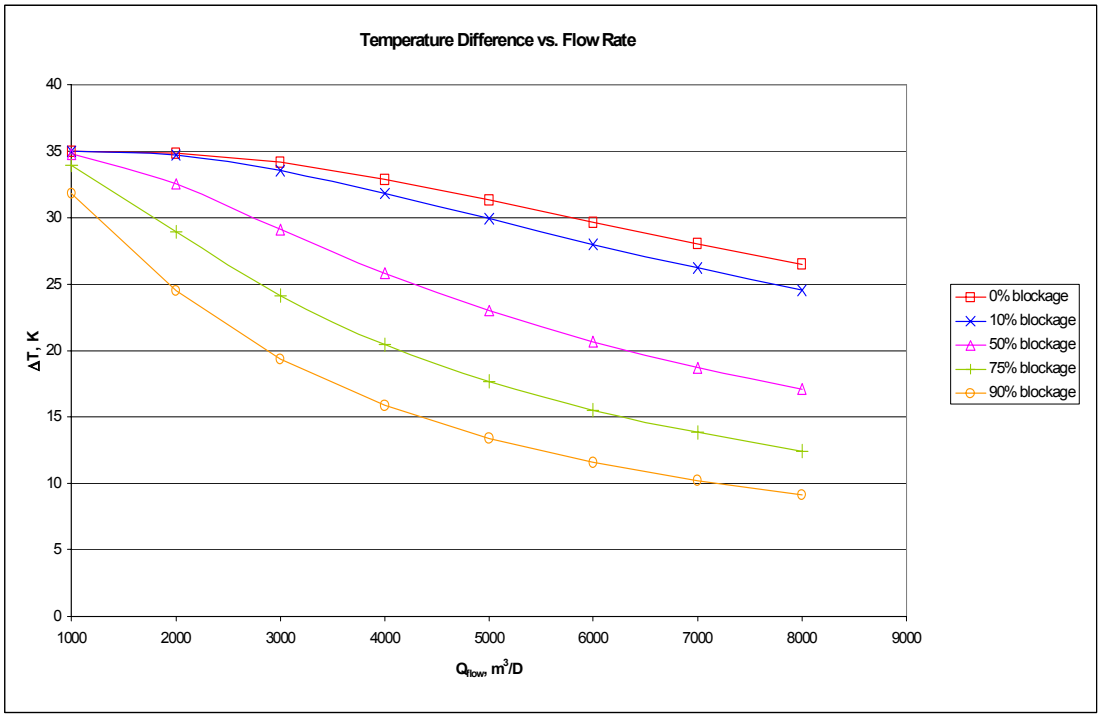

Fig. 3–Temperature drop variation with flow rate (Cartesian plot).

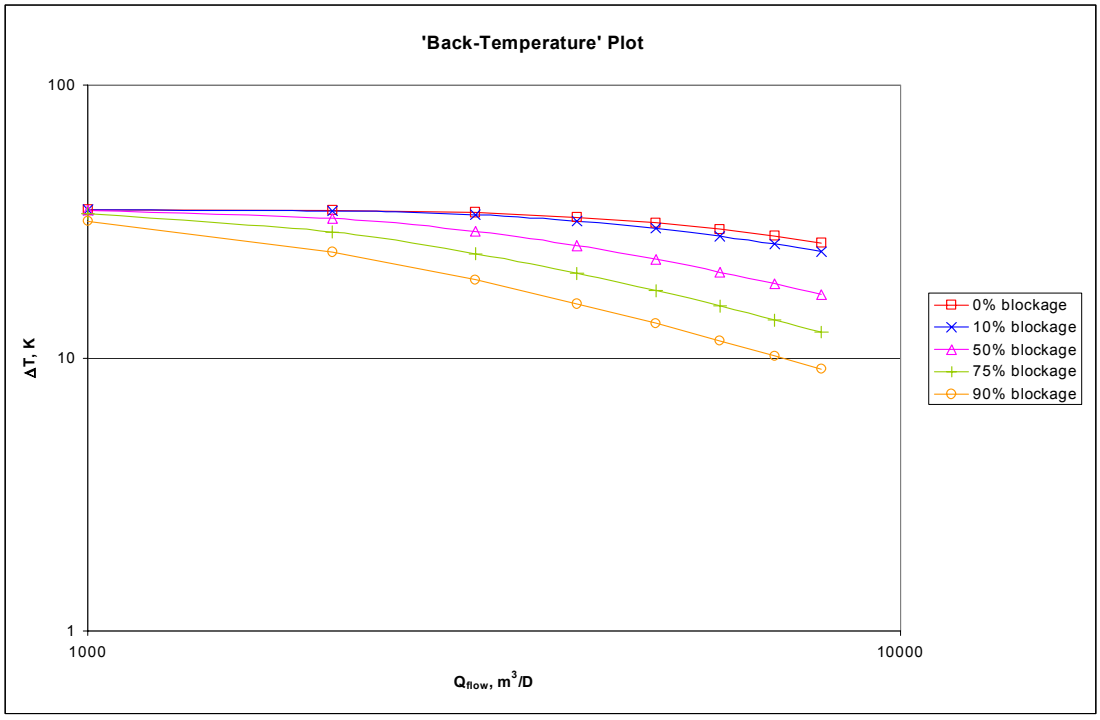

Fig. 4–Temperature drop variation with flow rate (back-temperature plot).

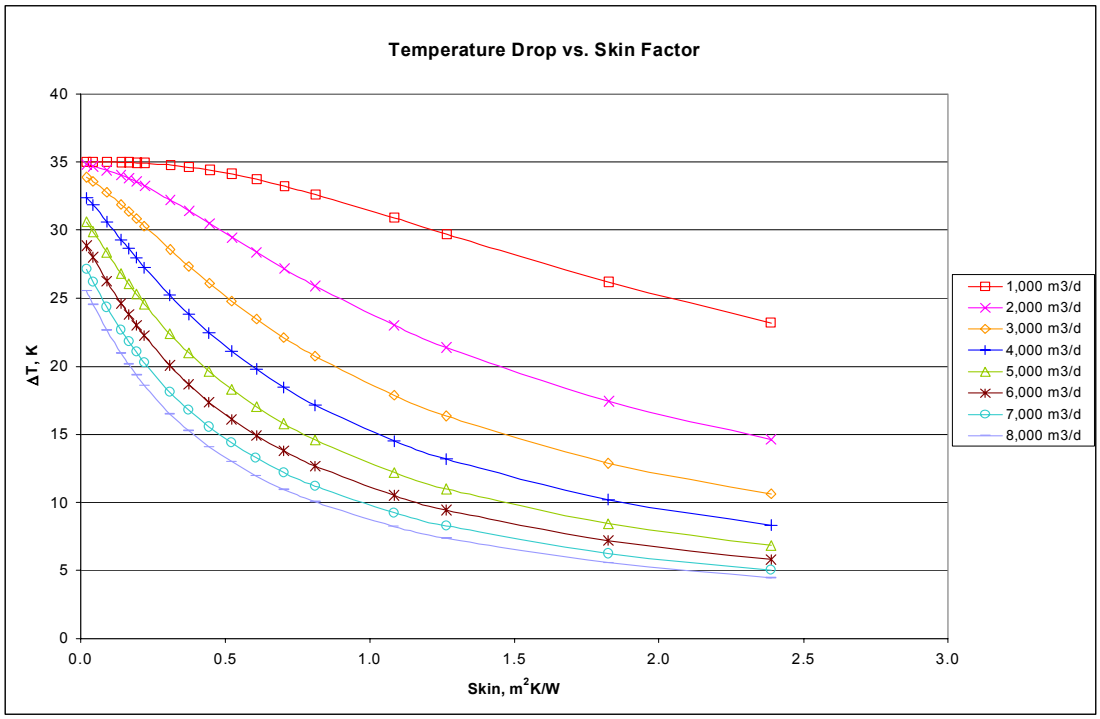

Fig. 5–Temperature drop variation with skin factor.

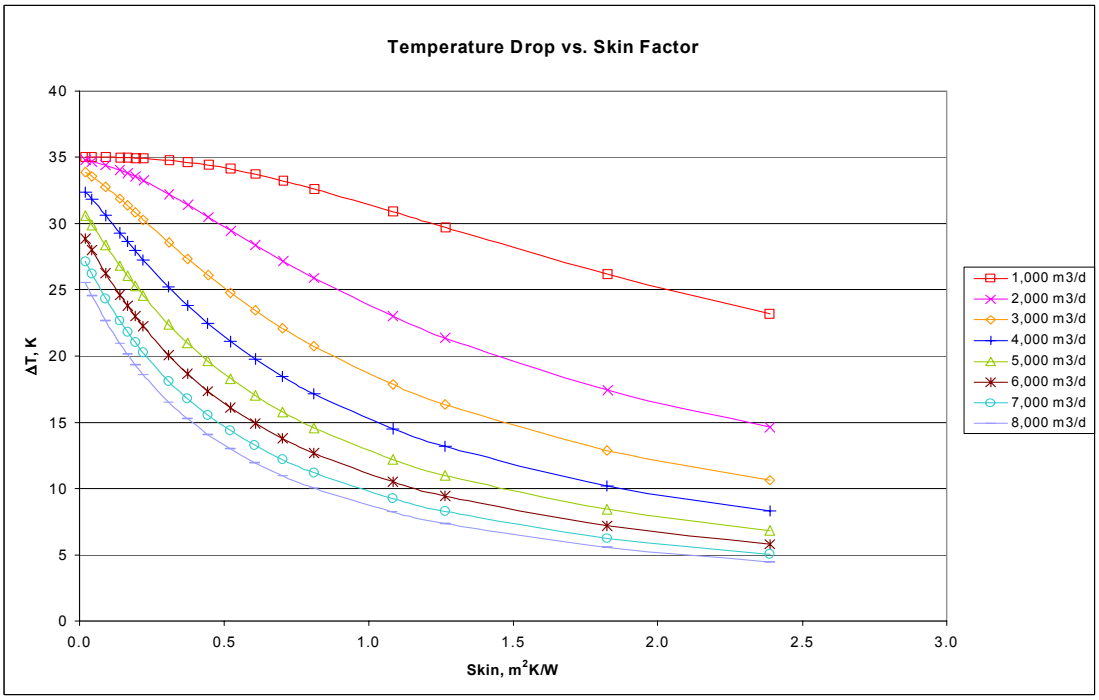

Fig. 6–Outlet temperature variation with flow rate and blockage.

Discussion

Fig. 3 shows that the greater the flow rate, the lower the temperature drop because higher flow rates imply greater volumes of fluid, higher heat contents (mC_p) and a greater overall retention of heat in the system. At higher flow rates, the heat transfer (loss) rate is lower and therefore the temperature drop from pipe inlet to outlet is lower. This is consistent with results obtained by Golzynski and Niesen;[34] they state, "At lower flowrates, the temperature losses to the environment will be increased, as there is less input to the system. The lower flowrates contribute less overall thermal mass to the system, and, as such, cannot maintain the high temperatures as easily as the flowrates do."

Fig. 4, essentially a "back temperature" representation of the information in Fig. 3, depicts the effect of a uniform blockage on fluid flow in a pipeline as a departure from the zero-blockage line. A blockage in a pipeline will manifest on a 'back-temperature' plot as a shift in trend below the zero-blockage line: the greater the blockage, the greater the shift. The 'shift' is as a result of the insulating effect of the wax blockages deposited. As the blockage increases in cross-sectional area, it reduces the overall heat loss rate causing the temperature drop from pipe inlet to outlet to decrease.

Fig. 5 clearly illustrates the inverse relationship between temperature drop from pipe inlet to outlet and skin factor. As the skin factor increases, the temperature drop

decreases. Also, at higher flow rates, the temperature drop is more sensitive to skin factor than at lower flow rates.

Fig. 6 shows the variation in outlet temperature with flow rate with different extents of blockage. Clearly, the outlet temperature is higher than expected when a blockage is present. The difference between the inlet temperature and the observed outlet temperature is a function of flow rate and blockage extent: the greater these two factors, the higher the outlet temperature and consequently, the lower the temperature drop.

THE HEAT-BALANCE MODEL FOR A PARTIALLY-BLOCKED PIPELINE

The base relations are summarized below (see Appendix C for details of development of the model).

1) Intermediate Heat-Balance Equation (see Eq. A-39 in Appendix)

$$\frac{T_{\text{amb}} - T_{mo}}{T_{\text{amb}} - T_{mi}} = \exp\left\{ \frac{-2\pi r_o L_p}{Q_{\text{flow}} \rho C_p \left(\frac{r_o}{h_i (r_i - \partial_w)} + \frac{r_o}{k_w} \ln \frac{r_i}{r_i - \partial_w} + \frac{r_o}{k_p} \ln \frac{r_o}{r_i} + \frac{1}{h_o} \right)} \right\} \quad \text{.... (39)}$$

2) Intermediate Heat-Balance Equation (written for the blocked section of pipe)

$$\frac{T_{amb} - T_{m2}}{T_{amb} - T_{m1}} = \exp\left\{ \frac{-2\pi r_o L_B}{Q_{\text{flow}} \rho C_p \left(\frac{r_o}{h_i (r_i - \partial_w)} + \frac{r_o}{k_w} \ln \frac{r_i}{r_i - \partial_w} + \frac{r_o}{k_p} \ln \frac{r_o}{r_i} + \frac{1}{h_o} \right)} \right\} \quad \text{.... (40)}$$

3) Intermediate Heat-Balance Equation (written for the unblocked section of pipe)

$$\frac{T_{amb} - T_{m3}}{T_{amb} - T_{m2}} = \exp\left\{ \frac{-2\pi r_o (L_p - L_B)}{Q_{\text{flow}} \rho C_p \left(\frac{r_o}{h_i r_i} + \frac{r_o}{k_p} \ln \frac{r_o}{r_i} + \frac{1}{h_o} \right)} \right\} \quad \text{..... (41)}$$

4) Heat-Balance Model

$$\frac{T_{amb}-T_{mo}}{T_{amb}-T_{mi}}=\exp\left\{-\left(\frac{2\pi r_o L_p}{Q_{\text{flow}}\rho C_p\left(\frac{r_o}{h_i r_i}+\frac{r_o}{k_p}\ln\frac{r_o}{r_i}+\frac{1}{h_o}\right)}+\frac{2\pi r_o L_B}{Q_{\text{flow}}\rho C_p}\left(\frac{1}{\frac{r_o}{h_i r_B}+\frac{r_o}{k_w}\ln\frac{r_i}{r_B}+\frac{r_o}{k_p}\ln\frac{r_o}{r_i}+\frac{1}{h_o}}-\frac{1}{\frac{r_o}{h_i r_i}+\frac{r_o}{k_p}\ln\frac{r_o}{r_i}+\frac{1}{h_o}}\right)\right)\right\} \quad (42)$$

5) Final Heat-Balance Model for a Partially-Blocked Pipeline (expressed as a temperature drop)

$$T_{mi}-T_{mo}=T_{amb}\left[\exp(-Y)-1\right]+T_{mi}\left[1-\exp(-Y)\right] \quad \text{..... (43)}$$

where $$Y=\frac{2\pi r_o L_p}{Q_{\text{flow}}\rho C_p\left(\frac{r_o}{h_i r_i}+\frac{r_o}{k_p}\ln\frac{r_o}{r_i}+\frac{1}{h_o}\right)}+\frac{2\pi r_o L_B}{Q_{\text{flow}}\rho C_p}\left(\frac{1}{\frac{r_o}{h_i r_B}+\frac{r_o}{k_w}\ln\frac{r_i}{r_B}+\frac{r_o}{k_p}\ln\frac{r_o}{r_i}+\frac{1}{h_o}}-\frac{1}{\frac{r_o}{h_i r_i}+\frac{r_o}{k_p}\ln\frac{r_o}{r_i}+\frac{1}{h_o}}\right) \quad (44)$$

TEMPERATURE SKIN FACTOR FOR A PARTIALLY-BLOCKED FLOWLINE

Eq. 42 is the heat model expression for a partially blocked pipe. For an unblocked pipe, $L_B = 0$ and Eq. 42 is simplified to Eq. 45.

$$\frac{T_{amb} - T_{mo}}{T_{amb} - T_{mi}} = \exp\left\{-\left(\frac{2\pi r_o L_p}{Q_{\text{flow}}\rho C_p\left(\frac{r_o}{h_i r_i} + \frac{r_o}{k_p}\ln\frac{r_o}{r_i} + \frac{1}{h_o}\right)}\right)\right\} \quad \text{..... (45)}$$

Comparing Eqs. 42 and 45 reveals an extra term, which accounts for the blockage. Again, this is the skin factor for a partial blockage in a flowline. It can be written as:

$$S = \frac{2\pi r_o L_B}{Q_{\text{flow}}\rho C_p}\left(\frac{1}{\frac{r_o}{h_i r_B} + \frac{r_o}{k_w}\ln\frac{r_i}{r_B} + \frac{r_o}{k_p}\ln\frac{r_o}{r_i} + \frac{1}{h_o}} - \frac{1}{\frac{r_o}{h_i r_i} + \frac{r_o}{k_p}\ln\frac{r_o}{r_i} + \frac{1}{h_o}}\right) \quad \text{..... (46)}$$

The heat model for a partially blocked pipe contains two unknowns, r_B and L_B. This model requires that either r_B or L_B be known either from the momentum- or the mass-balance approach; or the mass- or momentum-balance equation be solved simultaneously with the heat-balance equation for r_B and L_B.

The expression for skin factor reveals a direct relationship between the skin factor and the blockage length. The skin factor is observed to always be negative. The graphical results showing variations in parameters such as flow rate and blockage length for a partially-blocked pipeline are presented in **Figs. 7 through 18**.

GRAPHICAL REPRESENTATION OF HEAT-BALANCE MODEL FOR A FLOWLINE WITH A LOCALIZED BLOCKAGE AT INLET

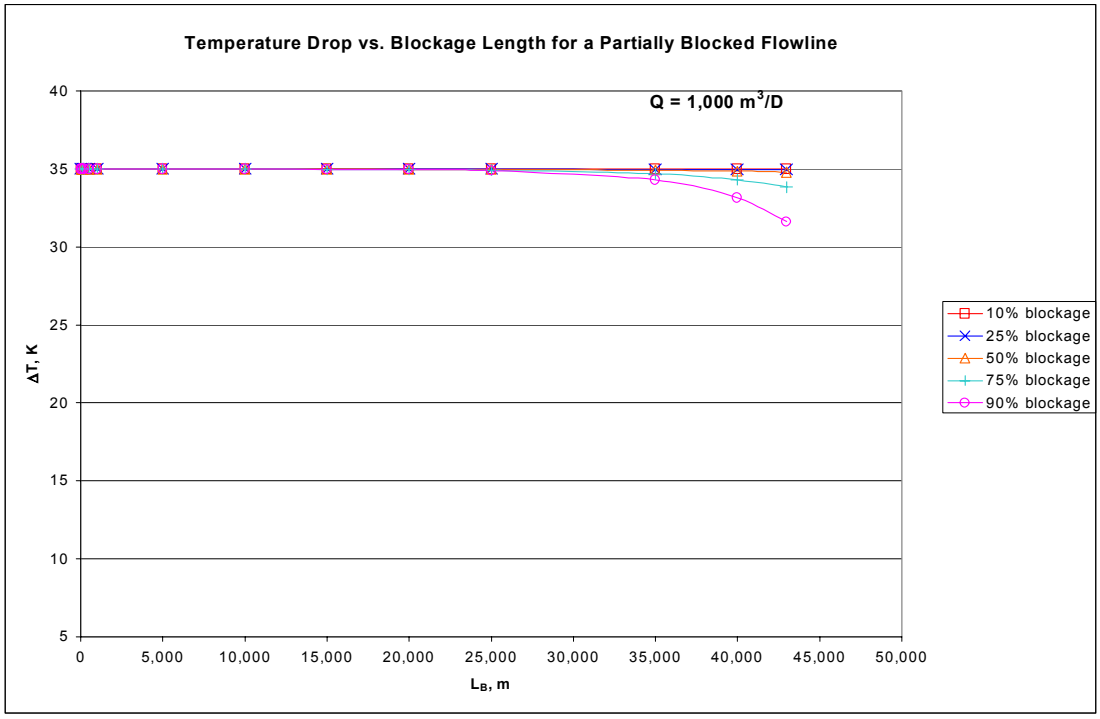

Fig. 7–Temperature drop variation with blockage length and cross-sectional area (1000 m^3/d).

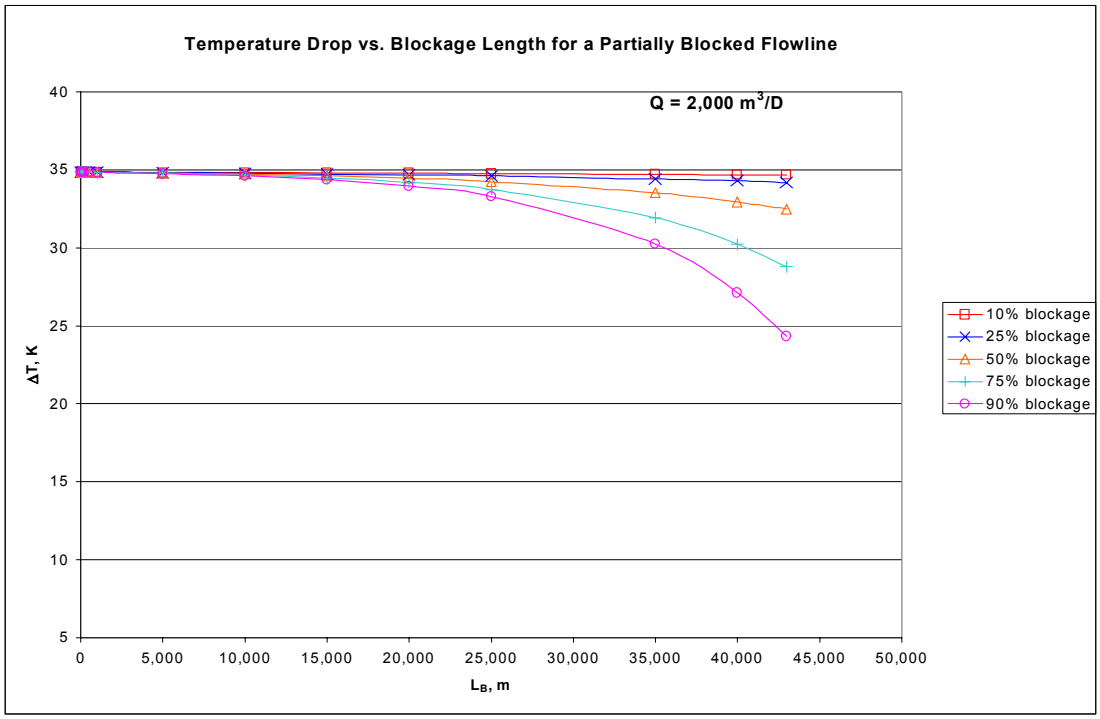

Fig. 8–Temperature drop variation with blockage length and cross-sectional area (2000 m^3/d).

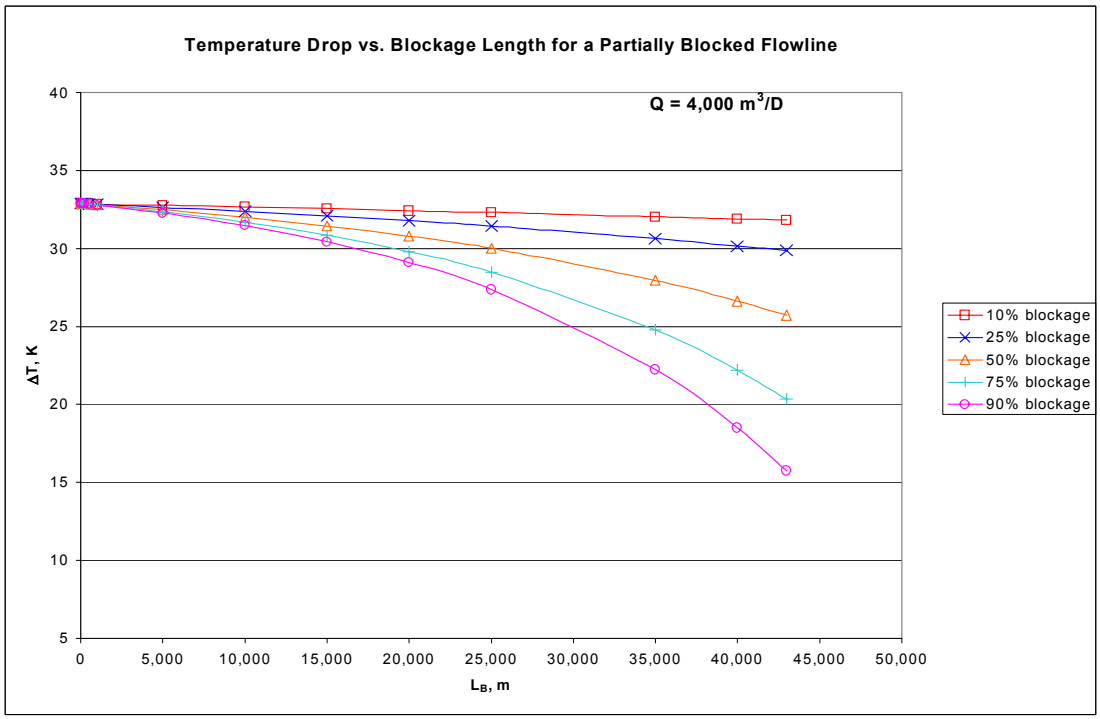

Fig. 9–Temperature drop variation with blockage length and cross-sectional area (4000 m^3/d).

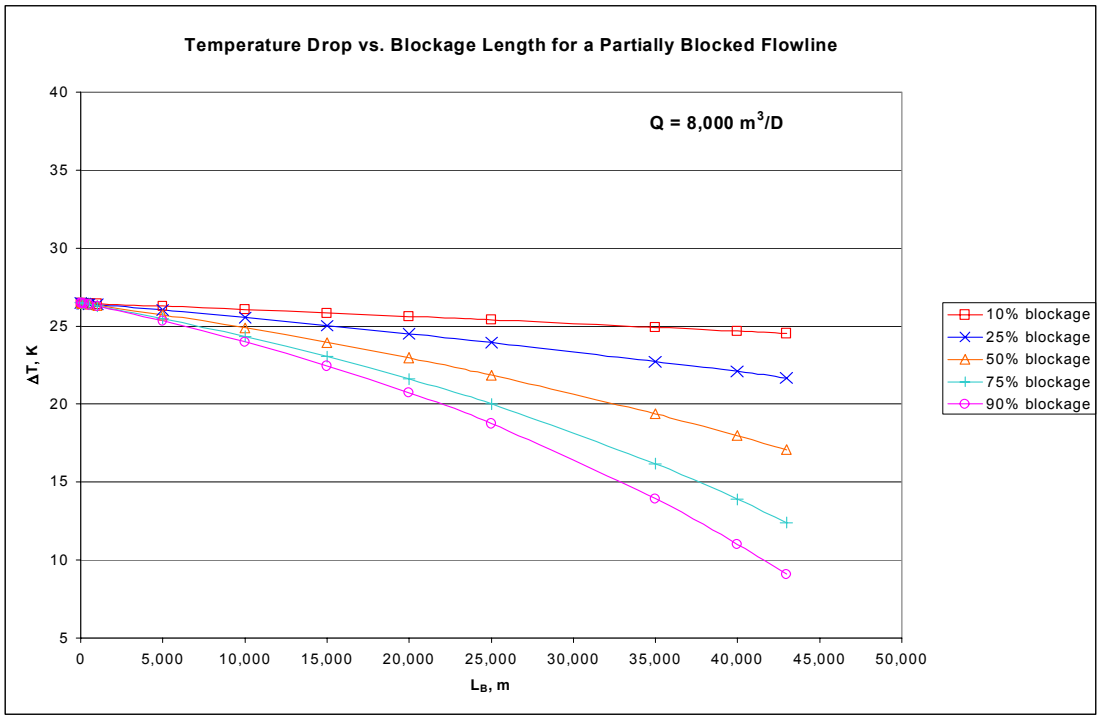

Fig. 10–Temperature drop variation with blockage length and cross-sectional area (8000 m^3/d).

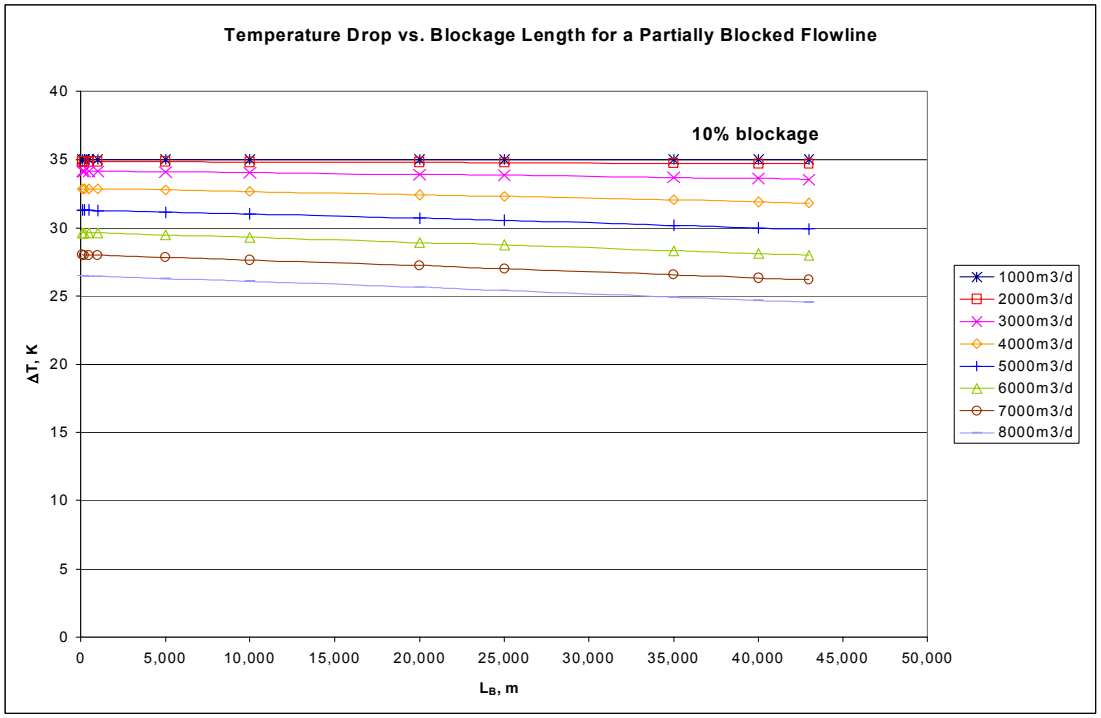

Fig. 11–Temperature drop variation with blockage length and flow rate (10% blockage).

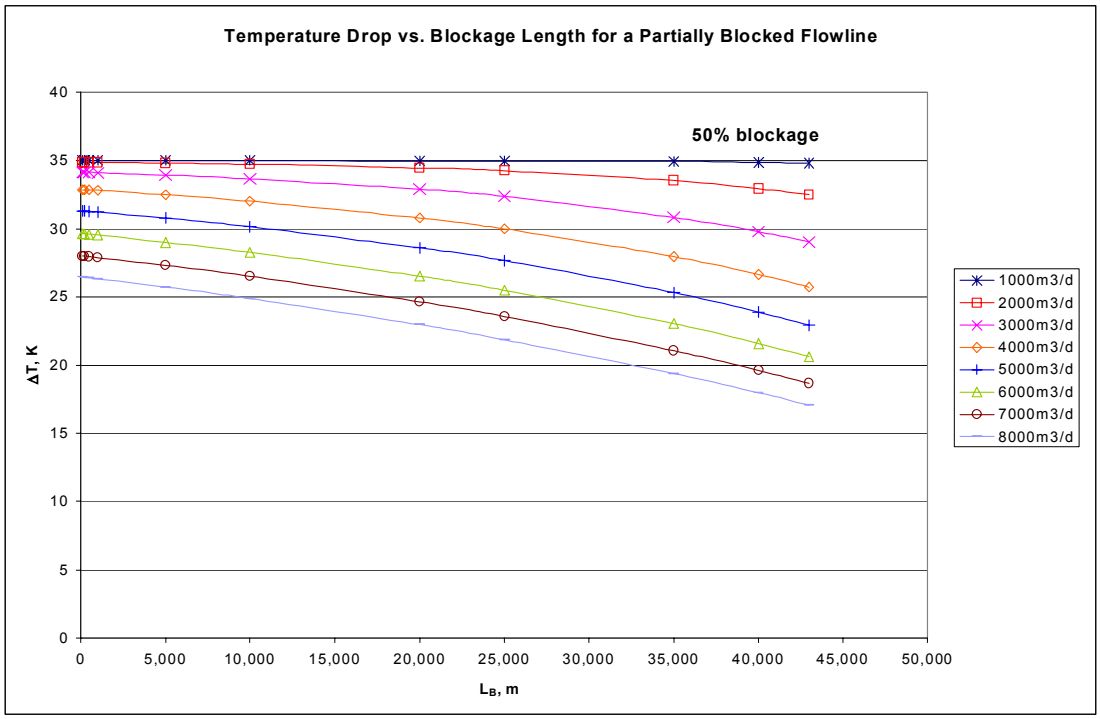

Fig. 12–Temperature drop variation with blockage length and flow rate (50% blockage).

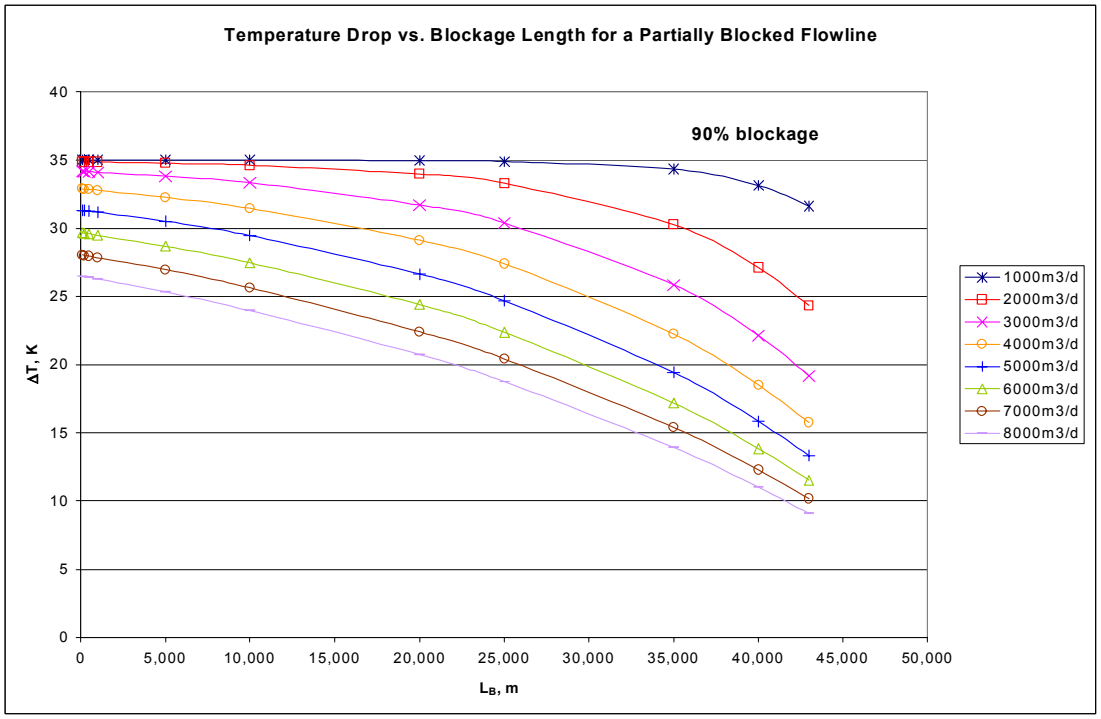

Fig. 13–Temperature drop variation with blockage length and flow rate (90% blockage).

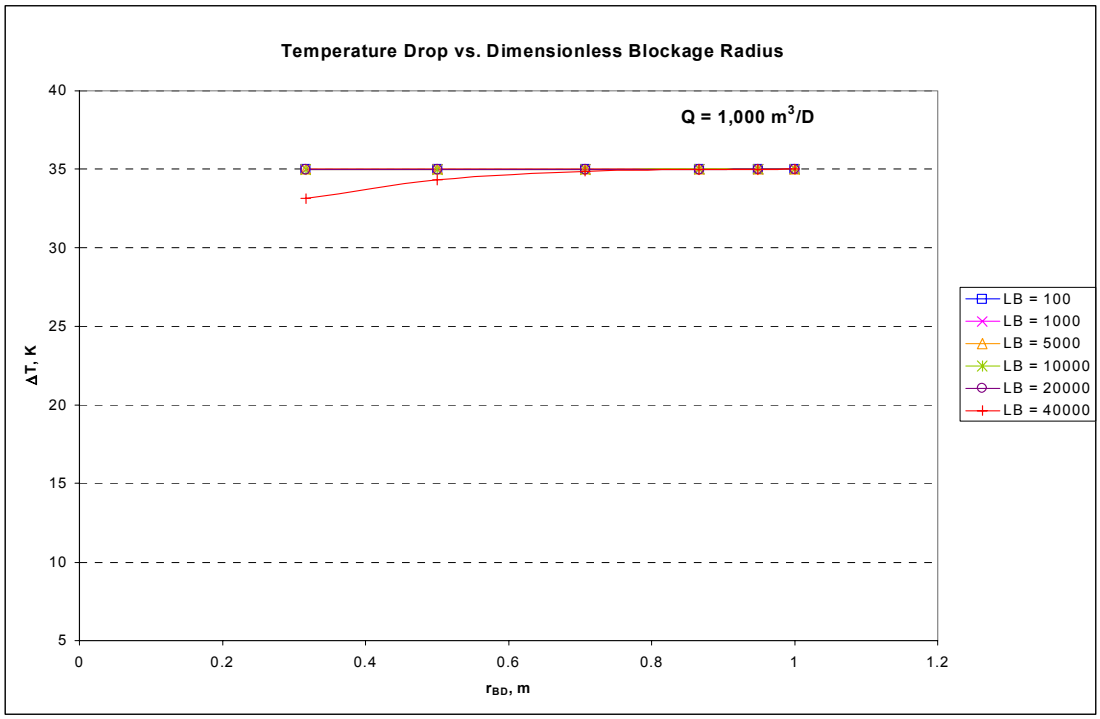

Fig. 14–Temperature drop variation with dimensionless blockage radius and length (1000 m^3/d).

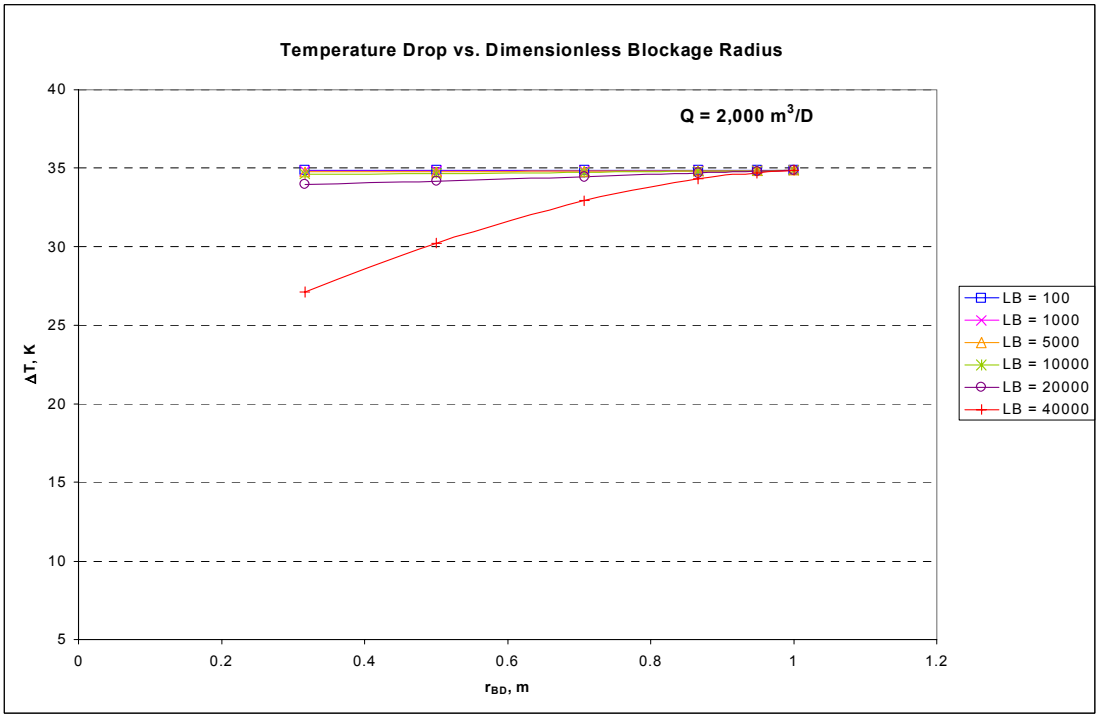

Fig. 15–Temperature drop variation with dimensionless blockage radius and length (2000 m^3/d).

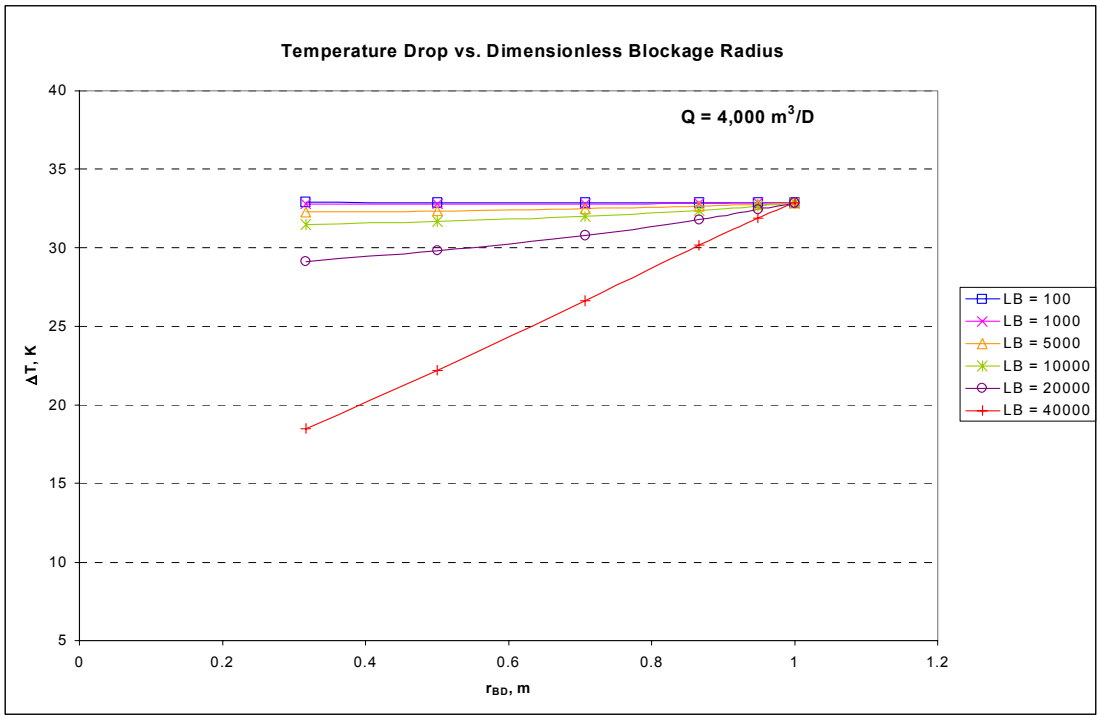

Fig. 16–Temperature drop variation with dimensionless blockage radius and length (4000 m^3/d).

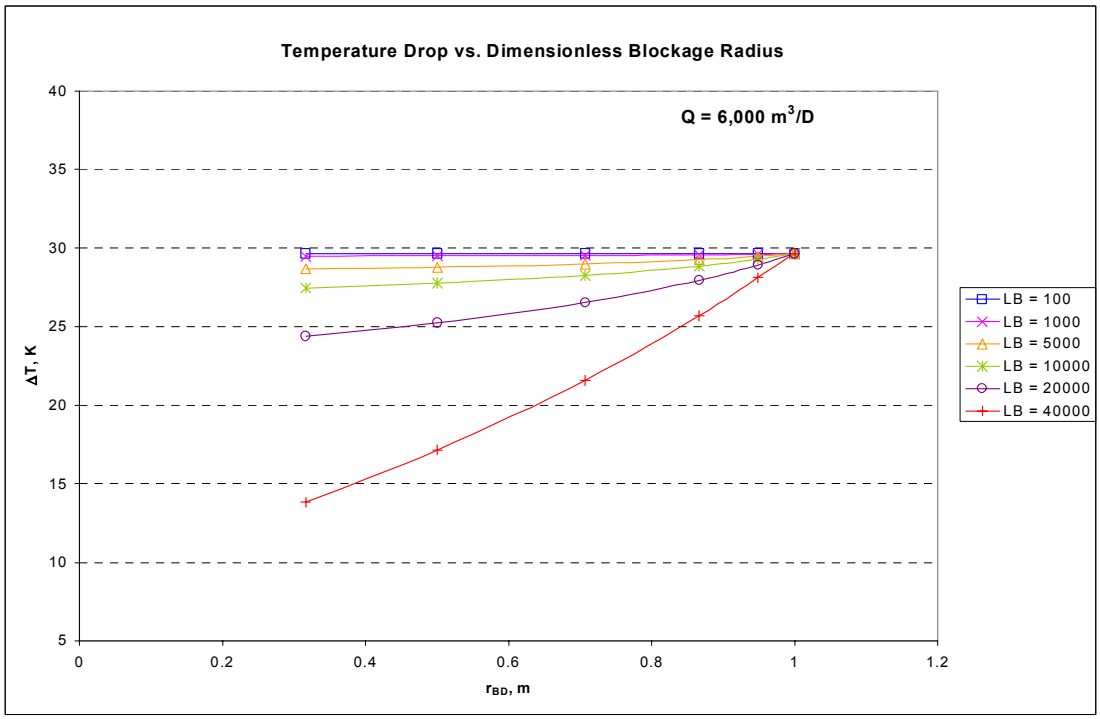

Fig. 17–Temperature drop variation with dimensionless blockage radius and length (6000 m^3/d).

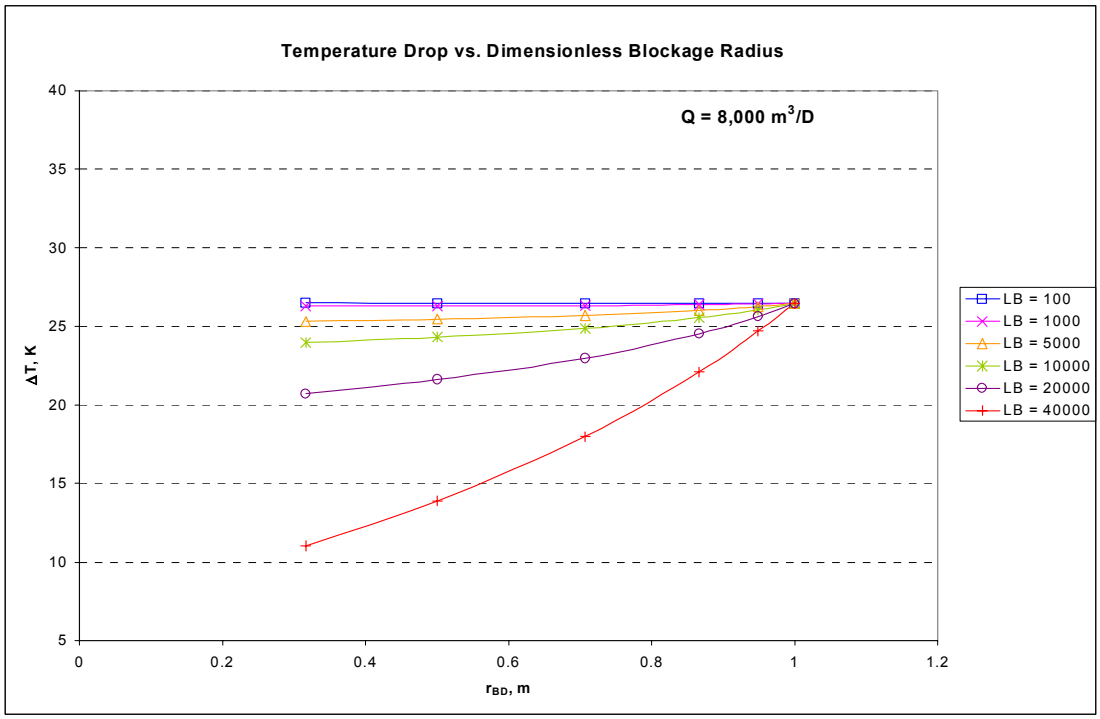

Fig. 18–Temperature drop variation with dimensionless blockage radius and length (8000 m^3/d).

Discussion

The same insulating effect of the wax layer from the fully-blocked pipeline appears for the partially blocked pipeline; the greater the wax length, the lower the temperature drop from inlet to outlet, hence the greater the insulation. Also, the greater the flow rate, the less the temperature drop. At higher flow rates, the greater amount of fluid volume per unit pipe volume provides a greater surface area and heat capacity. The insulating effect observed at higher flow rates has less to do with the deposited wax and more to do with the greater heat content of the fluid.

At low flow rates and for 'short' blockages (0-20,000m), the effect of dimensionless blockage radius, in other words, the cross-sectional area available for flow, on temperature drop cannot be detected. Only extremely long blockages (40,000 m) show a variation in temperature drop with blockage radius. As flow rate increases, the effect of blockage radius on temperature drop for shorter blockages becomes more apparent.

THE DIMENSIONLESS HEAT-BALANCE MODEL FOR A PARTIALLY-BLOCKED PIPE

The base relations are summarized below (see Appendix E for details of development).

1) The Dimensionless Heat-Balance Model for a Partially-Blocked Pipe

$$T_D = \left[\exp\left(-\frac{2\pi L_p}{Q_{\text{flow}} \rho C_p} F_{TB}\right) - 1 \right] + \frac{T_{mi}}{T_{amb}} \left[1 - \exp\left(-\frac{2\pi L_p}{Q_{\text{flow}} \rho C_p} F_{TB}\right) \right] \quad \text{..... (47)}$$

2) The Dimensionless Temperature-Based Blockage Factor (F_{TB})

$$F_{TB} = \left[\frac{L_{BD}}{\frac{1}{h_i r_i r_{BD}} + \frac{1}{k_w} \ln \frac{1}{r_{BD}} + \frac{1}{k_p} \ln \frac{r_o}{r_i} + \frac{1}{h_o r_o}} + \frac{1}{\frac{1}{h_i r_i} + \frac{1}{k_p} \ln \frac{r_o}{r_i} + \frac{1}{h_o r_o}} - \frac{L_{BD}}{\frac{1}{h_i r_i} + \frac{1}{k_p} \ln \frac{r_o}{r_i} + \frac{1}{h_o r_o}} \right] \quad \text{(48)}$$

The dimensionless temperature drop factor (F_{TB}) also called the dimensionless temperature-based blockage factor defined in Eq. 48 has three unknowns: r_{BD}, L_{BD} and T_D. Two of these unknowns must be determined from the mass- and momentum-balance equations or experimentally for Eq. 48 to be useful. An example of the usefulness of F_{TB} is shown by a graphical solution of the heat- and momentum-balance models for an arbitrary case in **Fig. 19**. Graphical plots of equations 47 and 48 for certain values of flow rate and blockage radii are also presented in **Figs. 20 through 25**.

GRAPHICAL SOLUTION OF HEAT- AND VOLUME-BALANCE MODELS

Suppose we consider an average flow rate of 8000 m^3/d of crude oil with properties as summarized in Table 2 flowing through the same North Sea pipeline described in Table 1. If F_{VB} is determined to be 0.75 from volumetric tests and F_{TB} is calculated as 0.2 from Eq. 48 using temperature measurements and fluid properties, the graphical solution of the volume-balance and heat-balance equations is shown in Fig. 19. There is a unique solution of blockage parameters that satisfy both models; they are L_B = 13,760m and D_B = 0.1672m (equivalent to 77% cross-sectional blockage).

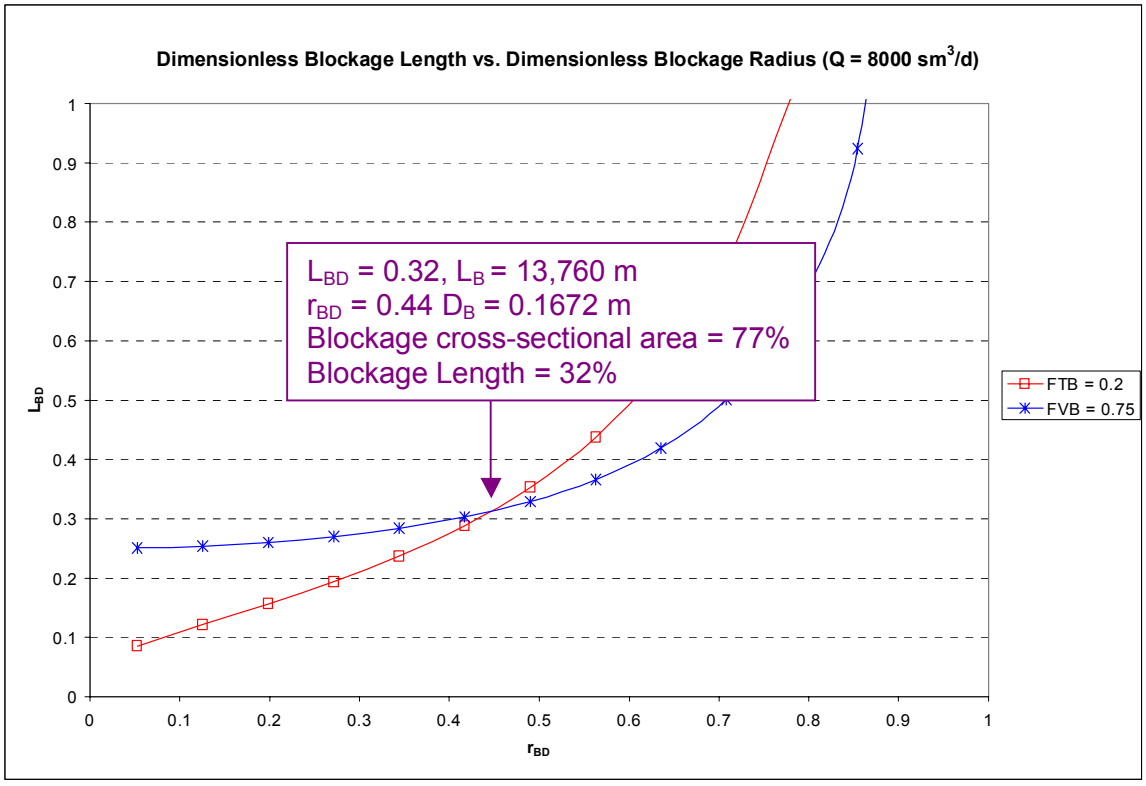

Fig. 19–Graphical solution of heat- and volume-balance models for blockage characterization of an arbitrary case.

DIMENSIONLESS TEMPERATURE DROP BLOCKAGE MAPS

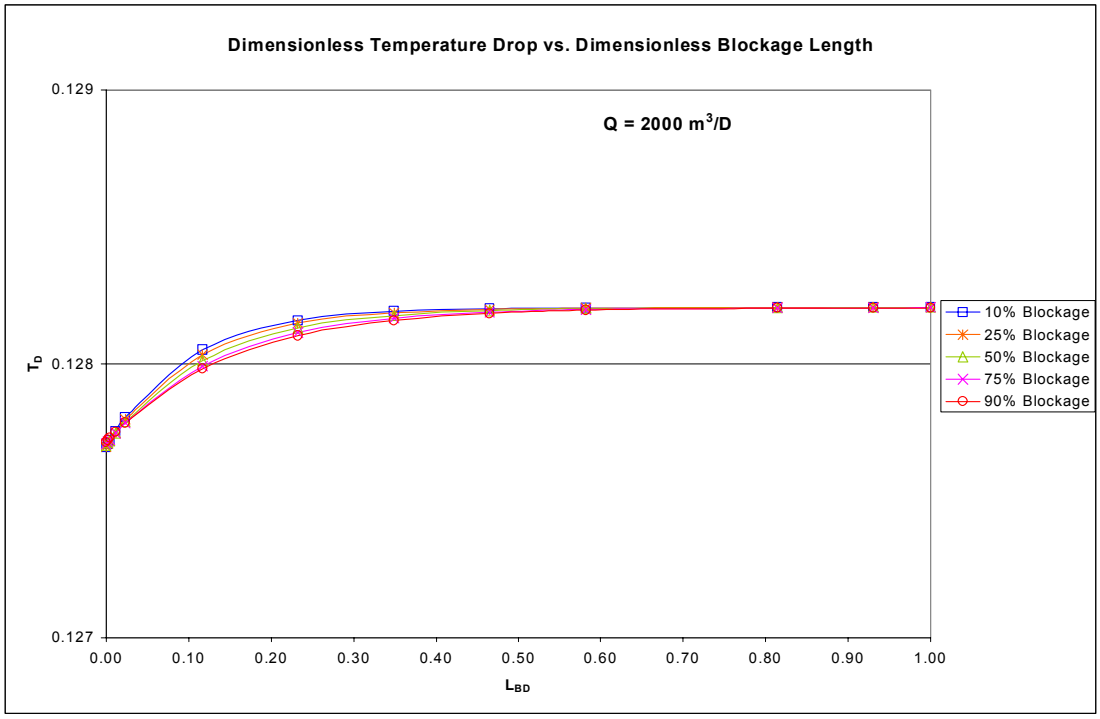

Fig. 20–Dimensionless temperature drop blockage map (2000 m^3/d).

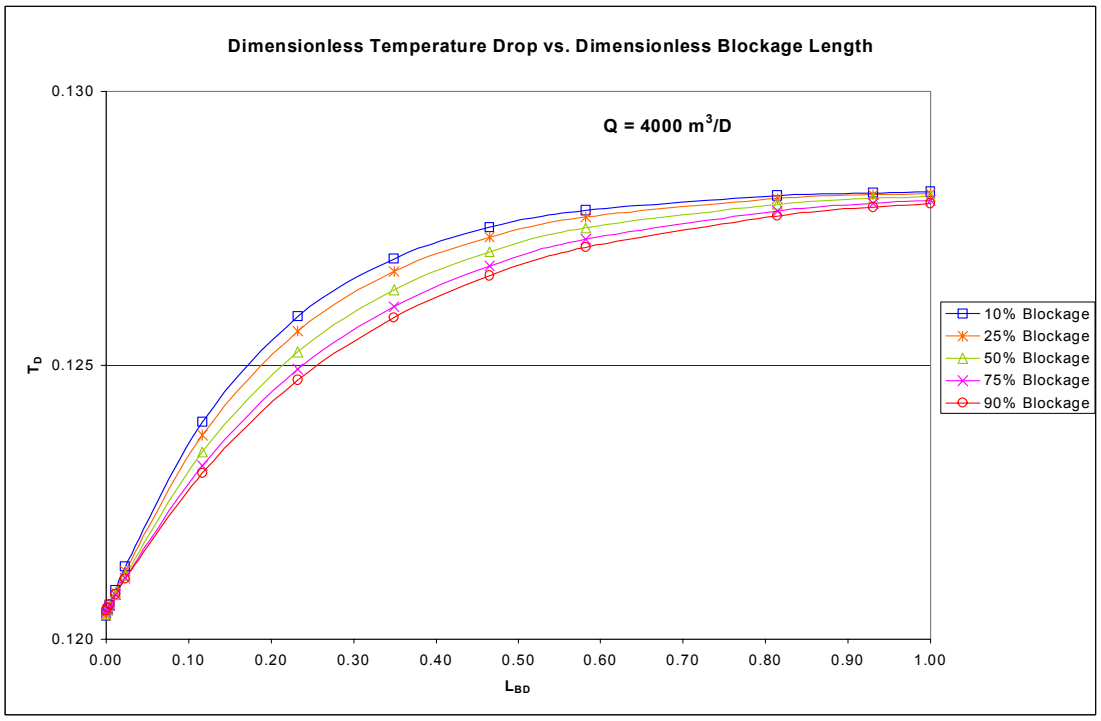

Fig. 21–Dimensionless temperature drop blockage map (4000m^3/d).

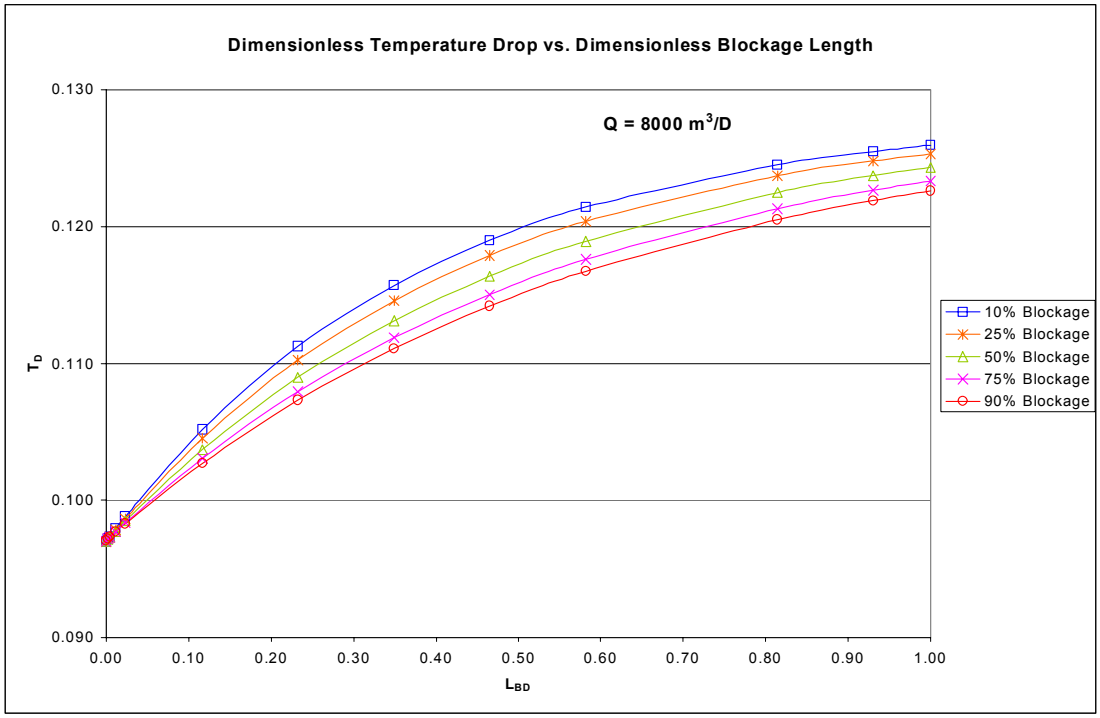

Fig. 22–Dimensionless temperature drop blockage map (8000 m^3/d).

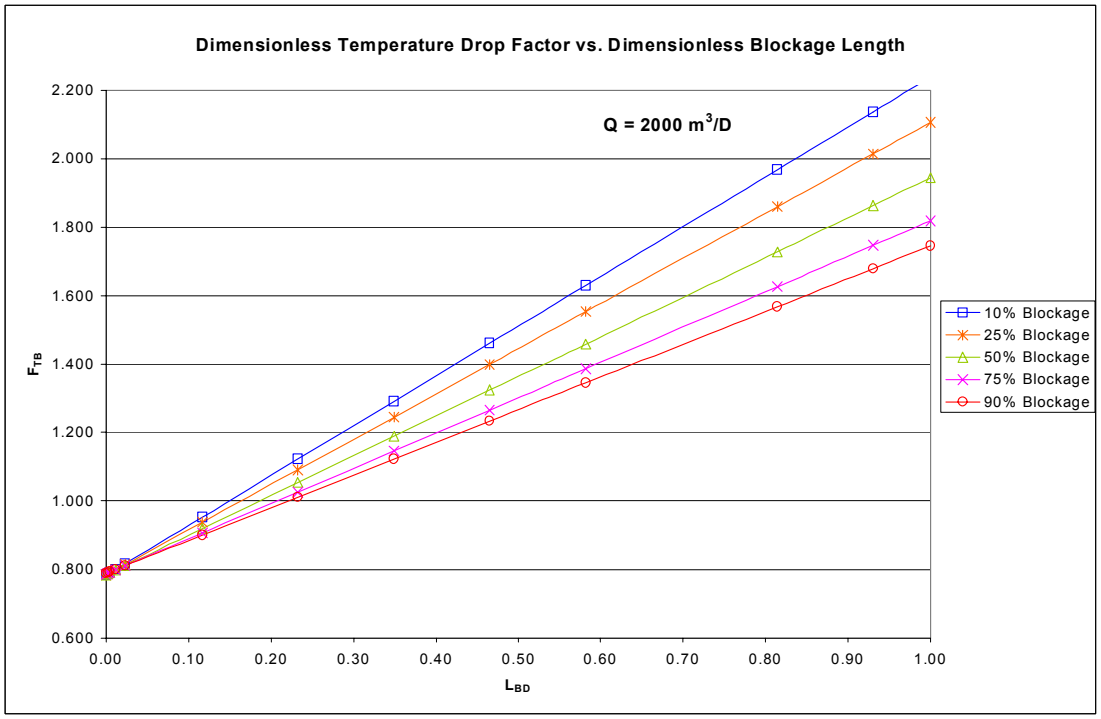

Fig. 23–Dimensionless temperature drop factor blockage map (2000 m^3/d).

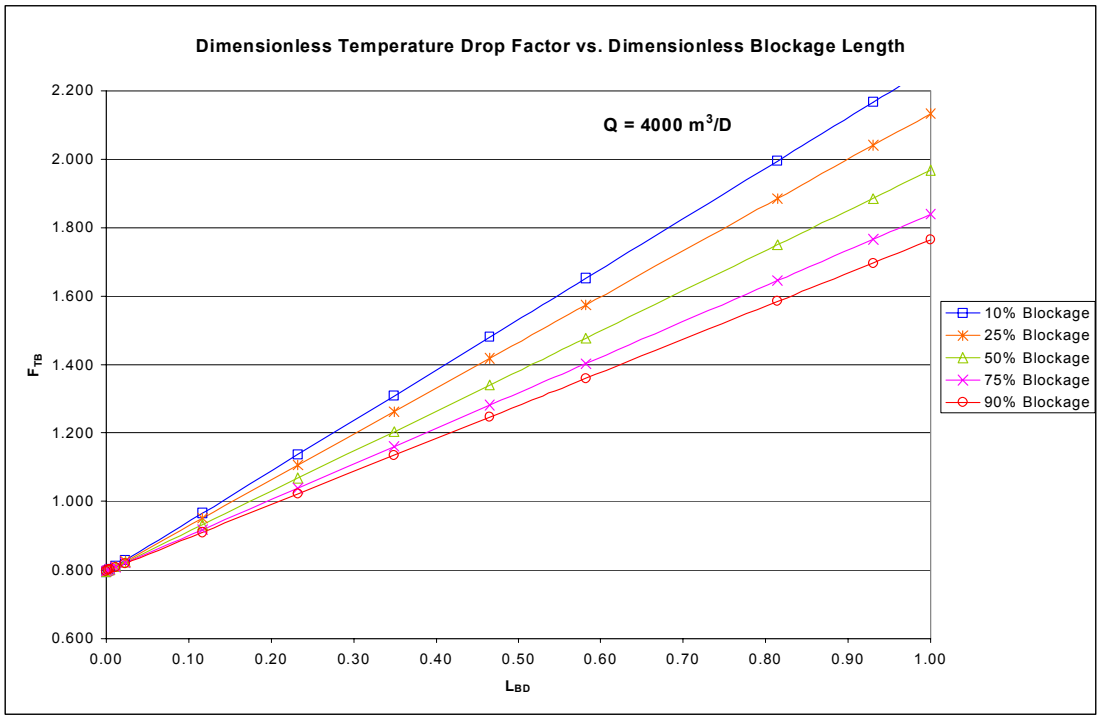

Fig. 24– Dimensionless temperature drop factor blockage map (4000 m^3/d).

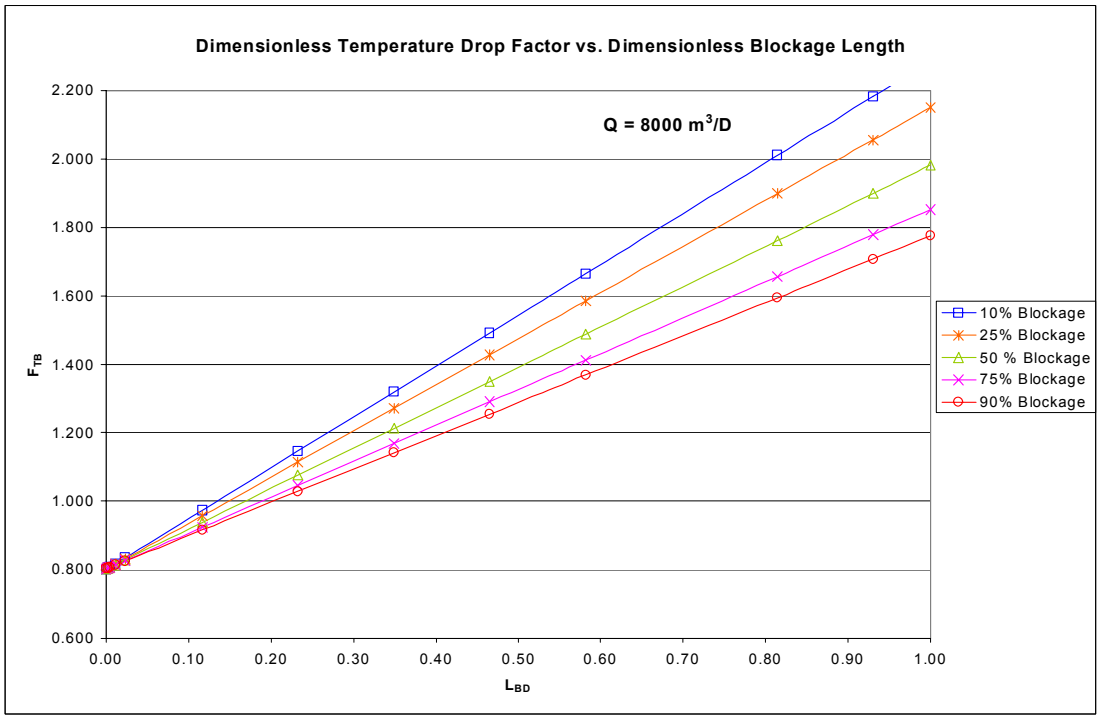

Fig. 25–Dimensionless temperature drop factor blockage map (8000 m^3/d).

Discussion

The usefulness of these blockage maps comes in when armed with either the dimensionless blockage radius r_{BD} or dimensionless blockage length L_{BD} from other approaches and the average flow rate of the operational pipeline. This is illustrated in Fig. 19, which shows the graphical solution of F_{TB} and F_{VB} to determine the blockage parameters; L_B and r_B.

The dimensionless temperature drop maps show increased sensitivity of T_D to L_{BD} as flow rate increases while the dimensionless temperature drop factor maps F_{TB} essentially appear the same for all flow rates but have subtle differences in the actual values used to generate the plots.

Note:

$$r_{BD} = \sqrt{1 - \left(\frac{B}{100}\right)}$$

where B = Blockage, %.

UNCERTAINTY IN BLOCKAGE CHARACTERIZATION

There is some uncertainty associated with the temperature measurements and all the other measured physical properties of the system. The uncertainty is related to the detectable blockage characteristics such as blockage length and diameter and therefore requires some investigation.

An arbitrary case of F_{TB} = 2.2 and F_{VB} = 0.75 is chosen. **Fig. 26** is a blockage map depicting the effect of uncertainty on temperature-based (F_{TB}) and volume-based factors (F_{VB}). **Figs. 27** through **29** depict the variation in dimensionless blockage length with dimensionless blockage radius as well as the graphical solution of blockage parameters for the cases of a 10%, 25% and 50% uncertainty in F_{TB} and F_{VB} for the case chosen.

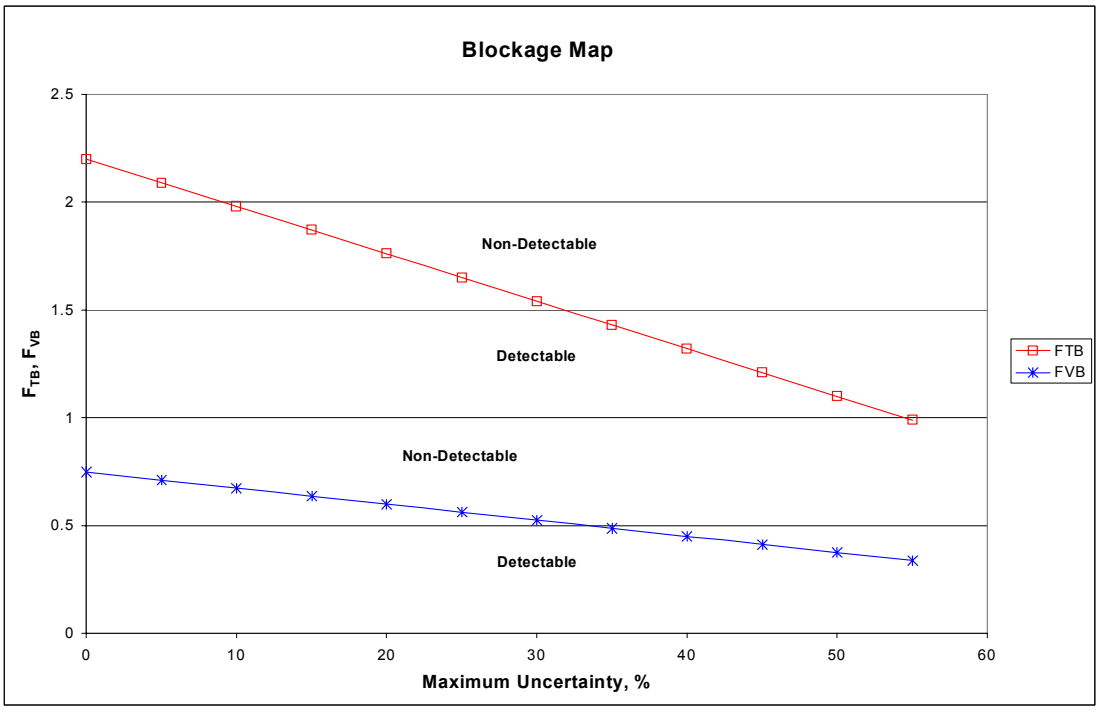

Fig. 26–Blockage map showing detectable blockage regions.

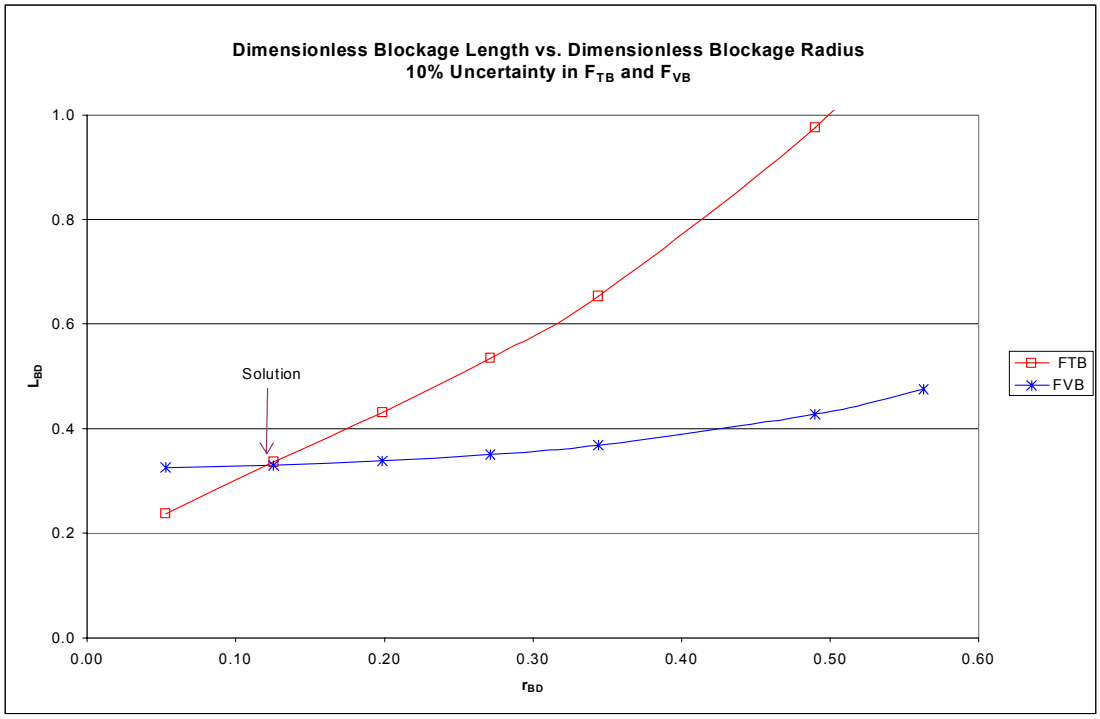

Fig. 27–Graphical solution of heat- and volume-balance models for blockage characterization incorporating 10% uncertainty.

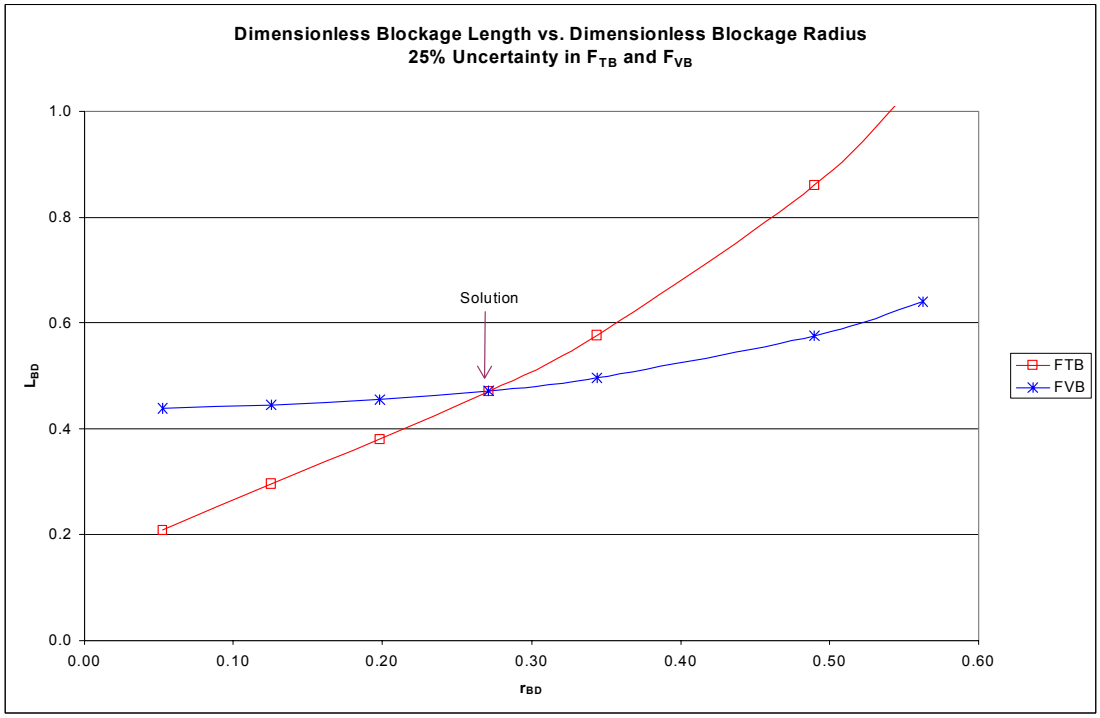

Fig. 28–Graphical solution of heat- and volume-balance models for blockage characterization incorporating 25% uncertainty.

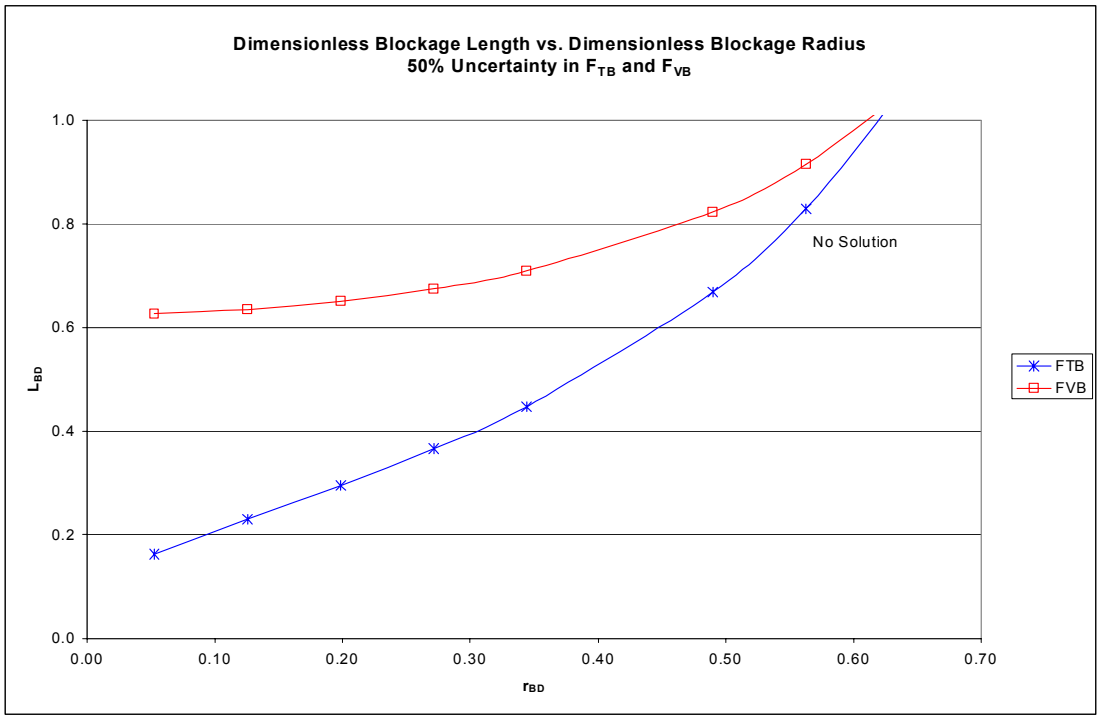

Fig. 29–Graphical plot of heat- and volume-balance models for blockage characterization incorporating 50% uncertainty. (No solution)

Discussion

The blockage map in Fig. 26 shows the ranges of F_{TB} and F_{VB} for an arbitrary case where the blockage can be detected assuming some level of uncertainty in the measurements of the physical properties of the system. Figs. 27 through 29 show that the possibility of characterizing a blockage by obtaining solutions of blockage parameters decreases with increasing uncertainty.

MODEL VERIFICATION

The model requires experimental verification, but because no facilities were available for this, the verification was restricted to the use of PIPESIM, a pipeline simulation software with inherent limitations that require that caution be exercised when making comparisons between its results and those from the model developed.

PIPESIM VERIFICATION

The pipeline was built with a source supplying the inlet temperature and pressure at one end and a boundary node at the other end, which provides the unknown outlet temperature used to calculate the temperature drop across the pipe.

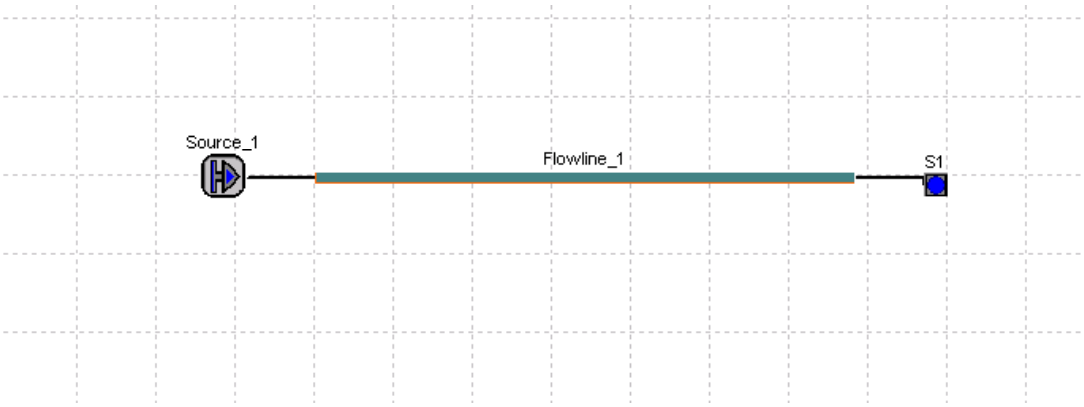

Fig. 30–PIPESIM network built for comparison of results with heat model.

PIPESIM INPUT DATA

The input data into PIPESIM is summarized in **Tables 3 and 4**.

Table 3–Pipeline Input Data to PIPESIM

Inlet Pressure	5000 psia
Inlet Temperature	35 ^{o}C
Pipe length	43 km
Inner Diameter	0.38 m
Outer Diameter	0.4054 m
Ambient Temperature	0 ^{o}C
Pipe Thermal Conductivity	43.25 W/mK

Table 4–Fluid Input Data to PIPESIM

GOR	300 scf/STB
API	30
Wax Thermal Conductivity	0.25 W/mK

The wax deposition module in PIPESIM, a separate module requiring BP or Shell security is unavailable for unlicensed users. This problem was circumvented by using the "detailed pipeline description" to model the wax layer as a coating of insulation, but with the thermal conductivity of the wax.

GRAPHICAL COMPARISON OF PIPESIM AND MODEL PREDICTIONS

The wax thickness was varied and the simulation was run for various inlet-pressure and flow-rate combinations. The software was unable to simulate certain combinations of blockage and flow conditions, most likely because the pressure was insufficient for the prescribed flow rate. The results are presented as **Figs. 31 through 53**.

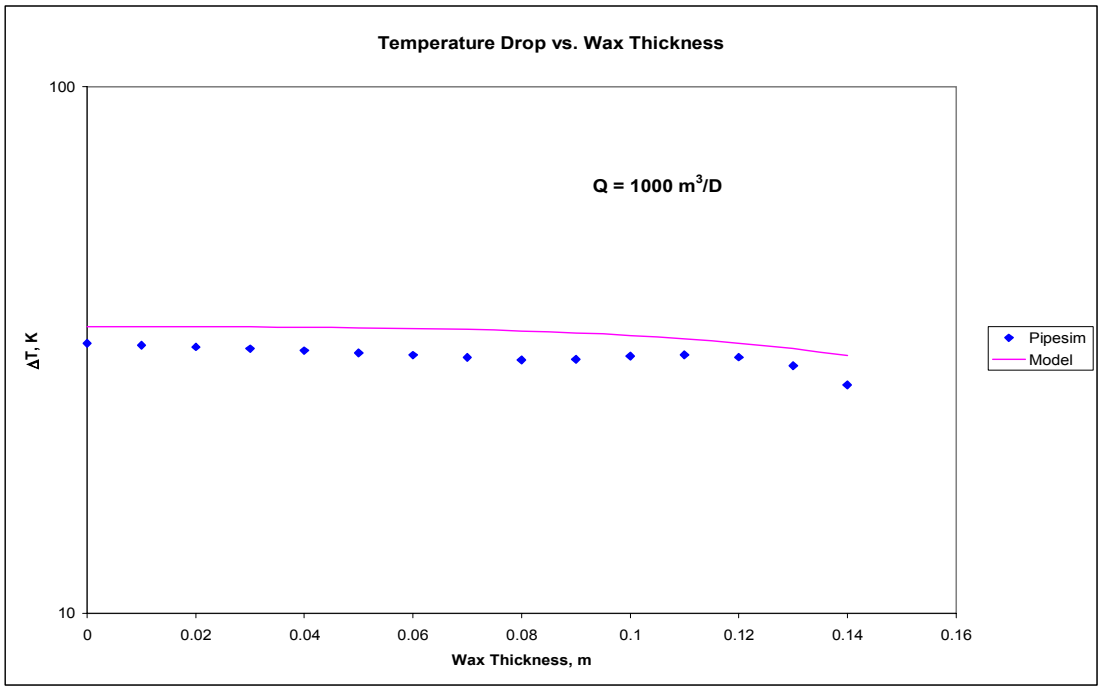

Fig. 31–Comparison of temperature drop variation with wax thickness predicted by PIPESIM and Model – semi log plot (1000 m^3/d).

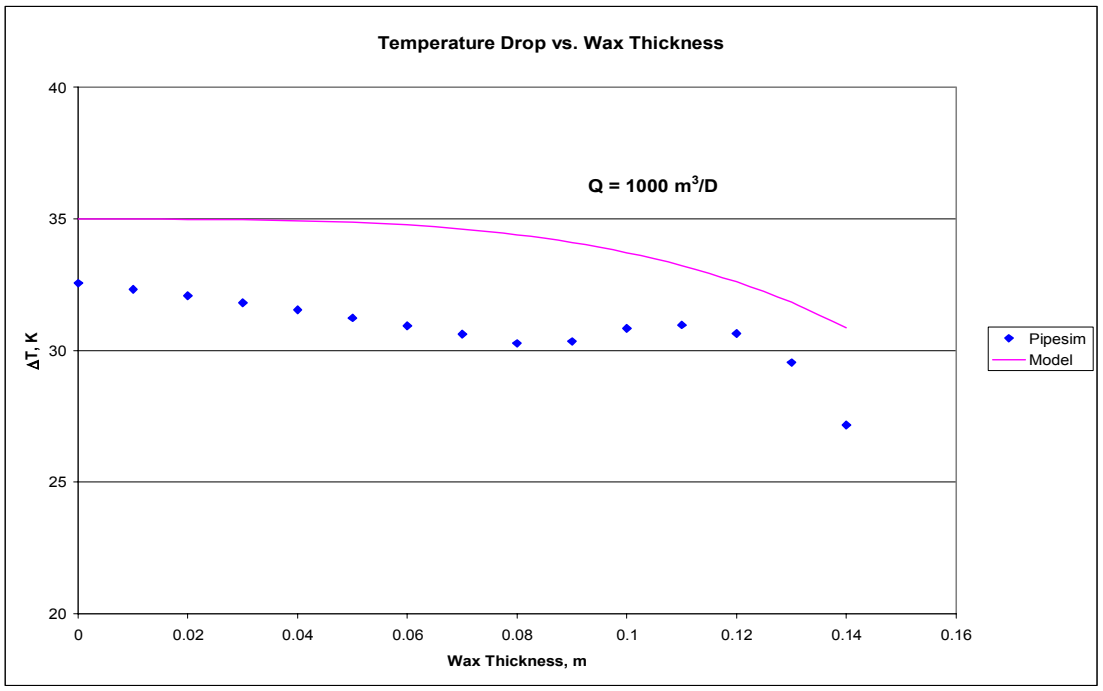

Fig. 32–Comparison of temperature drop variation with wax thickness predicted by PIPESIM and Model – Cartesian plot (1000 m^3/d).

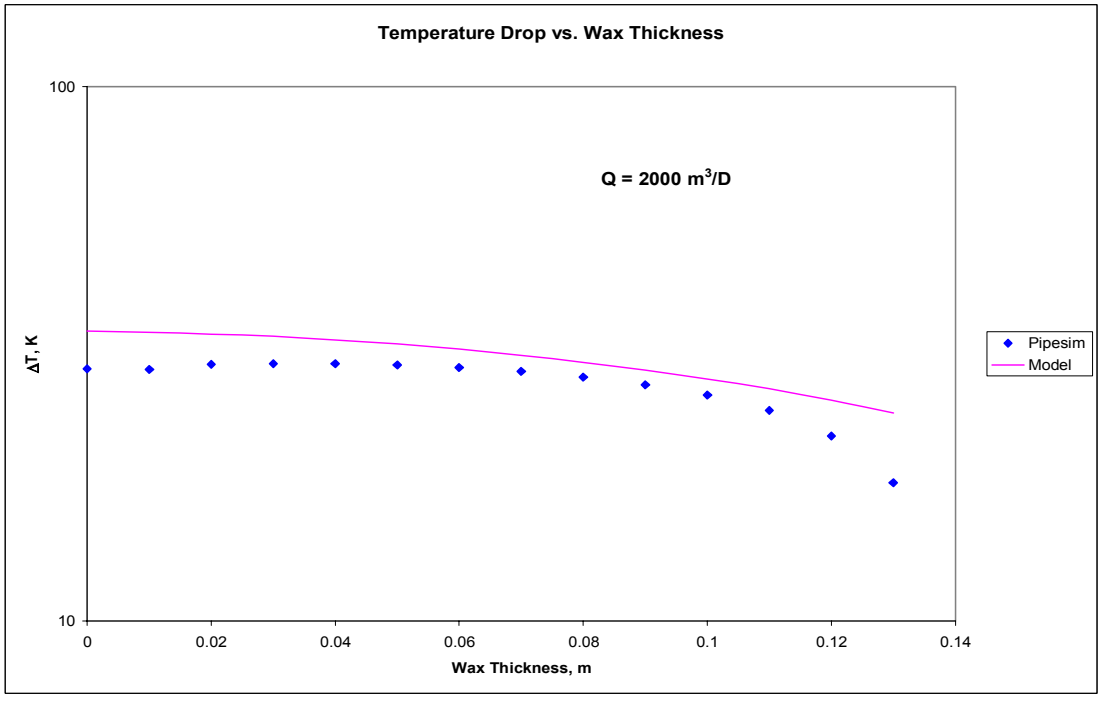

Fig. 33–Comparison of temperature drop variation with wax thickness predicted by PIPESIM and Model – semi log plot (2000 m^3/d).

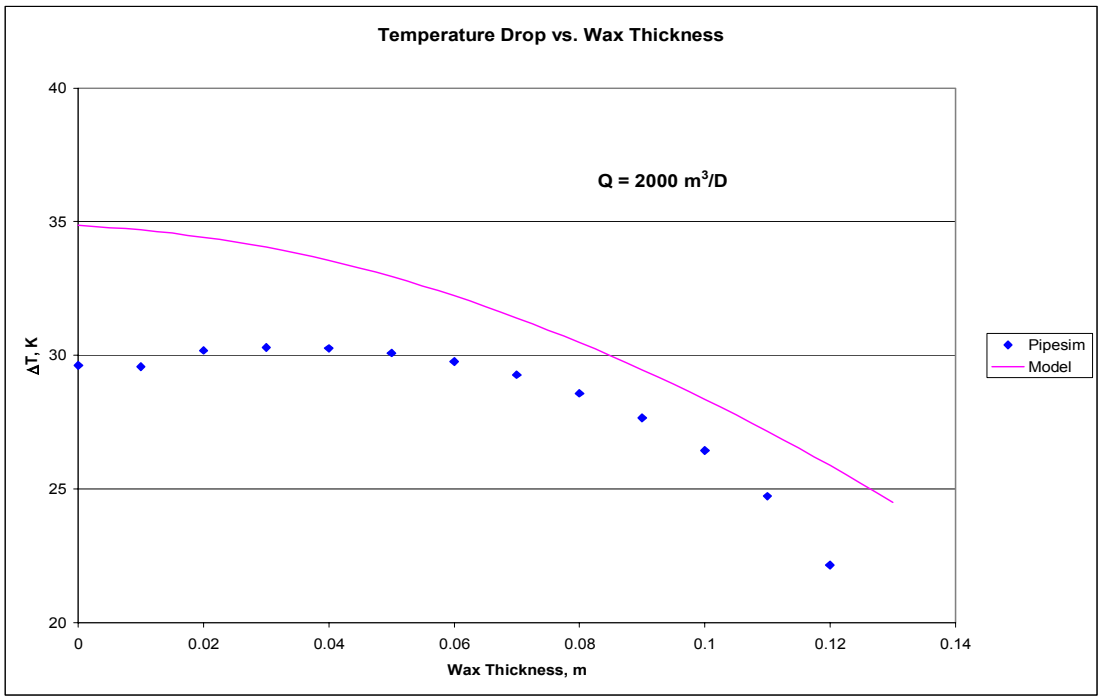

Fig. 34–Comparison of temperature drop variation with wax thickness predicted by PIPESIM and Model – Cartesian plot (2000 m^3/d).

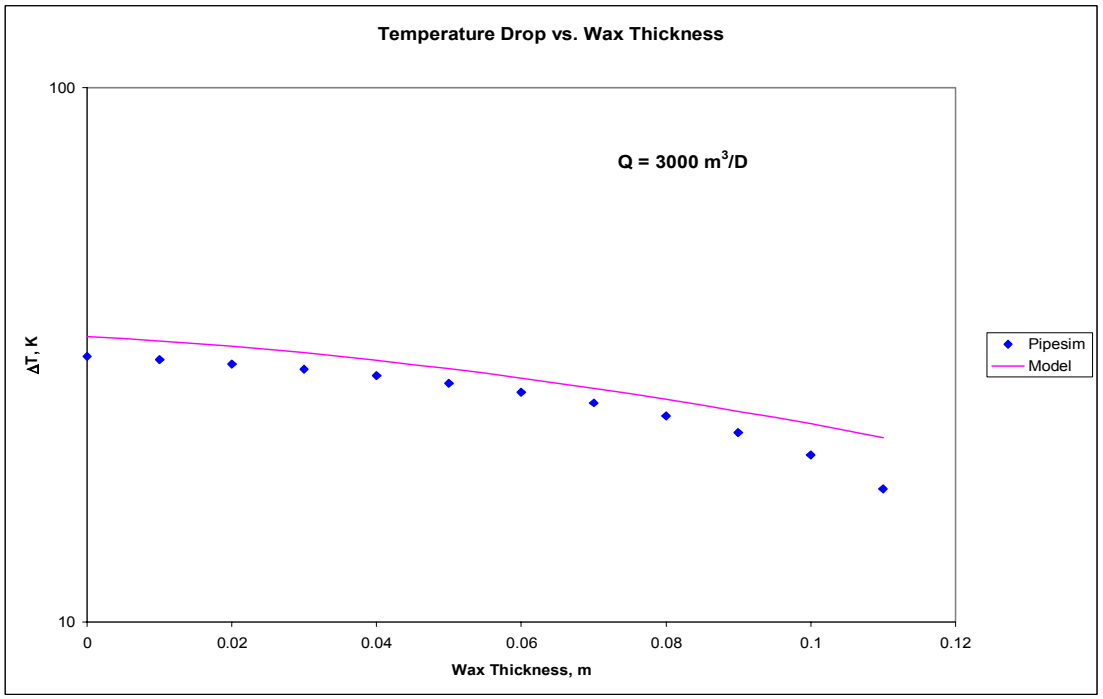

Fig. 35–Comparison of temperature drop variation with wax thickness predicted by PIPESIM and Model – semi log plot (3000 m^3/d).

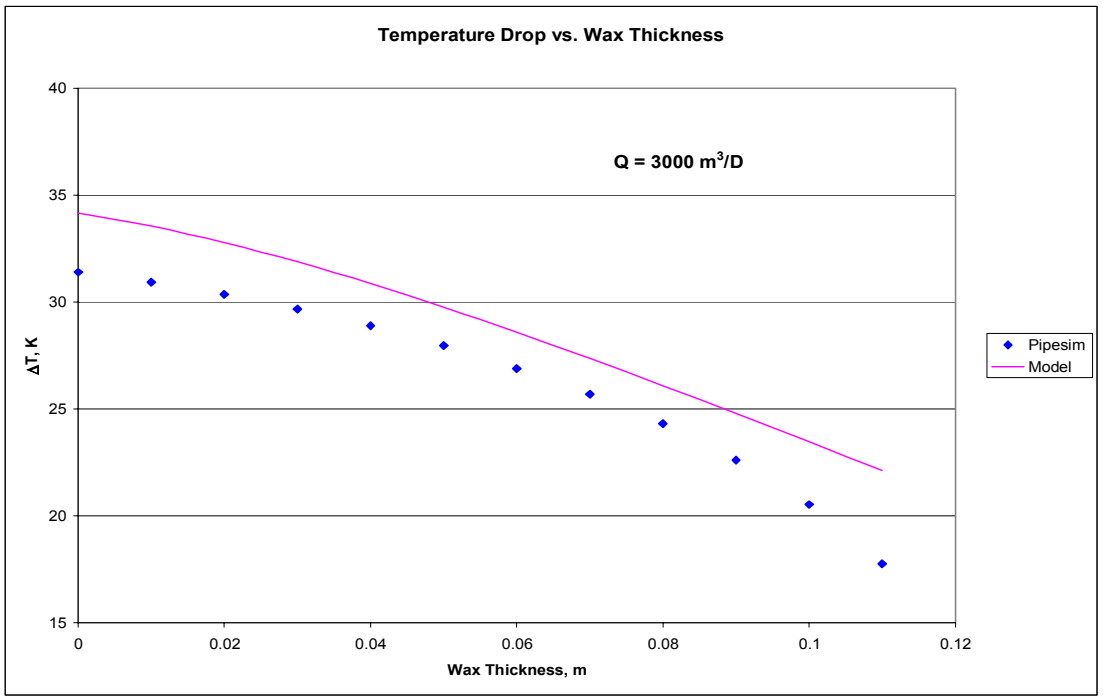

Fig. 36–Comparison of temperature drop variation with wax thickness predicted by PIPESIM and Model – Cartesian plot (3000 m^3/d).

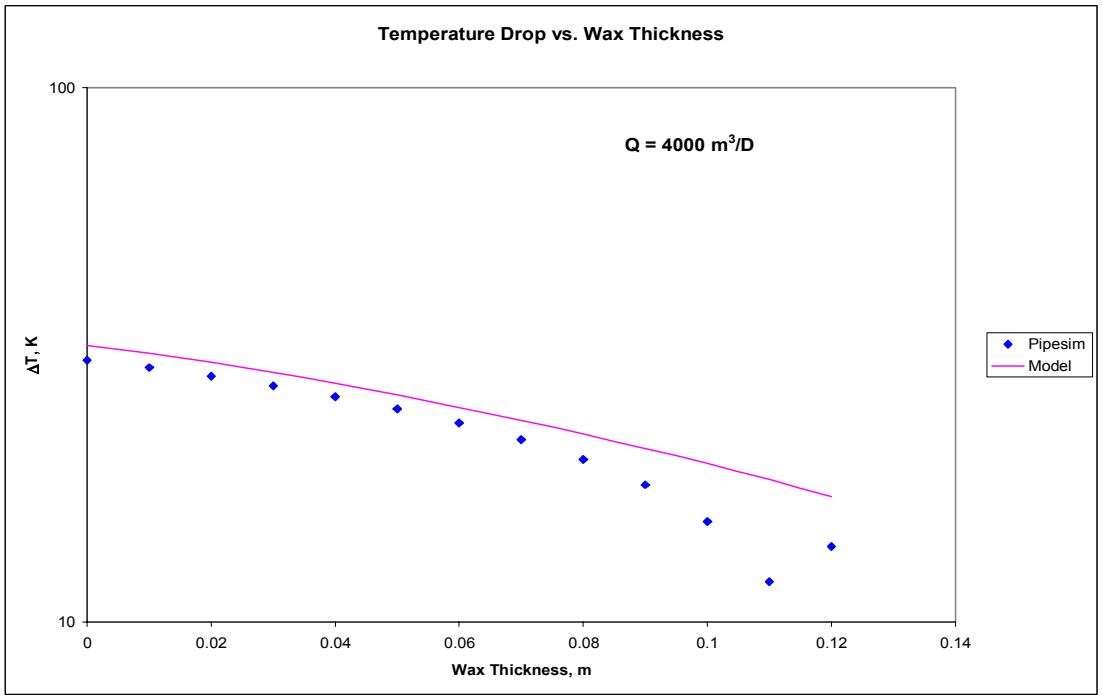

Fig. 37–Comparison of temperature drop variation with wax thickness predicted by PIPESIM and Model – semi log plot (4000 m^3/d)

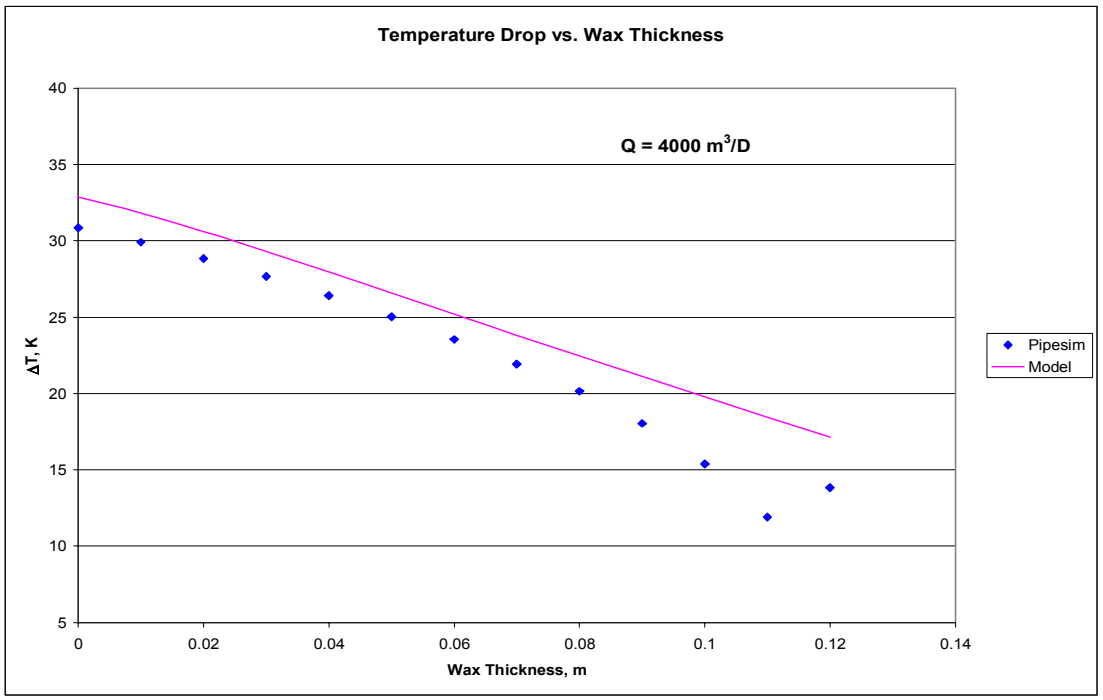

Fig. 38–Comparison of temperature drop variation with wax thickness predicted by PIPESIM and Model – Cartesian plot (4000 m^3/d).

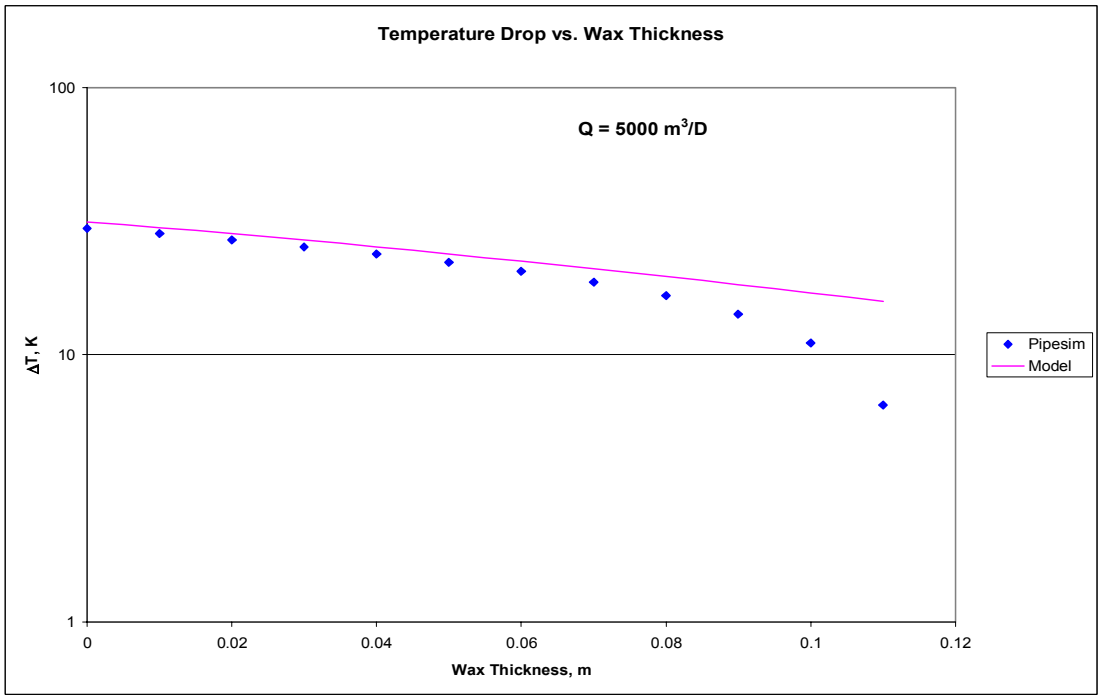

Fig. 39–Comparison of temperature drop variation with wax thickness predicted by PIPESIM and Model –semi log plot (5000 m^3/d)

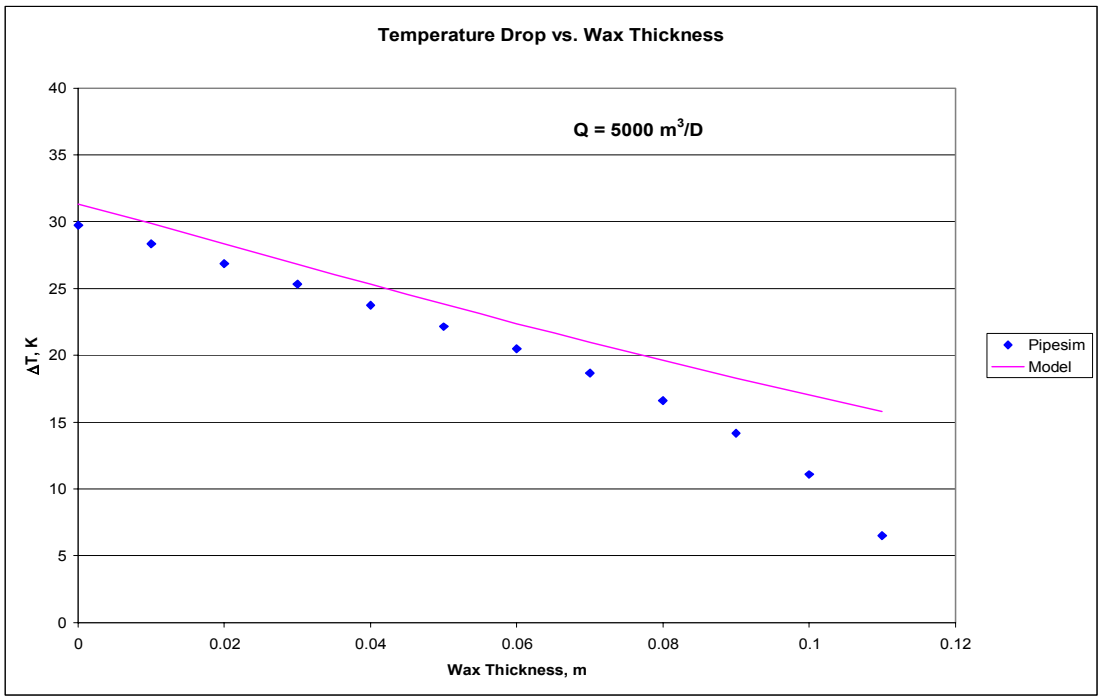

Fig. 40–Comparison of temperature drop variation with wax thickness predicted by PIPESIM and Model – Cartesian plot (5000 m^3/d).

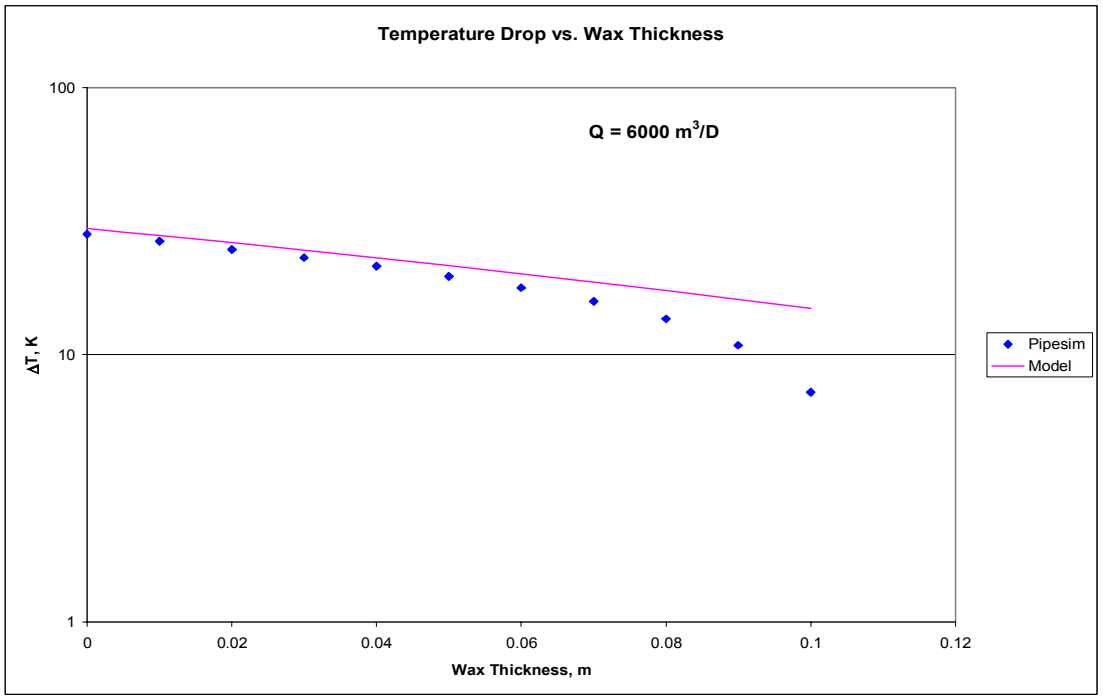

Fig. 41–Comparison of temperature drop variation with wax thickness predicted by PIPESIM and Model – semi log plot (6000 m^3/d).

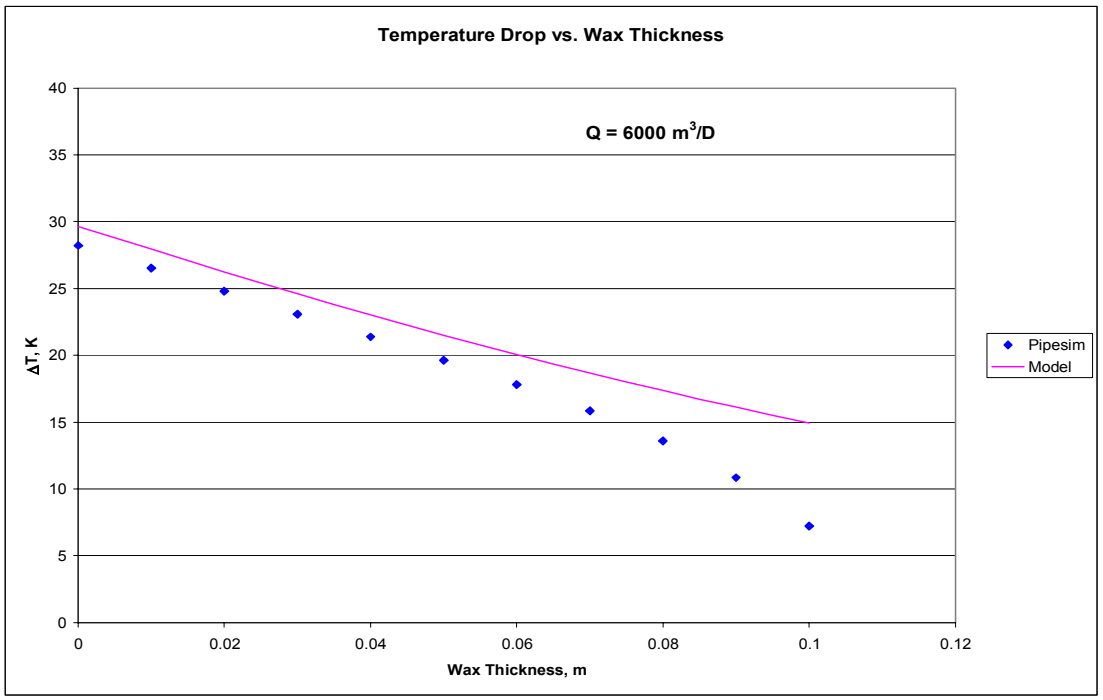

Fig. 42–Comparison of temperature drop variation with wax thickness predicted by PIPESIM and Model – Cartesian plot (6000 m^3/d).

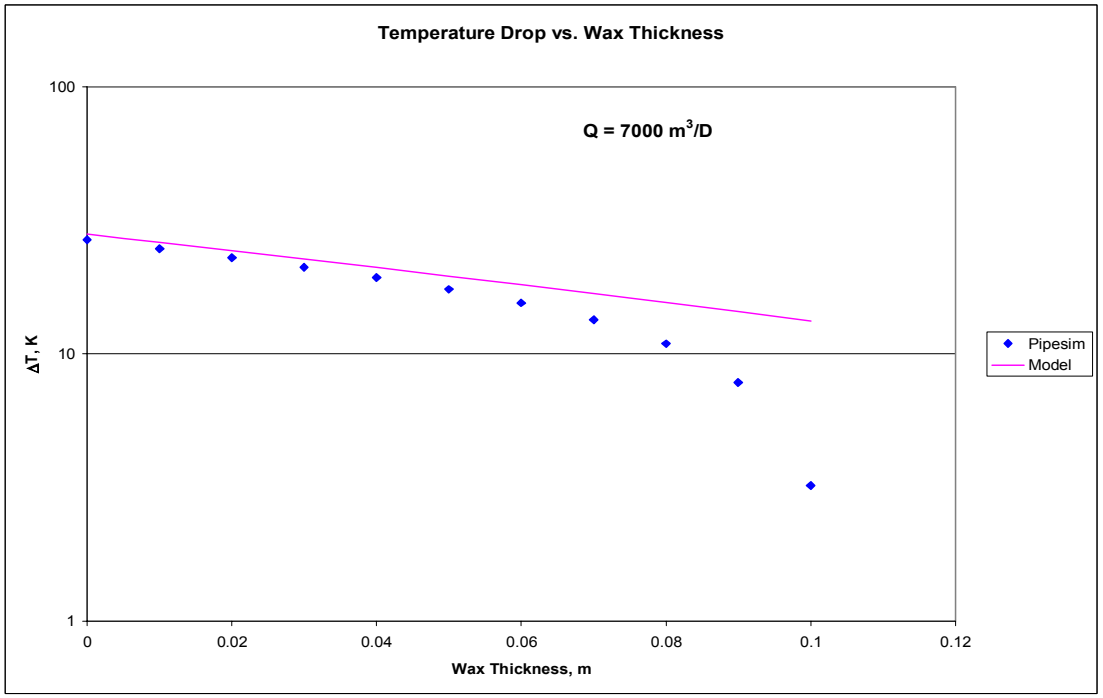

Fig. 43–Comparison of temperature drop variation with wax thickness predicted by PIPESIM and Model – semi log plot (7000 m^3/d).

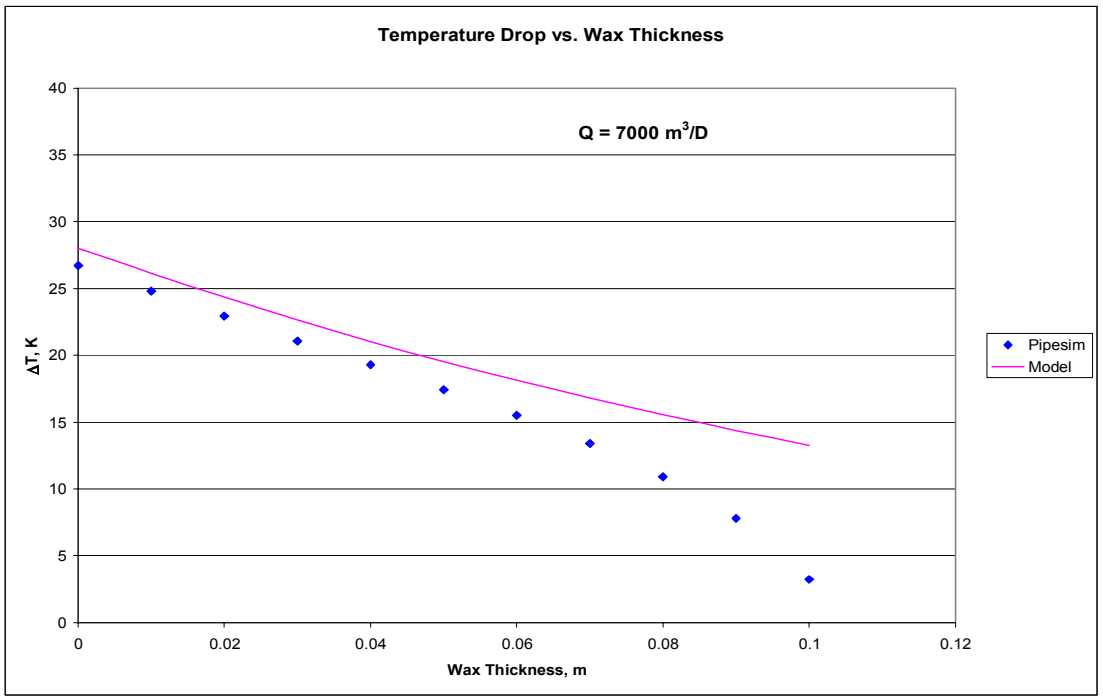

Fig. 44–Comparison of temperature drop variation with wax thickness predicted by PIPESIM and Model – Cartesian plot (7000 m^3/d).

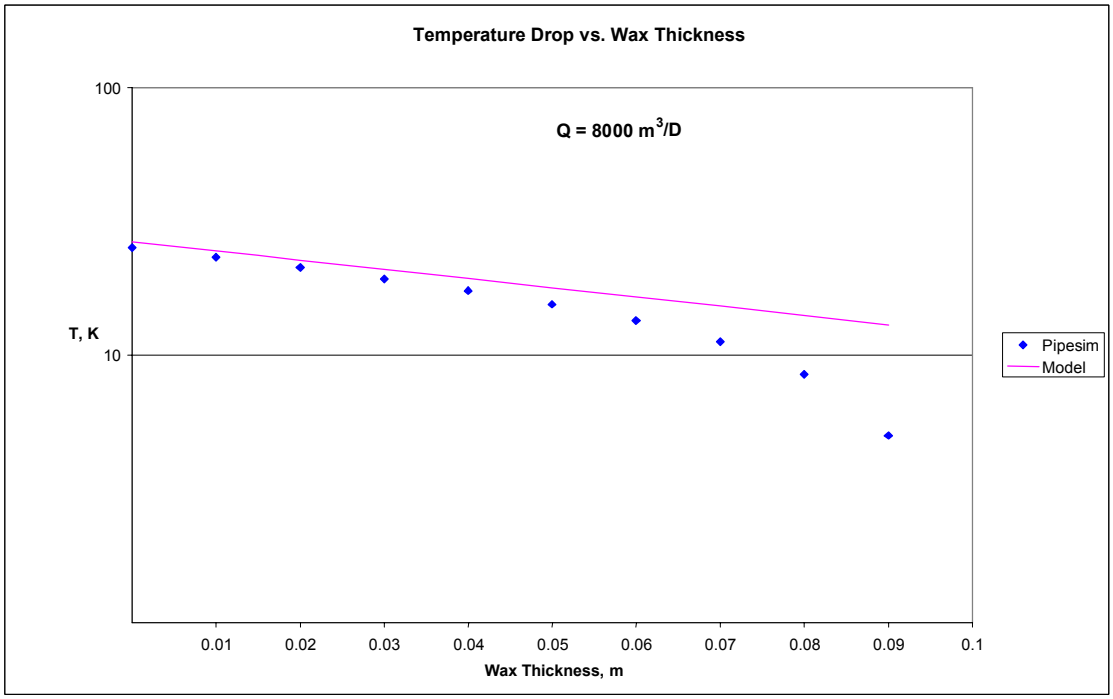

Fig. 45–Comparison of temperature drop variation with wax thickness predicted by PIPESIM and Model – semi log plot (8000 m^3/d).

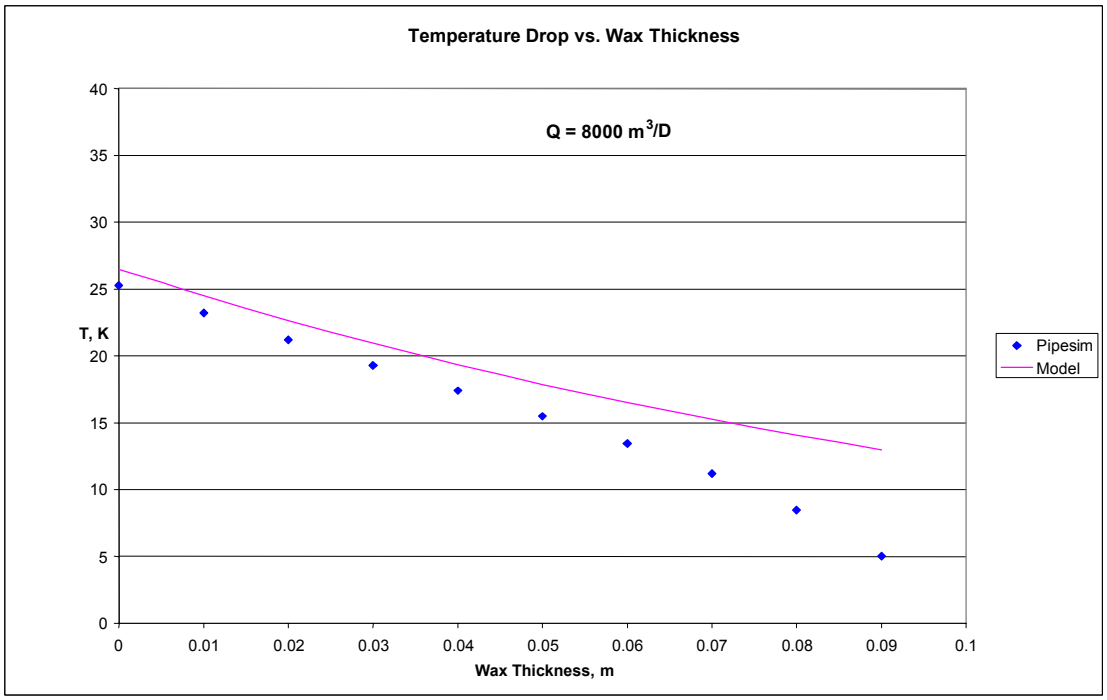

Fig. 46–Comparison of temperature drop variation with wax thickness predicted by PIPESIM and Model – Cartesian plot (8000 m^3/d).

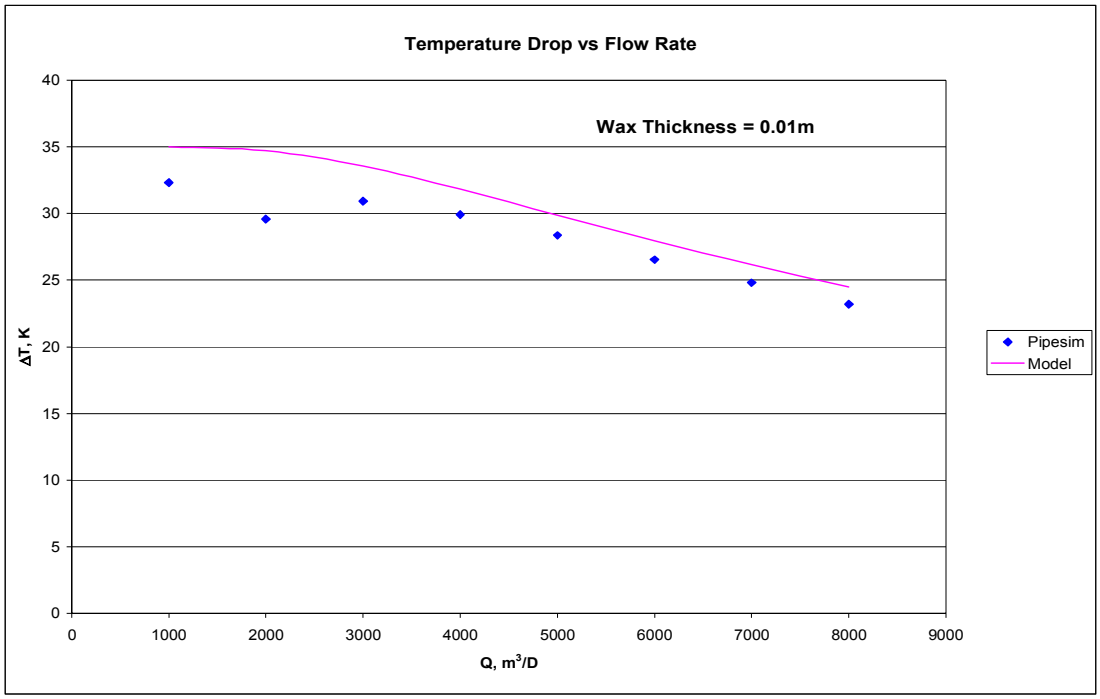

Fig. 47–Comparison of temperature drop variation with flow rate predicted by PIPESIM and Model (Wax Thickness = 0.01 m).

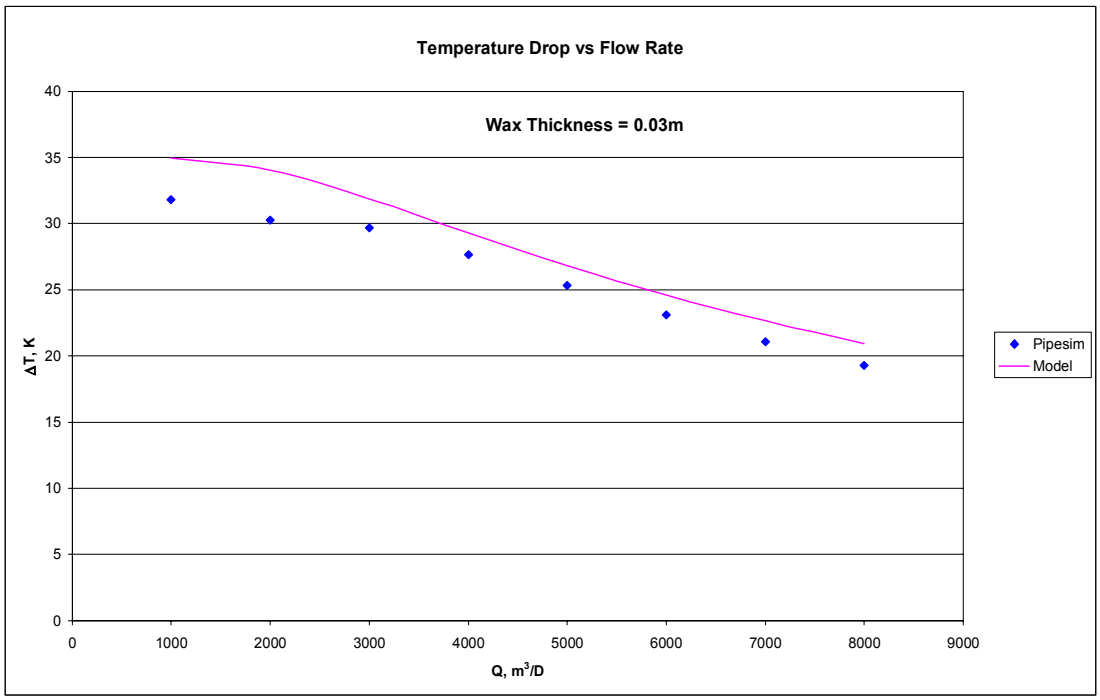

Fig. 48–Comparison of temperature drop variation with flow rate predicted by PIPESIM and Model (Wax Thickness = 0.03 m).

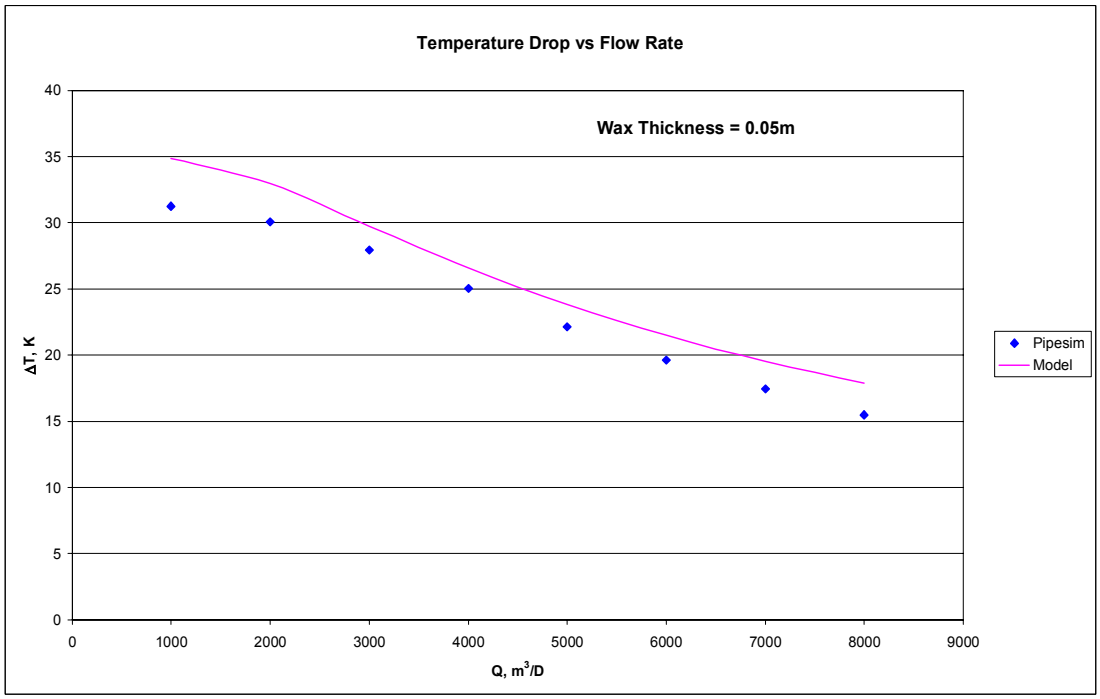

Fig. 49–Comparison of temperature drop variation with flow rate predicted by PIPESIM and Model (Wax Thickness = 0.05 m).

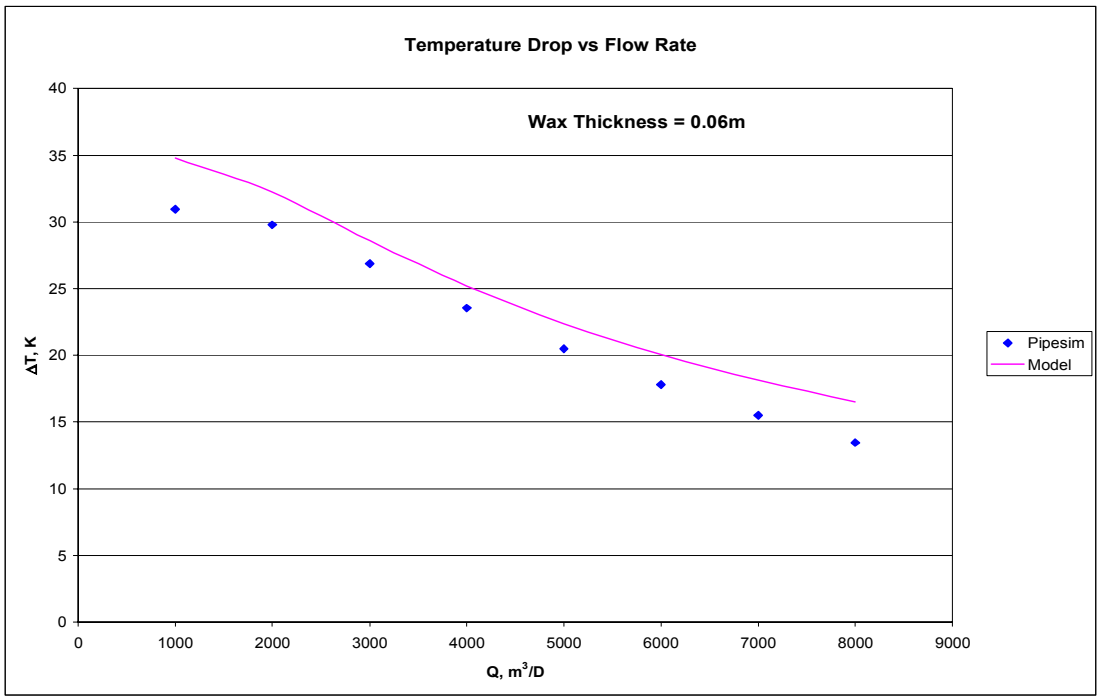

Fig. 50–Comparison of temperature drop variation with flow rate predicted by PIPESIM and Model (Wax Thickness = 0.06 m).

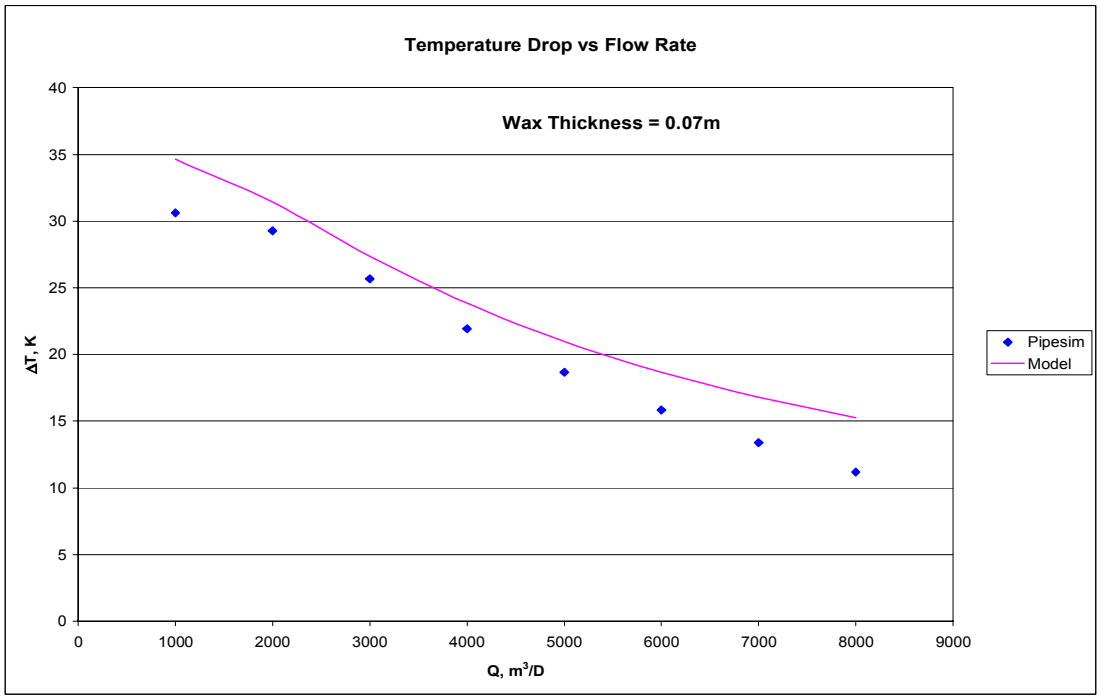

Fig. 51–Comparison of temperature drop variation with flow rate predicted by PIPESIM and Model (Wax Thickness = 0.07 m).

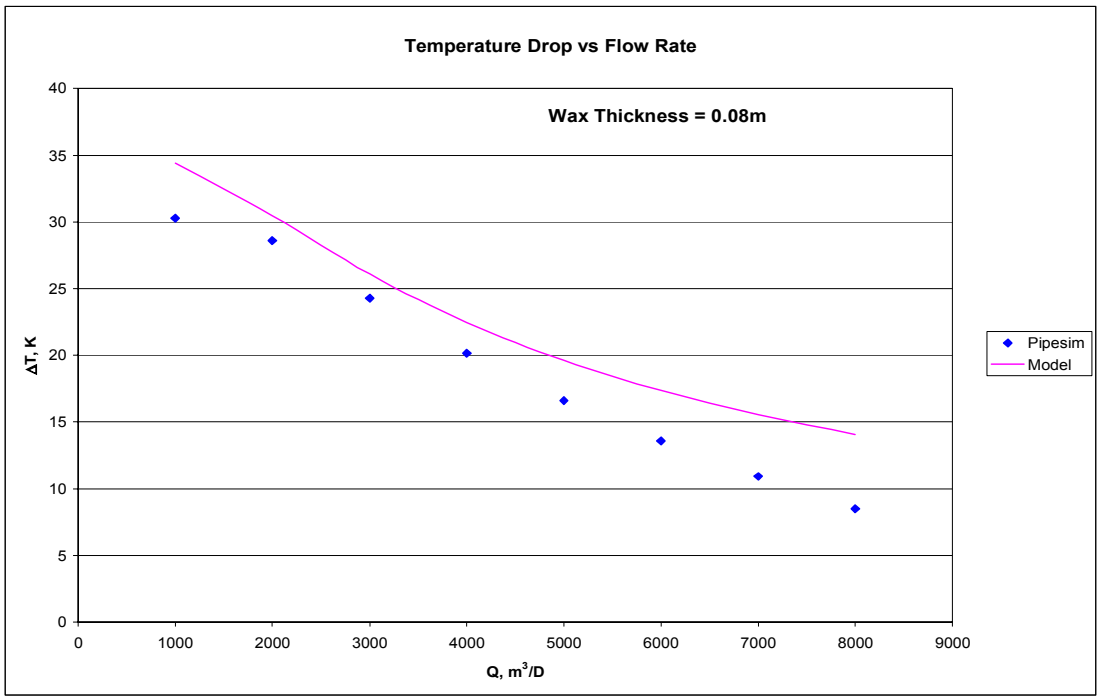

Fig. 52–Comparison of temperature drop variation with flow rate predicted by PIPESIM and Model (Wax Thickness = 0.08 m).

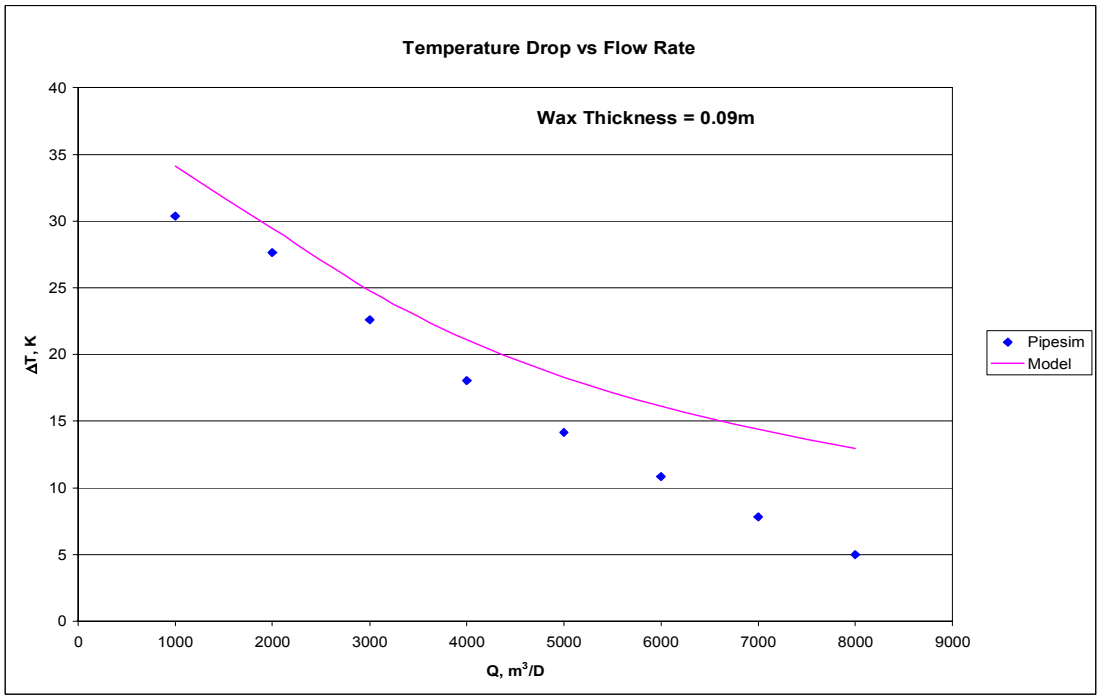

Fig. 53–Comparison of temperature drop variation with flow rate predicted by PIPESIM and Model (Wax Thickness = 0.09 m).

Discussion of Results

Overall, the match between the PIPESIM and model predictions is good. However, for all conditions of wax thickness and flow rate, the actual temperature drop simulated by PIPESIM is consistently lower than the temperature drop predicted by the model. This implies that the model is actually under-predicting the insulating effect of the wax layer.

There are two distinct regions where the match is poor: the first one is at low flow rates and thin layers of wax deposited and the second is at high flow rates and thick wax layers. For the first region, the PIPESIM prediction shows an overall inconsistent trend, which the model fails to match. At very low flow rates, (implying very low thermal masses) and without the benefit of the effect of pressure as modeled by PIPESIM, the model predicts a complete loss of heat energy coming into the pipe. The model does not take into account the effect of inlet pressure; and this, combined with the low thermal mass flowing in a very long pipeline results in a complete loss of heat energy into the system; to the extent that the insulating effect of the wax becomes negligible and the discrepancy between the temperature drop predicted by the model and PIPESIM is much wider in this region. This seems to indicate that for a given pipeline system, there is a minimum thermal heat content input required for accurate comparison of temperature drop predictions.

For the second region, the increasing wax thicknesses imply a reduction in effective cross-sectional area for flow; and this, combined with increasing flow rates results in

increased frictional heating, which the model fails to capture, making it predict higher temperature drops than PIPESIM. The dynamic PIPESIM simulation takes into account parameters such as pressure and friction factor, which are able to model this effect. The model does not incorporate these factors and this may be one of the major causes of the discrepancy between the results at the second extreme condition.

Clearly, there may be regions of flow and blockage conditions for which the model is inapplicable. These regions of inapplicability must be investigated to determine the limits of the model and ensure its robustness. This model might require tuning, like an equation of state, for the unique conditions of the operational pipeline, to improve its ability to accurately reproduce the expected temperature drop for a given layer of deposited wax.

The approach used here of adding the wax layer as a coating may also be a limitation. Investigating the model using an actual wax deposition module that incorporates the mechanisms of wax deposition such as diffusion and shear dispersion would provide simulated results that are more representative of wax deposition conditions in a pipeline, and help assess and improve the accuracy of the model predictions.

CONCLUSIONS

1) The heat model developed here is theoretically consistent. It correctly predicts the insulating effect of wax deposited in a pipeline by relating the thickness of wax deposited to the observed temperature drop, which is consistently lower than the temperature drop that would result if no wax blockage were present.
2) A temperature-based factor (F_{TB}) similar to the volume-based factor (F_{VB}) and friction-based factor (F_{FB}) was developed and correlated to blockage length and effective pipe diameter for a partially blocked pipeline. Dimensionless blockage maps developed here for unique flow conditions require knowledge of at least two of the three unknown variables (dimensionless blockage radius, length and temperature drop) to determine the third variable.
3) A back-temperature plot is developed similar to a backpressure plot but with a negative slope. The effect of a uniform blockage can be seen on a back-temperature plot as a shift in trend below the zero-blockage line (for the baseline case). The greater the blockage, the greater the departure from the zero-blockage line.
4) The overall reduction in temperature drop from pipe inlet to outlet is actually the result of the combined effect of the insulation from the wax layer and the flow rates. It is observed that for a fixed blockage, the temperature drop from pipe inlet to outlet decreases with increasing flow rate. This is because higher flow rates imply greater volumes of fluid, higher heat contents (mC_p), a greater overall retention of heat in the system and a lower temperature drop from inlet to outlet.

5) A skin factor is developed as the extra term in the denominator of the overall heat transfer coefficient for a blocked pipeline. The skin factor accounts for the insulating effect of the blockage and has an inverse relationship to the temperature drop from pipe inlet to outlet.
6) It is also noted that the temperature drop is more sensitive to skin factor or the effects of blockage at higher flow rates than at lower flow rates. At low flow rates and for 'short' blockages (0-20,000 m), the effect of blockage radius (the cross-sectional area available for flow) on temperature drop cannot be detected. Only extremely long blockages (40,000 m) show a variation in temperature drop with blockage radius. As flow rate increases, the effect of blockage radius on temperature drop for shorter blockages becomes more apparent.
7) Overall, there is a good match between the temperature drop predictions from the model and PIPESIM simulation. The results from the model are consistently lower than the PIPESIM predictions indicating that the model is under-estimating the insulating effect of the deposited wax.
8) It is also noted the match between the model and PIPESIM seems to be optimal for certain regions of flow conditions, possibly indicating that the model has regions of applicability that must be further investigated.
9) There appear to be two distinct regions where the match between the model and PIPESIM is poor: the first one is at low flow rates and thin layers of wax deposited and the second is at high flow rates and thick wax layers. Low flow rates imply low thermal heat content into the system, which for extensive pipeline lengths, result in a

complete loss of heat energy, if inlet pressure is unaccounted for. The difference between the temperature drop predictions by PIPESIM and the model is that PIPESIM, unlike the model, incorporates inlet pressure, which provides a 'pressure boost' minimizing temperature drop along the pipeline. This results in PIPESIM predicting temperature drops that are consistently lower than the model predictions in this region.

For the second region, the combination of high flow rates and high wax thickness result in increased frictional heating, accounted for by the PIPESIM simulation, but unaccounted for in the model. The increased frictional heating results in a lower system heat loss and a lower temperature drop prediction by PIPESIM.

RECOMMENDATIONS

1) Improvement of the accuracy of the model may be achieved by investigating and incorporating the effects of:
   a. Variation of fluid physical properties (such as μ and ρ) with temperature and pressure,
   b. Friction on temperature drop for severely restricted pipes,
   c. Sensitivity of the model to the internal convective heat transfer coefficient (h_i). The Dittus-Boelter correlation used in this study is noted to have errors as large as 25%.
2) The model requires rigorous investigation to determine its regions of validity. The ideal approach would be experimental validation.
3) The model needs to be extended to multiphase flow.
4) In the absence of experimental validation, a license for the Wax Deposition module of PIPESIM should be sought to enable a more realistic simulation of wax deposition, to enable validation of this model.
5) The possibility of becoming part of the Joint Industry Project on Paraffin Deposition Prediction in Multiphase Flowlines and Wellbores headed by the University of Tulsa should be explored. This would enable access to the large resources of information already available.

PROPOSED EXTENSION TO MULTIPHASE FLOW

The model has been developed for single phase flow applications but requires extension to multiphase flowing conditions to gain widespread relevance and usefulness. The multiple phases would affect the internal convective heat transfer coefficient (h_i). The 2-phase internal convective heat transfer coefficient ($h_i^{2-\phi}$) would be a function of the flow regime and liquid hold-up. The h_i for each phase would need to be determined from correlations; and weighted by the liquid hold-up (such as density, viscosity and other 2-phase properties) to obtain the two-phase internal convective heat transfer ($h_i^{2-\phi}$).

NOMENCLATURE

T_{amb}	=	Ambient air or sea temperature
B	=	Blockage (%)
T_m	=	Bulk fluid temperature
h	=	Convective heat transfer coefficient
ρ	=	Density
d	=	Diameter
n	=	Exponent
f	=	Fanning friction factor
v	=	Fluid velocity
F_{FB}	=	Friction-based blockage factor
c	=	Friction coefficient
R	=	Gas constant
Q	=	Heat energy
L	=	Length
$\dot{m}$	=	Mass flow rate
U	=	Overall heat transfer coefficient
P	=	Pressure
r	=	Radius
S	=	Skin factor
C_p	=	Specific heat capacity

A	=	Surface area
T	=	Temperature
F_{TB}	=	Temperature-based blockage factor
k	=	Thermal conductivity
δ	=	Thickness
μ	=	Viscosity
V	=	Volume
F_{VB}	=	Volume-based blockage factor
Q_{flow},	=	Volumetric flow rate

Subscripts and superscripts

B	=	Blocked pipe (or blockage for L_B)
D	=	Dimensionless
o	=	External/outside pipe wall (or outlet)
f	=	Friction
i	=	Internal/inside pipe wall (or inlet)
L	=	Liquid
w	=	Wax
P	=	Unblocked pipe

REFERENCES

1. Scott, S.L. and Satterwhite, L.A.: "Evaluation of the Backpressure Technique for Blockage Detection in Gas Flowlines," *J. of Energy Resources Technology* (March 1998) **120**, 27.

2. Chen, X.T., Butler, T., Volk, M. and Brill, J.P.: "Techniques for Measuring Wax Thickness During Single and Multiphase Flow," paper SPE 38773 presented at the 1997 SPE Annual Technical Conference and Exhibition, San Antonio, Texas, 5-8 October.

3. Brill, J.P. and Mukherjee, H.: *Multiphase Flow in Wells,* Monograph Series, SPE, Richardson, Texas (1999) **1**, 13-17.

4. Ramey, H.J.: "Wellbore Heat Transmission," paper SPE 96, *JPT* (April 1962) 427-435; *Trans*. AIME, **225**.

5. Hasan, A.R., and Kabir, C.S.: "Heat Transfer During Two-Phase Flow in Wellbores: Part I-Formation Temperature," paper SPE 22866 presented at the 1991 SPE Annual Technical Conference and Exhibition, Dallas, Texas, 6-9 October.

6. Ajienka, J.A. and Ikoku, C.U.: "Waxy Crude Oil Handling in Nigeria: Practices, Problems and Prospects," *Energy Sources* (1990) **12**, 463.

7. "Paraffin and Asphaltene Controllers," available at http://www.bakerhughes.com /bakerpetrolite/oilgas/paraffin.htm (accessed on 8 August 2004).

8. OLGA 2000 User's Manual, Scandpower Petroleum Technology AS, Oslo, Norway.

9. PIPESIM 2003 User Guide, Geoquest, the software division of Schlumberger Information Systems, Houston, Texas.

10. Labes-Carrier, C., Rønningsen, H.P., Kolnes, J. and Leporcher, E.: "Wax Deposition in North Sea Gas Condensate and Oil Systems: Comparison Between Operational Experience and Model Prediction," paper SPE 77573 presented at the 2002 SPE Annual Technical Conference and Exhibition, San Antonio, Texas, 29 September-2 October.

11. Won K. W., "Continuous Thermodynamics of Solid-Liquid Equilibria: Wax Formation from Heavy Hydrocarbon Mixtures," AIChE Spring National Meeting, Mar. 24-28, 1986.

12. Pedersen, K.S.: "Wax Formation and Inhibition," *Properties of Natural Gases*, Gulf Publishing Co., Houston (1989) Chap. 14, 208-219.

13. Pedersen, K.S.: "Prediction of Cloud Point Temperatures and Amount of Wax Precipitation," paper SPE 27629, *SPEPF* (Feb. 1993) 46.

14. Hansen, J.H.: "A Thermodynamic Model for Predicting Wax Formation in Crude Oils," *AICHE J.* (1988) **38**, 1937.

15. Erbar, J.H., "Three Phase Equilibrium Calculations," *Proc.*, Fifty-Second Annual GPA Convention, Dallas, Texas, 26-28 March 1973.

16. Majeed, A., Bringedal, B. and Overå, S.: "Model Calculates Wax Deposition in North Sea Oils," *Oil & Gas J.*, (18 June 1990) **88**, No. 25, 63.

17. Burger, E.D., Perkins, T.K. and Striegler, J.H.: "Studies of Wax Deposition in the Trans Alaska Pipeline," *JPT* (June 1981) 1075.

18. Bern, P.A., Withers, V.R. and Cairns, R.J.R.: "Wax Deposition in Crude Oil Pipelines," paper EUR 206 presented at the 1980 European Offshore Petroleum Conference and Exhibition, London, England, Oct. 21-24.

19. Brown, T.S., Niesen, V.G. and Erickson, D.D.: "The Effects of Light Ends and High Pressure on Paraffin Formation," paper SPE 28505 presented at the 1994 SPE Annual Technical Conference and Exhibition, New Orleans, LA, 25-28 September.

20. Shields, D.: "Predicting Asphaltene and Wax Deposition Problems in Mexican Wells," *Offshore* (September 2000) 84.

21. McClaflin, G.G. and Whitfill, D.L.: "Control of Paraffin Deposition in Production Operations," paper SPE 12204 presented at the 1983 SPE of AIME Annual Technical Conference and Exhibition, San Francisco, California, 5-8 October.

22. Barker, K.M.: "Formation Damage Related to Hot Oiling," paper SPE 16230 presented at the 1989 SPE Production Operations Symposium, Oklahoma City, Oklahoma, 8-10 March.

23. Marques, L.C., Rocha, N.O., Machado, A.L. Neves, G.B., Vierra, L.C. *et al.*: "Study of Paraffin Crystallization Process Under the Influence of Magnetic Fields and Chemicals," paper SPE 38990 presented at the Fifth Annual Latin American and Carribean Petroleum Engineering Conference and Exhibition, Rio de Janeiro, Brazil, 30 August-3 September 1997.

24. Scott, S.L.: "Multiphase Pumping Addresses a Wide Range of Operating Problems," *Oil & Gas J.,* (29 September 2003) **101**, No. 37, 59.

25. "Case Study Flow Assurance Monitoring of Flowlines & Risers," available at http://www.sensa.org/pipeline/index.html (accessed on 12 September 2004).

26. Biao, W. and Lijian, D.: "Paraffin Characteristics of Waxy Crude Oils in China and the Methods of Paraffin Removal and Inhibition," paper SPE 29954 presented at the Intl. Meeting on Petroleum Engineering, Beijing, PR China, 15-17 November 1995.

27. Balakirev, V.A., Sotnikov, G.V., Tkach, Y.V. and Yatsenko, T.Y.: "Removal of Asphalt-Paraffin Deposits in Oil Pipelines by a Moving Source of High-Frequency Electromagnetic Radiation," *Technical Physics* (September 2001) **46**, No. 9, 1069.

28. "Overview About Wax and Asphaltenes," available at www.peer.caltech.edu/ projects/of_chem1.ppt (accessed on 10 August 2004).

29. "About Pigs," available at www.piggingassnppsa.com/about.htm (accessed on 5 October 2004).

30. Kleinhans, J.W., Niesen, V.G. and Brown, T.S.: "Pompano Paraffin Calibration Field Trials," paper SPE 62946 presented at the 2000 SPE Annual Technical Conference and Exhibition, Dallas, Texas, 1-4 October.

31. Scott, S.L. and Yi, J.: "Flow Testing Methods to Detect and Characterize Partial Blockages in Looped Subsea Flowlines," *J. of Energy Resources Technology* (September 1999) 155; Trans., ASME, **121**.

32. Weingarten, J.S. and Euchner, J.A.: "Methods of Predicting Wax Precipitation and Deposition," *SPEPE* (Feb. 1988) 121-126.

33. Incropera, F.P. and Dewitt, D.P.: "Internal Flow," *Fundamentals of Heat and Mass Transfer*, Fifth edition, John Wiley & Sons Inc., New York (2002) Chap. 8, 466–491.

34. Golczynski, T.S. and Niesen, V.G: "A Tale of Two Trees: Flow Assurance Challenges for Wet Tree and Dry Tree Systems in Ultradeepwater," paper SPE 71545 presented at the 2001 SPE Annual Technical Conference and Exhibition, Dallas, Texas, 30 September–3 October.

APPENDIX A

DEVELOPMENT OF THE HEAT-BALANCE MODEL FOR A FULLY-BLOCKED PIPELINE

Consider **Fig. A-1** depicting a pipeline of length L_p blocked along its entire length such that $L_B = L_p$. The fluid flowing internally has the properties shown below and the pipeline is exposed to ambient air conditions.

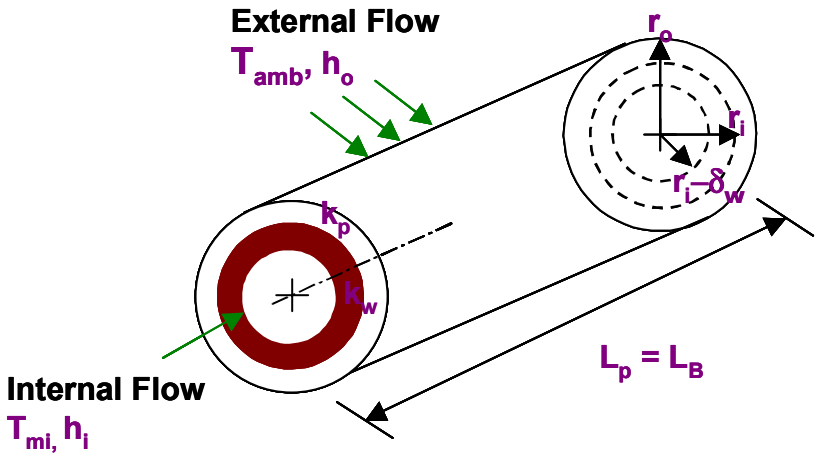

Fig. A-1–Schematic of a pipeline fully-blocked along its entire length.

Assumptions

1) Single-phase liquid.
2) Steady-state conditions.
3) Pipe of uniform radial geometry.
4) Wax thickness uniform over entire length of pipe.
5) Non-adiabatic system.

Taking a heat balance;

$$\Delta Q = Q_{in} - Q_{out} \quad \text{..... (A-1)}$$

where ΔQ is the change in heat energy, Q_{in} the heat energy entering the pipe, and Q_{out} the heat energy leaving the pipe.

The change in heat energy is predominantly made up of heat losses from conduction, convection and radiation. The expressions for each component of the heat loss from the system can now be evaluated independently.

For now, let's take a unit volume element of the pipe and assume that the bulk fluid temperature is uniform and equal to T_m. (Note the wax thickness is ∂_w).

The system above could be reduced to an equivalent electrical circuit:

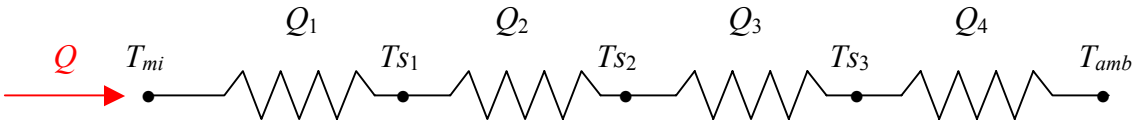

Fig. A-2–Illustration of thermal circuit represented as equivalent electrical circuit.

The heat energy across the unit volume element is made up of 4 components;

1) Q_1 – internal convection (from the fluid).
2) Q_2 – conduction through the wax layer.
3) Q_3 – conduction through the pipe wall.
4) Q_4 – external convection (to the ambient air).

We note that:

$$Q_{out} = Q = Q_1 = Q_2 = Q_3 = Q_4 \quad \text{(A-2)}$$

For a radial system,

The convective heat component is given by Eq. A-3,

$$Q = hA\Delta T \quad \text{(A-3)}$$

and Eq. A-4 gives the conductive heat component.

$$Q = kA\frac{dT}{dr} = \frac{2\pi Lk\Delta T}{\ln\left(r_o / r_i\right)} \quad \text{(A-4)}$$

The overall temperature gradient from the pipe inlet to the ambient conditions is given by:

$$T_{amb} - T_{\text{mi}} = (T_i - Ts_1) + (Ts_1 - Ts_2) + (Ts_2 - Ts_3) + (Ts_3 - T_{\text{amb}}) \quad \text{... (A-5)}$$

Each temperature gradient may be expressed in terms of a resistance.

$$\Delta T = \frac{Q}{R} \quad \text{..... (A-6)}$$

Eq. A-5 can then be expressed as Eq. A-7:

$$\Delta T = T_{amb} - T_{\text{mi}} = \frac{Q}{R_{tot}} = \frac{Q}{h_i A} + \frac{Q \ln\left(r_i / r_i - \partial_w\right)}{2\pi L k_w} + \frac{Q \ln\left(r_o / r_i\right)}{2\pi L k_p} + \frac{Q}{h_o A} \quad \text{(A-7)}$$

This can be further simplified to Eq. A-8:

$$T_{amb} - T_{\text{mi}} = Q\left[\frac{1}{h_i A} + \frac{\ln\left(r_i / r_i - \partial_w\right)}{2\pi L k_w} + \frac{\ln\left(r_o / r_i\right)}{2\pi L k_p} + \frac{1}{h_o A}\right] \quad \text{..... (A-8)}$$

$$Q = \frac{T_{amb} - T_{mi}}{\frac{1}{h_i A_i} + \frac{\ln\left(r_i / r_i - \partial_w\right)}{2\pi L k_w} + \frac{\ln\left(r_o / r_i\right)}{2\pi L k_p} + \frac{1}{h_o A_o}} \quad \text{..... (A-9)}$$

Eq. A-9 is the general expression for the heat loss from a unit volume element of pipe with a fluid flowing through it. It can be further simplified by substituting the expressions for the internal and external surface areas.

$$A_o = 2\pi r_o L_p \quad \text{..... (A-10)}$$

$$A_i = 2\pi r_i L_p \quad \text{..... (A-11)}$$

Eq. A-9 becomes:

$$Q = \frac{T_{amb} - T_{mi}}{\frac{1}{2\pi\left(r_i - \partial_w\right) L_p h_i} + \frac{\ln\left(r_i / r_i - \partial_w\right)}{2\pi L k_w} + \frac{\ln\left(r_o / r_i\right)}{2\pi L k_p} + \frac{1}{2\pi r_o L_p h_o}} \quad \text{(A-12)}$$

Basing the heat flow on the external area of the pipe yields:

$$Q = q''A = 2\pi r_o L_p q'', \quad \text{(A-13)}$$

where q'' is the heat flux (heat flow per unit area).

Substituting equation (A-13) into (A-12) yields:

$$2\pi r_o L_p q'' = \frac{T_{amb} - T_{mi}}{\frac{1}{2\pi (r_i - \partial_w) L_p h_i} + \frac{\ln\left(r_i / r_i - \partial_w\right)}{2\pi L k_w} + \frac{\ln\left(r_o / r_i\right)}{2\pi L k_p} + \frac{1}{2\pi r_o L_p h_o}} \quad \text{(A-14)}$$

$$q'' = \frac{T_{amb} - T_{mi}}{\frac{r_o}{h_i (r_i - \partial_w)} + \frac{r_o}{k_w} \ln \frac{r_i}{r_i - \partial_w} + \frac{r_o}{k_p} \ln \frac{r_o}{r_i} + \frac{1}{h_o}} \quad \text{(A-15)}$$

Eq. A-15 is the final expression for the heat flux from a unit volume element of pipe. However, we know that the temperature of the fluid will vary from inlet to outlet over the entire pipeline; and it is this gradient ($T_{mi} - T_{mo}$) that we are interested in, so we need to do some further manipulation:

We can rewrite Eq. A-15 in general terms as:

$$Q = UA\,\Delta T \quad \text{..... (A-16)}$$

$$UA = \frac{Q}{\Delta T} = \frac{1}{R} = \frac{1}{\frac{1}{2\pi(r_i - \partial_w)L_p h_i} + \frac{\ln\left(r_i / r_i - \partial_w\right)}{2\pi L k_w} + \frac{\ln\left(r_o / r_i\right)}{2\pi L k_p} + \frac{1}{2\pi r_o L_p h_o}} \quad \text{(A-17)}$$

where U is the overall heat transfer coefficient and;

$$\Delta T = T_{amb} - T_{mi} \quad \text{..... (A-18)}$$

For the entire pipe, the overall heat input is given by:

$$Q_{in} = q = \dot{m} C_p dT_m \quad \text{..... (A-19)}$$

Therefore,

$$\dot{m} C_p dT_m = q'' A = UA\Delta T = U(Pdx)\Delta T \text{ , ... (A-20)}$$

where P is the perimeter of the pipe.

$$dT_m = T_{mi} - T_{mo} \equiv -\left[\left(T_{amb} - T_{mi}\right) - \left(T_{amb} - T_{mo}\right)\right] = -d(\Delta T) \text{ .. (A-21)}$$

From Eq. A-20;

$$\frac{dT_m}{dx} = \frac{-d(\Delta T)}{dx} = \frac{P}{\dot{m}C_p} U\Delta T \quad \text{..... (A-22)}$$

Separating variables and integrating from inlet to outlet yields:

$$\int_{\Delta T_i}^{\Delta T_o} \frac{-d(\Delta T)}{\Delta T} = \int_0^{L_p} \frac{P}{\dot{m}C_p} U dx \quad \text{..... (A-23)}$$

$$\ln \frac{\Delta T_o}{\Delta T_i} = -\frac{PL_p}{\dot{m}C_p}\overline{U} = -\frac{\overline{U}A}{\dot{m}C_p} \quad \text{..... (A-24)}$$

$$\dot{m}C_p = -\frac{\overline{U}A}{\ln \frac{\Delta T_i}{\Delta T_o}} \quad \text{..... (A-25)}$$

Multiplying both sides by $(\Delta T_o - \Delta T_i)$ yields:

$$Q = \dot{m}C_p(\Delta T_o - \Delta T_i) = -\overline{U}A\frac{\Delta T_o - \Delta T_i}{\ln \frac{\Delta T_o}{\Delta T_i}} \equiv -\overline{U}A_s\Delta T_{lm} \quad \text{, ... (A-26)}$$

$$\Delta T_{lm} = \frac{\Delta T_o - \Delta T_i}{\ln \frac{\Delta T_o}{\Delta T_i}} \text{ , } \quad \text{(A-27)}$$

where $\overline{U}$ is the overall heat transfer coefficient and ΔT_{lm} the logarithmic mean temperature difference.

Basing the overall heat transfer coefficient on the outside surface area,

$$A_o = 2\pi r_o L_p \quad \text{(A-28)}$$

$$\overline{U}_o = \overline{U} A_o = 2\pi r_o L_p \overline{U} \quad \text{(A-29)}$$

where $\overline{U}_o$ is the overall heat transfer coefficient based on the external surface area. Equating Eqs. A-17 and A-29,

$$2\pi r_o L_p \overline{U} = \frac{1}{\frac{1}{2\pi (r_i - \partial_w) L_p h_i} + \frac{\ln\left(r_i / r_i - \partial_w\right)}{2\pi L k_w} + \frac{\ln\left(r_o / r_i\right)}{2\pi L k_p} + \frac{1}{2\pi r_o L_p h_o}} \quad \text{(A-30)}$$

This simplifies to Eq. A-31:

$$\overline{U} = \frac{1}{\frac{r_o}{h_i(r_i - \partial_w)} + \frac{r_o}{k_w}\ln\frac{r_i}{r_i - \partial_w} + \frac{r_o}{k_p}\ln\frac{r_o}{r_i} + \frac{1}{h_o}} \quad \text{..... (A-31)}$$

Going back to Eq. A-26, the temperature gradients can be expanded as follows:

$$\Delta T_o = T_{amb} - T_{mo} \quad \text{..... (A-32)}$$

$$\Delta T_i = T_{amb} - T_{mi} \quad \text{..... (A-33)}$$

Substituting Eqs. A-32 and A-33 into A-26 yields:

$$Q = \dot{m}C_p(\Delta T_o - \Delta T_i) = \left[\frac{-2\pi r_o L_p \left(\frac{(T_{\text{amb}} - T_{mo}) - (T_{\text{amb}} - T_{mi})}{\ln\frac{T_{\text{amb}} - T_{mo}}{T_{\text{amb}} - T_{mi}}} \right)}{\frac{r_o}{h_i(r_i - \partial_w)} + \frac{r_o}{k_w}\ln\frac{r_i}{r_i - \partial_w} + \frac{r_o}{k_p}\ln\frac{r_o}{r_i} + \frac{1}{h_o}} \right] \quad \text{(A-34)}$$

Defining the mass flow rate,

$$\dot{m} = \rho Q_{\text{flow}} \quad \text{..... (A-35)}$$

The pipe wall resistance, though negligible when compared to the other resistances because its thermal conductivity (k_p) tends to infinity, is included in all calculations.

$$Q = \rho Q_{\text{flow}} C_p (T_{mi} - T_{mo}) = \left[\frac{-2\pi r_o L_p \left(\frac{(T_{\text{amb}} - T_{mo}) - (T_{\text{amb}} - T_{mi})}{\ln \frac{T_{\text{amb}} - T_{mo}}{T_{\text{amb}} - T_{mi}}} \right)}{\frac{r_o}{h_i (r_i - \partial_w)} + \frac{r_o}{k_w} \ln \frac{r_i}{r_i - \partial_w} + \frac{r_o}{k_p} \ln \frac{r_o}{r_i} + \frac{1}{h_o}} \right] \quad \text{(A-36)}$$

$$Q_{\text{flow}} = \left[\frac{-2\pi r_o L_p \left(\frac{(T_{mi} - T_{mo})}{\ln \frac{T_{\text{amb}} - T_{mo}}{T_{\text{amb}} - T_{mi}}} \right)}{\left(\frac{r_o}{h_i (r_i - \partial_w)} + \frac{r_o}{k_w} \ln \frac{r_i}{r_i - \partial_w} + \frac{r_o}{k_p} \ln \frac{r_o}{r_i} + \frac{1}{h_o} \right) \rho C_p (T_{mi} - T_{mo})} \right] \quad \text{(A-37)}$$

$$Q_{\text{flow}} = \left[\frac{-2\pi r_o L_p}{\rho C_p \ln \left(\frac{T_{\text{amb}} - T_{mo}}{T_{\text{amb}} - T_{mi}} \right) \left(\frac{r_o}{h_i (r_i - \partial_w)} + \frac{r_o}{k_w} \ln \frac{r_i}{r_i - \partial_w} + \frac{r_o}{k_p} \ln \frac{r_o}{r_i} + \frac{1}{h_o} \right)} \right] \quad \text{(A-38)}$$

$$\frac{T_{\text{amb}} - T_{mo}}{T_{\text{amb}} - T_{mi}} = \exp\left\{ \frac{-2\pi r_o L_p}{Q_{\text{flow}} \rho C_p \left(\frac{r_o}{h_i (r_i - \partial_w)} + \frac{r_o}{k_w} \ln \frac{r_i}{r_i - \partial_w} + \frac{r_o}{k_p} \ln \frac{r_o}{r_i} + \frac{1}{h_o} \right)} \right\} \quad \text{(A-39)}$$

Eq. A-39 can be expressed simply as:

$$\frac{T_{\text{amb}} - T_{mo}}{T_{\text{amb}} - T_{mi}} = \exp\left\{ \frac{-\overline{U} A_o}{Q_{\text{flow}} \rho C_p} \right\} \quad \text{(A-40)}$$

where;

$$\overline{U} = \frac{1}{\frac{r_o}{h_i (r_i - \partial_w)} + \frac{r_o}{k_w} \ln \frac{r_i}{r_i - \partial_w} + \frac{r_o}{k_p} \ln \frac{r_o}{r_i} + \frac{1}{h_o}} \quad \text{(A-41)}$$

$A_o = 2\pi r_o L_p$, is based on the pipe external surface area and C_p is the specific heat capacity of the oil.

Eq. A-41 can be further manipulated to yield a temperature drop:

$$T_{\text{amb}} - T_{mo} = T_{amb} \exp\left\{ \frac{-\overline{U} A_o}{Q_{\text{flow}} \rho C_p} \right\} - T_{mi} \exp\left\{ \frac{-\overline{U} A_o}{Q_{\text{flow}} \rho C_p} \right\} \quad \text{(A-42)}$$

$$T_{mi} - T_{mo} = T_{mi} - T_{amb} + T_{amb} \exp\left\{\frac{-\overline{U}A_o}{Q_{\text{flow}}\rho C_p}\right\} - T_{mi} \exp\left\{\frac{-\overline{U}A_o}{Q_{\text{flow}}\rho C_p}\right\} \text{ ..... (A-43)}$$

Eq. A-44 gives the final heat-balance model for a fully-blocked pipeline.

$$T_{mi} - T_{mo} = T_{amb}\left[\exp\left\{\frac{-\overline{U}A_o}{Q_{\text{flow}}\rho C_p}\right\} - 1\right] + T_{mi}\left[1 - \exp\left\{\frac{-\overline{U}A_o}{Q_{\text{flow}}\rho C_p}\right\}\right] \text{ ..... (A-44)}$$

APPENDIX B

EXCEL SPREADSHEET FOR THE HEAT-BALANCE MODEL FOR A FULLY-BLOCKED PIPELINE AND DATA FOR FIGS. 3 AND 6

Heat Transfer Approach to Blockage Detection

Blocked Pipe (Uniform blockage over entire length of pipe)

Reference pipe-North Sea Field

Lp = 43000 m
Di = 0.38 m
Do = 0.4054 m
Δt = 0.0127 m
r_i = 0.19 m
r_o = 0.2027 m
kp = 43.25 W/mK
As = 54765 m^2

Ts = 32 °C 305 K
Inlet T T_{m1} = 35 °C 308 K

Crude Oil Properties

ρ = 0.8753 g/cm^3 875.32 kg/m^3
μ = 1.0603 cp 0.0010603 kg/ms
C_p = 1890 J/kgK
k_w = 0.25 W/mK
k_f = 0.1312 W/mK

Air Properties

ρ = 1.271 kg/m3
T_{amb} = 0 °C 273 K
k_{air} = 0.026 W/mK
v_{air} = 0.0305 m/s
C_p = 1005 J/kgK
μ_{air} = 0.0175 cp
h_o = 4 W/m^2K

S	r	B, %	r_B/r_i	r_B	v, m/s	Q, m^3/d	Q, m^3/s	R				U	EXP	T_{m3}, K	T_{m1} - T_{m3}, K	Re	Pr	Nu_D	h_i
0.021	0.014	5	0.97	0.19	0.102	1000	0.0116	0.014	0.021	0.000	0.250	3.50	0.000	273.002	34.998	32846	15	214	76
0.043	0.013	10	0.95	0.18				0.014	0.043			3.26	0.000	273.003	34.997	33747		219	80
0.067	0.013	15	0.92	0.18				0.014	0.066			3.03	0.000	273.006	34.994	34725		224	84
0.092	0.012	20	0.89	0.17				0.013	0.090			2.82	0.000	273.011	34.989	35794		229	88
0.118	0.011	25	0.87	0.16				0.013	0.117			2.63	0.001	273.019	34.981	36968		235	94
0.147	0.011	30	0.84	0.16				0.013	0.145			2.45	0.001	273.031	34.969	38265		242	100
0.177	0.010	35	0.81	0.15				0.012	0.175			2.29	0.001	273.051	34.949	39709		249	107
0.210	0.009	40	0.77	0.15				0.012	0.207			2.13	0.002	273.079	34.921	41331		257	115
0.245	0.009	45	0.74	0.14				0.012	0.242			1.98	0.003	273.120	34.880	43169		266	124
0.284	0.008	50	0.71	0.13				0.011	0.281			1.84	0.005	273.180	34.820	45276		276	135
0.327	0.007	55	0.67	0.13				0.011	0.324			1.71	0.008	273.263	34.737	47725		288	148
0.430	0.006	65	0.59	0.11				0.010	0.426			1.46	0.015	273.540	34.460	54115		319	186
0.492	0.005	70	0.55	0.10				0.009	0.488			1.34	0.022	273.763	34.237	58451		339	214
0.566	0.004	75	0.50	0.10				0.008	0.562			1.22	0.031	274.073	33.927	64030		365	252
0.657	0.003	80	0.45	0.08				0.008	0.652			1.10	0.043	274.513	33.487	71587		399	308
0.773	0.003	85	0.39	0.07				0.007	0.769			0.97	0.062	275.157	32.843	82662		447	399
0.937	0.002	90	0.32	0.06				0.006	0.933			0.84	0.090	276.162	31.838	101240		526	575
1.218	0.001	95	0.22	0.04				0.004	1.214			0.68	0.143	277.996	30.004	143175		694	1072
0.000	0.015	0	1.00	0.19				0.015	0.000			3.77	0.000	273.001	34.999	32015		209	72

S	r	B, %	r_B/r_i	r_B	v, m/s	Q, m^3/d	Q, m^3/s	R				U	EXP	$T_{m3,}$ K	$T_{m1} - T_{m3,}$ K	Re	Pr	Nu_D	h_i
0.021	0.008	3	0.97	0.19	0.204	2000	0.0231	0.008	0.021	0.000	0.250	3.58	0.006	273.209	34.791	65693	15	372	132
0.043	0.008	5	0.95	0.18				0.008	0.043			3.32	0.009	273.303	34.697	67493		380	139
0.067	0.007	8	0.92	0.18				0.008	0.066			3.09	0.012	273.425	34.575	69450		389	146
0.091	0.007	11	0.89	0.17				0.008	0.090			2.87	0.017	273.578	34.422	71587		399	154
0.118	0.007	13	0.87	0.16				0.008	0.117			2.67	0.022	273.768	34.232	73935		409	163
0.146	0.006	16	0.84	0.16				0.007	0.145			2.49	0.029	274.000	34.000	76530		421	174
0.176	0.006	19	0.81	0.15				0.007	0.175			2.31	0.037	274.278	33.722	79419		433	186
0.209	0.005	23	0.77	0.15				0.007	0.207			2.15	0.046	274.608	33.392	82662		447	199
0.244	0.005	26	0.74	0.14				0.007	0.242			2.00	0.057	274.996	33.004	86338		463	216
0.283	0.005	29	0.71	0.13				0.006	0.281			1.86	0.070	275.449	32.551	90552		481	235
0.326	0.004	33	0.67	0.13				0.006	0.324			1.72	0.085	275.976	32.024	95450		502	258
0.428	0.003	41	0.59	0.11				0.006	0.426			1.47	0.123	277.292	30.708	108230		555	324
0.490	0.003	45	0.55	0.10				0.005	0.488			1.34	0.146	278.115	29.885	116902		590	372
0.564	0.002	50	0.50	0.10				0.005	0.562			1.22	0.174	279.082	28.918	128059		635	439
0.655	0.002	55	0.45	0.08				0.004	0.652			1.10	0.207	280.236	27.764	143175		694	536
0.772	0.002	61	0.39	0.07				0.004	0.769			0.98	0.247	281.653	26.347	165324		779	695
0.936	0.001	68	0.32	0.06				0.003	0.933			0.84	0.300	283.493	24.507	202479		916	1001
1.216	0.001	78	0.22	0.04				0.003	1.214			0.68	0.377	286.207	21.793	286349		1209	1867
0.000	0.008	0	1.00	0.19				0.008	0.000			3.86	0.004	273.139	34.861	64030		365	126
0.021	0.006	3	0.97	0.19	0.306	3000	0.0347	0.006	0.021	0.000	0.250	3.61	0.032	274.122	33.878	98539	15	515	182
0.043	0.006	5	0.95	0.18				0.006	0.043			3.35	0.041	274.441	33.559	101240		526	192
0.066	0.005	8	0.92	0.18				0.006	0.066			3.11	0.052	274.811	33.189	104175		538	202
0.091	0.005	11	0.89	0.17				0.006	0.090			2.89	0.064	275.232	32.768	107381		552	213
0.117	0.005	13	0.87	0.16				0.005	0.117			2.69	0.077	275.705	32.295	110903		566	226
0.145	0.004	16	0.84	0.16				0.005	0.145			2.50	0.092	276.232	31.768	114795		582	240
0.176	0.004	19	0.81	0.15				0.005	0.175			2.33	0.109	276.814	31.186	119128		599	257
0.208	0.004	23	0.77	0.15				0.005	0.207			2.16	0.127	277.453	30.547	123993		619	276
0.244	0.004	26	0.74	0.14				0.005	0.242			2.01	0.147	278.150	29.850	129506		641	298
0.282	0.003	29	0.71	0.13				0.005	0.281			1.87	0.169	278.909	29.091	135827		666	325
0.325	0.003	33	0.67	0.13				0.004	0.324			1.73	0.192	279.734	28.266	143175		694	357
0.427	0.002	41	0.59	0.11				0.004	0.426			1.47	0.246	281.612	26.388	162345		768	448
0.490	0.002	45	0.55	0.10				0.004	0.488			1.35	0.277	282.687	25.313	175352		817	515
0.564	0.002	50	0.50	0.10				0.004	0.562			1.23	0.311	283.878	24.122	192089		878	607
0.654	0.001	55	0.45	0.08				0.003	0.652			1.10	0.349	285.220	22.780	214762		960	742
0.771	0.001	61	0.39	0.07				0.003	0.769			0.98	0.394	286.773	21.227	247986		1077	961
0.935	0.001	68	0.32	0.06				0.002	0.933			0.84	0.448	288.668	19.332	303719		1267	1384
1.216	0.000	78	0.22	0.04				0.002	1.214			0.68	0.522	291.271	16.729	429524		1672	2583
0.000	0.006	0	1.00	0.19				0.006	0.000			3.90	0.024	273.850	34.150	96044		504	174

S	r	B, %	r_B/r_i	r_B	v, m/s	Q, m^3/d	Q, m^3/s	R				U	EXP	$T_{m3,}$ K	$T_{m1} - T_{m3,}$ K	Re	Pr	Nu_D	h_i
0.021	0.005	3	0.97	0.19	0.408	4000	0.0463	0.005	0.021	0.000	0.250	3.62	0.075	275.620	32.380	131386	15	648	230
0.043	0.004	5	0.95	0.18				0.005	0.043			3.36	0.091	276.169	31.831	134986		662	241
0.066	0.004	8	0.92	0.18				0.005	0.066			3.12	0.108	276.766	31.234	138900		678	254
0.091	0.004	11	0.89	0.17				0.004	0.090			2.90	0.126	277.411	30.589	143175		694	268
0.117	0.004	13	0.87	0.16				0.004	0.117			2.69	0.146	278.101	29.899	147870		712	284
0.145	0.004	16	0.84	0.16				0.004	0.145			2.51	0.167	278.835	29.165	153060		732	302
0.175	0.003	19	0.81	0.15				0.004	0.175			2.33	0.189	279.611	28.389	158838		754	323
0.208	0.003	23	0.77	0.15				0.004	0.207			2.17	0.212	280.430	27.570	165324		779	347
0.243	0.003	26	0.74	0.14				0.004	0.242			2.01	0.237	281.291	26.709	172675		807	376
0.282	0.003	29	0.71	0.13				0.004	0.281			1.87	0.263	282.196	25.804	181103		838	409
0.325	0.002	33	0.67	0.13				0.004	0.324			1.73	0.290	283.148	24.852	190899		874	450
0.427	0.002	41	0.59	0.11				0.003	0.426			1.47	0.349	285.212	22.788	216460		966	564
0.489	0.002	45	0.55	0.10				0.003	0.488			1.35	0.381	286.342	21.658	233803		1028	648
0.563	0.001	50	0.50	0.10				0.003	0.562			1.23	0.416	287.558	20.442	256118		1106	764
0.654	0.001	55	0.45	0.08				0.003	0.652			1.10	0.454	288.888	19.112	286349		1209	934
0.770	0.001	61	0.39	0.07				0.002	0.769			0.98	0.497	290.383	17.617	330647		1356	1210
0.935	0.001	68	0.32	0.06				0.002	0.933			0.84	0.547	292.150	15.850	404959		1595	1742
1.216	0.000	78	0.22	0.04				0.001	1.214			0.68	0.614	294.492	13.508	572698		2105	3251
0.000	0.005	0	1.00	0.19				0.005	0.000			3.92	0.061	275.124	32.876	128059		635	219
0.021	0.004	3	0.97	0.19	0.51	5000	0.0579	0.004	0.021	0.000	0.250	3.64	0.125	277.375	30.625	164232	15	775	275
0.043	0.004	5	0.95	0.18				0.004	0.043			3.37	0.146	278.098	29.902	168733		792	288
0.066	0.004	8	0.92	0.18				0.004	0.066			3.12	0.167	278.858	29.142	173625		810	303
0.091	0.003	11	0.89	0.17				0.004	0.090			2.90	0.190	279.651	28.349	178968		830	321
0.117	0.003	13	0.87	0.16				0.004	0.117			2.70	0.214	280.476	27.524	184838		852	340
0.145	0.003	16	0.84	0.16				0.004	0.145			2.51	0.238	281.328	26.672	191325		876	361
0.175	0.003	19	0.81	0.15				0.003	0.175			2.33	0.263	282.207	25.793	198547		902	386
0.208	0.003	23	0.77	0.15				0.003	0.207			2.17	0.289	283.112	24.888	206655		931	415
0.243	0.002	26	0.74	0.14				0.003	0.242			2.02	0.316	284.043	23.957	215844		964	449
0.282	0.002	29	0.71	0.13				0.003	0.281			1.87	0.343	285.000	23.000	226379		1002	489
0.325	0.002	33	0.67	0.13				0.003	0.324			1.73	0.371	285.987	22.013	238624		1045	538
0.427	0.002	41	0.59	0.11				0.003	0.426			1.47	0.430	288.065	19.935	270574		1155	674
0.489	0.001	45	0.55	0.10				0.003	0.488			1.35	0.462	289.172	18.828	292254		1229	775
0.563	0.001	50	0.50	0.10				0.002	0.562			1.23	0.496	290.343	17.657	320148		1322	913
0.654	0.001	55	0.45	0.08				0.002	0.652			1.11	0.531	291.601	16.399	357936		1445	1116
0.770	0.001	61	0.39	0.07				0.002	0.769			0.98	0.571	292.990	15.010	413309		1621	1446
0.935	0.001	68	0.32	0.06				0.002	0.933			0.84	0.617	294.602	13.398	506199		1907	2083
1.215	0.000	78	0.22	0.04				0.001	1.214			0.68	0.677	296.692	11.308	715873		2516	3886
0.000	0.004	0	1.00	0.19				0.004	0.000			3.93	0.106	276.693	31.307	160074		759	262

S	r	B, %	r_B/r_i	r_B	v, m/s	Q, m^3/d	Q, m^3/s	R				U	EXP	$T_{m3,}$ K	$T_{m1} - T_{m3,}$ K	Re	Pr	Nu_D	h_i
0.021	0.003	3	0.97	0.19	0.612	6000	0.0694	0.003	0.021	0.000	0.250	3.64	0.176	279.166	28.834	197079	15	897	318
0.043	0.003	5	0.95	0.18				0.003	0.043			3.37	0.200	280.008	27.992	202479		916	334
0.066	0.003	8	0.92	0.18				0.003	0.066			3.13	0.225	280.872	27.128	208350		937	351
0.091	0.003	11	0.89	0.17				0.003	0.090			2.91	0.250	281.754	26.246	214762		960	371
0.117	0.003	13	0.87	0.16				0.003	0.117			2.70	0.276	282.653	25.347	221805		985	393
0.145	0.003	16	0.84	0.16				0.003	0.145			2.51	0.302	283.564	24.436	229590		1013	418
0.175	0.002	19	0.81	0.15				0.003	0.175			2.34	0.328	284.488	23.512	238257		1044	447
0.208	0.002	23	0.77	0.15				0.003	0.207			2.17	0.355	285.424	22.576	247986		1077	480
0.243	0.002	26	0.74	0.14				0.003	0.242			2.02	0.382	286.372	21.628	259013		1116	520
0.282	0.002	29	0.71	0.13				0.003	0.281			1.87	0.410	287.334	20.666	271655		1159	566
0.325	0.002	33	0.67	0.13				0.003	0.324			1.73	0.437	288.311	19.689	286349		1209	622
0.427	0.001	41	0.59	0.11				0.002	0.426			1.47	0.495	290.331	17.669	324689		1337	780
0.489	0.001	45	0.55	0.10				0.002	0.488			1.35	0.525	291.387	16.613	350705		1422	897
0.563	0.001	50	0.50	0.10				0.002	0.562			1.23	0.557	292.491	15.509	384178		1529	1056
0.653	0.001	55	0.45	0.08				0.002	0.652			1.11	0.590	293.664	14.336	429524		1672	1291
0.770	0.001	61	0.39	0.07				0.002	0.769			0.98	0.627	294.944	13.056	495971		1876	1673
0.934	0.000	68	0.32	0.06				0.001	0.933			0.84	0.669	296.409	11.591	607438		2206	2410
1.215	0.000	78	0.22	0.04				0.001	1.214			0.68	0.722	298.283	9.717	859047		2911	4497
0.000	0.004	0	1.00	0.19				0.004	0.000			3.94	0.153	278.351	29.649	192089		878	303
0.021	0.003	3	0.97	0.19	0.714	7000	0.081	0.003	0.021	0.000	0.250	3.65	0.225	280.885	27.115	229925	15	1014	359
0.043	0.003	5	0.95	0.18				0.003	0.043			3.38	0.251	281.802	26.198	236226		1036	377
0.066	0.003	8	0.92	0.18				0.003	0.066			3.13	0.278	282.727	25.273	243075		1060	397
0.091	0.003	11	0.89	0.17				0.003	0.090			2.91	0.304	283.657	24.343	250555		1086	420
0.117	0.002	13	0.87	0.16				0.003	0.117			2.70	0.331	284.590	23.410	258773		1115	445
0.145	0.002	16	0.84	0.16				0.003	0.145			2.52	0.358	285.525	22.475	267855		1146	473
0.175	0.002	19	0.81	0.15				0.003	0.175			2.34	0.385	286.460	21.540	277966		1180	506
0.208	0.002	23	0.77	0.15				0.003	0.207			2.17	0.411	287.396	20.604	289317		1219	543
0.243	0.002	26	0.74	0.14				0.002	0.242			2.02	0.438	288.334	19.666	302181		1262	588
0.282	0.002	29	0.71	0.13				0.002	0.281			1.87	0.465	289.276	18.724	316930		1311	640
0.324	0.002	33	0.67	0.13				0.002	0.324			1.74	0.492	290.224	17.776	334074		1368	704
0.426	0.001	41	0.59	0.11				0.002	0.426			1.48	0.547	292.157	15.843	378804		1512	883
0.489	0.001	45	0.55	0.10				0.002	0.488			1.35	0.576	293.155	14.845	409155		1608	1014
0.563	0.001	50	0.50	0.10				0.002	0.562			1.23	0.605	294.188	13.812	448207		1730	1195
0.653	0.001	55	0.45	0.08				0.002	0.652			1.11	0.636	295.277	12.723	501111		1892	1461
0.770	0.001	61	0.39	0.07				0.001	0.769			0.98	0.670	296.455	11.545	578633		2122	1893
0.934	0.000	68	0.32	0.06				0.001	0.933			0.84	0.708	297.793	10.207	708678		2496	2726
1.215	0.000	78	0.22	0.04				0.001	1.214			0.68	0.757	299.485	8.515	1002222		3293	5087
0.000	0.003	0	1.00	0.19				0.003	0.000			3.95	0.199	279.980	28.020	224104		994	343

S	r	B, %	r_B/r_i	r_B	v, m/s	Q, m^3/d	Q, m^3/s	R				U	EXP	$T_{m3,}$ K	$T_{m1} - T_{m3,}$ K	Re	Pr	Nu_D	h_i
0.021	0.003	3	0.97	0.19	0.816	8000	0.0926	0.003	0.021	0.000	0.250	3.65	0.271	282.485	25.515	262772	15	1129	400
0.043	0.003	5	0.95	0.18				0.003	0.043			3.38	0.298	283.447	24.553	269973		1153	420
0.066	0.002	8	0.92	0.18				0.003	0.066			3.14	0.326	284.404	23.596	277799		1180	442
0.091	0.002	11	0.89	0.17				0.003	0.090			2.91	0.353	285.354	22.646	286349		1209	467
0.117	0.002	13	0.87	0.16				0.002	0.117			2.71	0.380	286.297	21.703	295740		1240	495
0.145	0.002	16	0.84	0.16				0.002	0.145			2.52	0.407	287.233	20.767	306120		1275	526
0.175	0.002	19	0.81	0.15				0.002	0.175			2.34	0.433	288.160	19.840	317676		1314	563
0.208	0.002	23	0.77	0.15				0.002	0.207			2.18	0.459	289.080	18.920	330647		1356	605
0.243	0.002	26	0.74	0.14				0.002	0.242			2.02	0.486	289.995	18.005	345350		1404	654
0.282	0.001	29	0.71	0.13				0.002	0.281			1.87	0.512	290.906	17.094	362206		1459	713
0.324	0.001	33	0.67	0.13				0.002	0.324			1.74	0.538	291.816	16.184	381799		1522	783
0.426	0.001	41	0.59	0.11				0.002	0.426			1.48	0.590	293.652	14.348	432919		1683	982
0.489	0.001	45	0.55	0.10				0.002	0.488			1.35	0.617	294.591	13.409	467606		1790	1129
0.563	0.001	50	0.50	0.10				0.002	0.562			1.23	0.645	295.558	12.442	512237		1925	1330
0.653	0.001	55	0.45	0.08				0.001	0.652			1.11	0.673	296.570	11.430	572698		2105	1626
0.770	0.001	61	0.39	0.07				0.001	0.769			0.98	0.705	297.658	10.342	661295		2361	2106
0.934	0.000	68	0.32	0.06				0.001	0.933			0.84	0.740	298.884	9.116	809918		2777	3033
1.215	0.000	78	0.22	0.04				0.001	1.214			0.68	0.784	300.424	7.576	1145397		3665	5660
0.000	0.003	0	1.00	0.19				0.003	0.000			3.95	0.244	281.523	26.477	256118		1106	382

Temperature Drop Variation with Flow Rate for a Fixed Cross-Sectional Area (Fig. 5)

Blockage, %	0	10	50	75	90
Q, m^3/d	ΔT				
1000	34.999	34.997	34.820	33.927	31.838
2000	34.861	34.697	32.551	28.918	24.507
3000	34.150	33.559	29.091	24.122	19.332
4000	32.876	31.831	25.804	20.442	15.850
5000	31.307	29.902	23.000	17.657	13.398
6000	29.649	27.992	20.666	15.509	11.591
7000	28.020	26.198	18.724	13.812	10.207
8000	26.477	24.553	17.094	12.442	9.116

Predicted Outlet Temperatures with Varying Blockage vs. Expected Outlet Temperature (Fig. 8)

Expected T_{mo}, K	Predicted T_{mo}, K			
B = 0%	B = 10%	B = 50%	B = 75%	B = 90%
273.001	273.003	273.180	274.073	276.162
273.139	273.303	275.449	279.082	283.493
273.850	274.441	278.909	283.878	288.668
275.124	276.169	282.196	287.558	292.150
276.693	278.098	285.000	290.343	294.602
278.351	280.008	287.334	292.491	296.409
279.980	281.802	289.276	294.188	297.793
281.523	283.447	290.906	295.558	298.884

APPENDIX C

DEVELOPMENT OF THE HEAT-BALANCE MODEL FOR A PIPELINE WITH A LOCALIZED BLOCKAGE

The model developed in the previous section was for a fully-blocked pipeline, i.e., a pipeline with a blockage along its entire length. In this section, a model is developed for the more common situation of a pipeline with a localized blockage.

Assumptions

1) Steady-state conditions
2) Constant surface temperature along the length of the pipe.
3) Uniform wax thickness deposited radially over length L_B of the pipe.
4) Non-adiabatic system.

Fig. C-1 shows a pipeline with a localized radial blockage of length L_B at the pipe inlet. The fluid and wax properties are shown below and the pipeline is exposed to ambient air conditions.

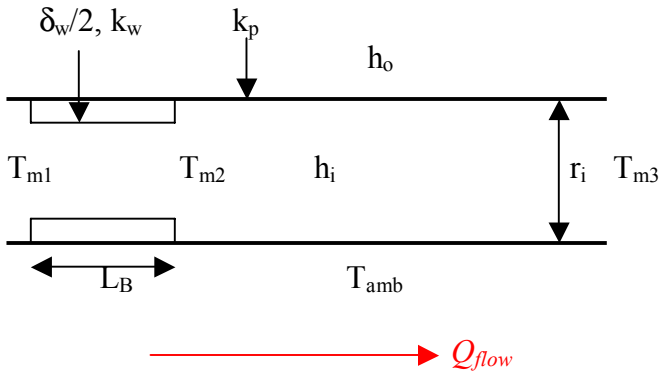

Fig. C-1–Illustration of a pipeline with a localized blockage at pipe inlet.

Recalling Eq. A-39,

$$\frac{T_{\text{amb}} - T_{mo}}{T_{\text{amb}} - T_{mi}} = \exp\left\{ \frac{-2\pi r_o L_p}{Q_{\text{flow}} \rho C_p \left(\frac{r_o}{h_i (r_i - \partial_w)} + \frac{r_o}{k_w} \ln \frac{r_i}{r_i - \partial_w} + \frac{r_o}{k_p} \ln \frac{r_o}{r_i} + \frac{1}{h_o} \right)} \right\} \quad \text{(A-39)}$$

Eq. A-39 can be written for the two sections of the pipe– the blocked and unblocked lengths respectively, as follows:

$$\frac{T_{amb} - T_{m2}}{T_{amb} - T_{m1}} = \exp\left\{ \frac{-2\pi r_o L_B}{Q_{\text{flow}} \rho C_p \left(\frac{r_o}{h_i (r_i - \partial_w)} + \frac{r_o}{k_w} \ln \frac{r_i}{r_i - \partial_w} + \frac{r_o}{k_p} \ln \frac{r_o}{r_i} + \frac{1}{h_o} \right)} \right\} \text{.. (C-1)}$$

$$\frac{T_{amb} - T_{m3}}{T_{amb} - T_{m2}} = \exp\left\{ \frac{-2\pi r_o (L_p - L_B)}{Q_{\text{flow}} \rho C_p \left(\frac{r_o}{h_i r_i} + \frac{r_o}{k_p} \ln \frac{r_o}{r_i} + \frac{1}{h_o} \right)} \right\} \text{..... (C-2)}$$

Setting $r_B = r_i - \delta_\omega$ and combining the above equations into Eq. C-4:

$$\frac{T_{amb}-T_{m2}}{T_{amb}-T_{m1}}\times\frac{T_{amb}-T_{m3}}{T_{amb}-T_{m2}}=\exp\left\{-\left(\frac{2\pi r_o L_B}{Q_{\text{flow}}\rho C_p\left(\frac{r_o}{h_i r_B}+\frac{r_o}{k_w}\ln\frac{r_i}{r_B}+\frac{r_o}{k_p}\ln\frac{r_o}{r_i}+\frac{1}{h_o}\right)}+\frac{2\pi r_o(L_p-L_B)}{Q_{\text{flow}}\rho C_p\left(\frac{r_o}{h_i r_i}+\frac{r_o}{k_p}\ln\frac{r_o}{r_i}+\frac{1}{h_o}\right)}\right)\right\}$$

(C-3)

$$\frac{T_{amb}-T_{m3}}{T_{amb}-T_{m1}}=\exp\left\{-\left(\frac{2\pi r_o L_p}{Q_{\text{flow}}\rho C_p\left(\frac{r_o}{h_i r_i}+\frac{r_o}{k_p}\ln\frac{r_o}{r_i}+\frac{1}{h_o}\right)}+\frac{2\pi r_o L_B}{Q_{\text{flow}}\rho C_p}\left(\frac{1}{\frac{r_o}{h_i r_B}+\frac{r_o}{k_w}\ln\frac{r_i}{r_B}+\frac{r_o}{k_p}\ln\frac{r_o}{r_i}+\frac{1}{h_o}}-\frac{1}{\frac{r_o}{h_i r_i}+\frac{r_o}{k_p}\ln\frac{r_o}{r_i}+\frac{1}{h_o}}\right)\right)\right\}$$

(C-4)

(Note: $T_{m1} = T_{mi}$ and $T_{m3} = T_{mo}$)

Eq. C-5 is the final expression for the heat-balance model for a partially-blocked pipe.

$$\frac{T_{amb}-T_{mo}}{T_{amb}-T_{mi}}=\exp\left\{-\left(\frac{2\pi r_o L_p}{Q_{\text{flow}}\rho C_p\left(\frac{r_o}{h_i r_i}+\frac{r_o}{k_p}\ln\frac{r_o}{r_i}+\frac{1}{h_o}\right)}+\frac{2\pi r_o L_B}{Q_{\text{flow}}\rho C_p}\left(\frac{1}{\frac{r_o}{h_i r_B}+\frac{r_o}{k_w}\ln\frac{r_i}{r_B}+\frac{r_o}{k_p}\ln\frac{r_o}{r_i}+\frac{1}{h_o}}-\frac{1}{\frac{r_o}{h_i r_i}+\frac{r_o}{k_p}\ln\frac{r_o}{r_i}+\frac{1}{h_o}}\right)\right)\right\}$$

(C-5)

Replacing the bracketed term by a variable, *Y*; Eq. C-5 can be expressed as a temperature drop as in Eq. C-6.

$$T_{mi} - T_{mo} = T_{amb}\left[\exp(-Y) - 1\right] + T_{mi}\left[1 - \exp(-Y)\right] \quad \text{..... (C-6)}$$

$$\text{where } Y = \frac{2\pi r_o L_p}{Q_{\text{flow}}\rho C_p\left(\frac{r_o}{h_i r_i} + \frac{r_o}{k_p}\ln\frac{r_o}{r_i} + \frac{1}{h_o}\right)} + \frac{2\pi r_o L_B}{Q_{\text{flow}}\rho C_p}\left(\frac{1}{\frac{r_o}{h_i r_B} + \frac{r_o}{k_w}\ln\frac{r_i}{r_B} + \frac{r_o}{k_p}\ln\frac{r_o}{r_i} + \frac{1}{h_o}} - \frac{1}{\frac{r_o}{h_i r_i} + \frac{r_o}{k_p}\ln\frac{r_o}{r_i} + \frac{1}{h_o}}\right) \quad \text{(C-7)}$$

APPENDIX D

SAMPLE EXCEL SPREADSHEET FOR THE HEAT-BALANCE MODEL FOR A PARTIALLY-BLOCKED PIPELINE ($Q = 2000\ m^3/d$) AND DATA FOR FIGS. 8 AND 11

Heat Transfer Approach to Blockage Detection

Partially Blocked Pipe

Reference pipe-North Sea Field

Lp =	43000	m
Di =	0.38	m
Do =	0.405	m
Δt =	0.013	m
r_i =	0.19	m
r_o =	0.203	m
kp =	43.25	W/mK
A_s =	54765	m^2

T_s =	32	°C	305 K
Inlet T T_{m1} =	35	°C	308 K

Crude Oil Properties

ρ =	0.8753	g/cm^3	875.3 kg/m^3
μ =	1.0603	cp	0.001 kg/ms
C_p =	1890	J/kgK	
k_w =	0.25	W/mK	
k_f =	0.1312	W/mK	

Air Properties

ρ =	1.271	kg/m3	
T_{amb} =	0	°C	273 K
k_{air} =	0.026	W/mK	
v_{air} =	0.0305	m/s	
C_p =	1005	J/kgK	
μ_{air} =	0.0175	cp	
h_o =	4	W/m^{2}K	

B, %	D_i, m	Q, m^3/d	Re	Pr	Nu_D	h_i
10	0.360	2000	60743.8	15	350	127
25	0.329		55451.3		325	130
50	0.269		45275.8		276	135
75	0.190		32014.8		209	145
90	0.120		20247.9		145	159
0	0.380		64029.6		365	126

$$T_{m1} - T_{m3} = T_{amb}\left[\exp(-Y) - 1\right] + T_{m1}\left[1 - \exp(-Y)\right]$$

$$Y = \frac{2\pi r_o L_p}{Q_{flow}\rho C_p\left(\frac{r_o}{h_i r_i} + \frac{r_o}{k_p}\ln\frac{r_o}{r_i} + \frac{1}{h_o}\right)} + \frac{2\pi r_o L_B}{Q_{flow}\rho C_p}\left(\frac{1}{\frac{r_o}{h_i r_B} + \frac{r_o}{k_w}\ln\frac{r_i}{r_B} + \frac{r_o}{k_p}\ln\frac{r_o}{r_i} + \frac{1}{h_o}} - \frac{1}{\frac{r_o}{h_i r_i} + \frac{r_o}{k_p}\ln\frac{r_o}{r_i} + \frac{1}{h_o}}\right)$$

$2\pi r_o L_B$	B, %	r_B/r_i	L_B, m	r_B	v, m/s	Q, m^3/	Q, m^3/s	R								LHS	RHS (Skin)	Y	EXP(-Y)	T_{m1} - T_{m3}, K	T_{m3}, K
0	10	0.949	0	0.180	0.2	2000	0.0231	0.009	0.043	0.0003	0.250	0.008	3.866	3.313	-0.553	5.528	0.000	5.528	0.004	34.8609	273.139
127	10	0.949	100	0.180				0.009	0.043					3.313	-0.553	5.528	-0.002	5.526	0.004	34.8607	273.139
255	10	0.949	200	0.180				0.009	0.043					3.313	-0.553	5.528	-0.004	5.525	0.004	34.8604	273.140
637	10	0.949	500	0.180				0.009	0.043					3.313	-0.553	5.528	-0.009	5.519	0.004	34.8597	273.140
1274	10	0.949	1,000	0.180				0.009	0.043					3.313	-0.553	5.528	-0.018	5.510	0.004	34.8584	273.142
6368	10	0.949	5,000	0.180				0.009	0.043					3.313	-0.553	5.528	-0.092	5.436	0.004	34.8476	273.152
12736	10	0.949	10,000	0.180				0.009	0.043					3.313	-0.553	5.528	-0.184	5.344	0.005	34.8329	273.167
19104	10	0.949	15,000	0.180				0.009	0.043					3.313	-0.553	5.528	-0.276	5.252	0.005	34.8168	273.183
25472	10	0.949	20,000	0.180				0.009	0.043					3.313	-0.553	5.528	-0.368	5.161	0.006	34.7992	273.201
31840	10	0.949	25,000	0.180				0.009	0.043					3.313	-0.553	5.528	-0.460	5.069	0.006	34.7798	273.220
44576	10	0.949	35,000	0.180				0.009	0.043					3.313	-0.553	5.528	-0.643	4.885	0.008	34.7354	273.265
50944	10	0.949	40,000	0.180				0.009	0.043					3.313	-0.553	5.528	-0.735	4.793	0.008	34.7099	273.290
54765	10	0.949	43,000	0.180				0.009	0.043					3.313	-0.553	5.528	-0.791	4.738	0.009	34.6934	273.307
$2\pi r_o L_B$	B, %	r_B/r_i	L_B, m	r_B	v, m/s	Q, m^3/	Q, m^3/s	R								LHS	RHS (Skin)	Y	EXP(-Y)	T_{m1} - T_{m3}, K	T_{m3}, K
0	25	0.866	0	0.165	0.2	2000	0.0231	0.010	0.117	0.0003	0.250	0.008	3.868	2.657	-1.211	5.532	0.000	5.532	0.004	34.8614	273.139
127	25	0.866	100	0.165				0.010	0.117					2.657	-1.211	5.532	-0.004	5.527	0.004	34.8608	273.139
255	25	0.866	200	0.165				0.010	0.117					2.657	-1.211	5.532	-0.008	5.523	0.004	34.8603	273.140
637	25	0.866	500	0.165				0.010	0.117					2.657	-1.211	5.532	-0.020	5.511	0.004	34.8586	273.141
1274	25	0.866	1,000	0.165				0.010	0.117					2.657	-1.211	5.532	-0.040	5.491	0.004	34.8557	273.144
6368	25	0.866	5,000	0.165				0.010	0.117					2.657	-1.211	5.532	-0.201	5.330	0.005	34.8305	273.170
12736	25	0.866	10,000	0.165				0.010	0.117					2.657	-1.211	5.532	-0.403	5.129	0.006	34.7926	273.207
19104	25	0.866	15,000	0.165				0.010	0.117					2.657	-1.211	5.532	-0.604	4.927	0.007	34.7463	273.254
25472	25	0.866	20,000	0.165				0.010	0.117					2.657	-1.211	5.532	-0.806	4.726	0.009	34.6897	273.310
31840	25	0.866	25,000	0.165				0.010	0.117					2.657	-1.211	5.532	-1.007	4.524	0.011	34.6205	273.380
44576	25	0.866	35,000	0.165				0.010	0.117					2.657	-1.211	5.532	-1.410	4.121	0.016	34.4322	273.568
50944	25	0.866	40,000	0.165				0.010	0.117					2.657	-1.211	5.532	-1.612	3.920	0.020	34.3055	273.695
54765	25	0.866	43,000	0.165				0.010	0.117					2.657	-1.211	5.532	-1.732	3.799	0.022	34.2163	273.784

$2\pi r_o L_B$	B, %	r_B/r_i	L_B, m	r_B	v, m/s	Q, m^3/	Q, m^3/s	R								LHS	RHS (Skin)	Y	EXP(-Y)	$T_{m1} - T_{m3}$, K	T_{m3}, K
0	50	0.707	0	0.134	0.2	2000	0.0231	0.011	0.281	0.0003	0.250	0.008	3.873	1.843	-2.030	5.539	0.000	5.539	0.004	34.8624	273.138
127	50	0.707	100	0.134				0.011	0.281					1.843	-2.030	5.539	-0.007	5.532	0.004	34.8614	273.139
255	50	0.707	200	0.134				0.011	0.281					1.843	-2.030	5.539	-0.013	5.525	0.004	34.8605	273.140
637	50	0.707	500	0.134				0.011	0.281					1.843	-2.030	5.539	-0.034	5.505	0.004	34.8576	273.142
1274	50	0.707	1,000	0.134				0.011	0.281					1.843	-2.030	5.539	-0.067	5.471	0.004	34.8528	273.147
6368	50	0.707	5,000	0.134				0.011	0.281					1.843	-2.030	5.539	-0.337	5.201	0.006	34.8071	273.193
12736	50	0.707	10,000	0.134				0.011	0.281					1.843	-2.030	5.539	-0.675	4.864	0.008	34.7297	273.270
19104	50	0.707	15,000	0.134				0.011	0.281					1.843	-2.030	5.539	-1.012	4.526	0.011	34.6212	273.379
25472	50	0.707	20,000	0.134				0.011	0.281					1.843	-2.030	5.539	-1.350	4.189	0.015	34.4691	273.531
31840	50	0.707	25,000	0.134				0.011	0.281					1.843	-2.030	5.539	-1.687	3.851	0.021	34.2560	273.744
44576	50	0.707	35,000	0.134				0.011	0.281					1.843	-2.030	5.539	-2.362	3.176	0.042	33.5389	274.461
50944	50	0.707	40,000	0.134				0.011	0.281					1.843	-2.030	5.539	-2.700	2.839	0.059	32.9524	275.048
54765	50	0.707	43,000	0.134				0.011	0.281					1.843	-2.030	5.539	-2.902	2.636	0.072	32.4928	275.507
$2\pi r_o L_B$	B, %	r_B/r_i	L_B, m	r_B	v, m/s	Q, m^3/	Q, m^3/s	R								LHS	RHS (Skin)	Y	EXP(-Y)	$T_{m1} - T_{m3}$, K	T_{m3}, K
0	75	0.5	0	0.095	0.2	2000	0.0231	0.015	0.562	0.0003	0.250	0.007	3.881	1.209	-2.672	5.550	0.000	5.550	0.004	34.8639	273.136
127	75	0.5	100	0.095				0.015	0.562					1.209	-2.672	5.550	-0.009	5.541	0.004	34.8627	273.137
255	75	0.5	200	0.095				0.015	0.562					1.209	-2.672	5.550	-0.018	5.532	0.004	34.8615	273.139
637	75	0.5	500	0.095				0.015	0.562					1.209	-2.672	5.550	-0.044	5.505	0.004	34.8577	273.142
1274	75	0.5	1,000	0.095				0.015	0.562					1.209	-2.672	5.550	-0.089	5.461	0.004	34.8513	273.149
6368	75	0.5	5,000	0.095				0.015	0.562					1.209	-2.672	5.550	-0.444	5.106	0.006	34.7878	273.212
12736	75	0.5	10,000	0.095				0.015	0.562					1.209	-2.672	5.550	-0.889	4.661	0.009	34.6691	273.331
19104	75	0.5	15,000	0.095				0.015	0.562					1.209	-2.672	5.550	-1.333	4.217	0.015	34.4840	273.516
25472	75	0.5	20,000	0.095				0.015	0.562					1.209	-2.672	5.550	-1.777	3.773	0.023	34.1954	273.805
31840	75	0.5	25,000	0.095				0.015	0.562					1.209	-2.672	5.550	-2.221	3.329	0.036	33.7454	274.255
44576	75	0.5	35,000	0.095				0.015	0.562					1.209	-2.672	5.550	-3.110	2.440	0.087	31.9492	276.051
50944	75	0.5	40,000	0.095				0.015	0.562					1.209	-2.672	5.550	-3.554	1.996	0.136	30.2428	277.757
54765	75	0.5	43,000	0.095				0.015	0.562					1.209	-2.672	5.550	-3.821	1.729	0.177	28.7896	279.210
$2\pi r_o L_B$	B, %	r_B/r_i	L_B, m	r_B	v, m/s	Q, m^3/	Q, m^3/s	R								LHS	RHS (Skin)	Y	EXP(-Y)	$T_{m1} - T_{m3}$, K	T_{m3}, K
0	90	0.316	0	0.060	0.2	2000	0.0231	0.021	0.933	0.0003	0.250	0.007	3.891	0.830	-3.061	5.564	0.000	5.564	0.004	34.8658	273.134
127	90	0.316	100	0.060				0.021	0.933					0.830	-3.061	5.564	-0.010	5.554	0.004	34.8644	273.136
255	90	0.316	200	0.060				0.021	0.933					0.830	-3.061	5.564	-0.020	5.543	0.004	34.8630	273.137
637	90	0.316	500	0.060				0.021	0.933					0.830	-3.061	5.564	-0.051	5.513	0.004	34.8588	273.141
1274	90	0.316	1,000	0.060				0.021	0.933					0.830	-3.061	5.564	-0.102	5.462	0.004	34.8514	273.149
6368	90	0.316	5,000	0.060				0.021	0.933					0.830	-3.061	5.564	-0.509	5.055	0.006	34.7768	273.223
12736	90	0.316	10,000	0.060				0.021	0.933					0.830	-3.061	5.564	-1.018	4.546	0.011	34.6286	273.371
19104	90	0.316	15,000	0.060				0.021	0.933					0.830	-3.061	5.564	-1.527	4.037	0.018	34.3822	273.618
25472	90	0.316	20,000	0.060				0.021	0.933					0.830	-3.061	5.564	-2.036	3.528	0.029	33.9722	274.028
31840	90	0.316	25,000	0.060				0.021	0.933					0.830	-3.061	5.564	-2.545	3.019	0.049	33.2903	274.710
44576	90	0.316	35,000	0.060				0.021	0.933					0.830	-3.061	5.564	-3.563	2.001	0.135	30.2684	277.732
50944	90	0.316	40,000	0.060				0.021	0.933					0.830	-3.061	5.564	-4.072	1.492	0.225	27.1286	280.871
54765	90	0.316	43,000	0.060				0.021	0.933					0.830	-3.061	5.564	-4.377	1.187	0.305	24.3175	283.683

$2\pi r_o L_B$	B, %	r_B/r_i	L_B, m	r_B	v, m/s	Q, m^3/	Q, m^3/s	R							LHS	RHS (Skin)	Y	EXP(-Y)	$T_{m1} - T_{m3}$, K	T_{m3}, K
0	0	1	0	0.190	0.2	2000	0.0231	0.008	0.000	0.0003	0.250	0.008	3.864	3.864	0.000	5.526	0.000	5.526	0.004	34.8607	273.139
127	0	1	100	0.190				0.008	0.000					3.864	0.000	5.526	0.000	5.526	0.004	34.8607	273.139
255	0	1	200	0.190				0.008	0.000					3.864	0.000	5.526	0.000	5.526	0.004	34.8607	273.139
637	0	1	500	0.190				0.008	0.000					3.864	0.000	5.526	0.000	5.526	0.004	34.8607	273.139
1274	0	1	1,000	0.190				0.008	0.000					3.864	0.000	5.526	0.000	5.526	0.004	34.8607	273.139
6368	0	1	5,000	0.190				0.008	0.000					3.864	0.000	5.526	0.000	5.526	0.004	34.8607	273.139
12736	0	1	10,000	0.190				0.008	0.000					3.864	0.000	5.526	0.000	5.526	0.004	34.8607	273.139
19104	0	1	15,000	0.190				0.008	0.000					3.864	0.000	5.526	0.000	5.526	0.004	34.8607	273.139
25472	0	1	20,000	0.190				0.008	0.000					3.864	0.000	5.526	0.000	5.526	0.004	34.8607	273.139
31840	0	1	25,000	0.190				0.008	0.000					3.864	0.000	5.526	0.000	5.526	0.004	34.8607	273.139
44576	0	1	35,000	0.190				0.008	0.000					3.864	0.000	5.526	0.000	5.526	0.004	34.8607	273.139
50944	0	1	40,000	0.190				0.008	0.000					3.864	0.000	5.526	0.000	5.526	0.004	34.8607	273.139
54765	0	1	43,000	0.190				0.008	0.000					3.864	0.000	5.526	0.000	5.526	0.004	34.8607	273.139

Temperature Variation with Blockage Length for a Fixed Blockage Cross-Sectional Area and Flow Rate (Fig. 8)

Q = 2000 m^3/d			L_B = 100	L_B = 1000	L_B = 5000	L_B = 10000	L_B = 20000	L_B = 40000
Blockage	r_B	r_{BD}	ΔT, K					
0	0.190	1.000	34.861	34.861	34.861	34.861	34.861	34.861
10	0.180	0.949	34.861	34.858	34.848	34.833	34.799	34.710
25	0.165	0.866	34.861	34.856	34.830	34.793	34.690	34.305
50	0.134	0.707	34.861	34.853	34.807	34.730	34.469	32.952
75	0.095	0.500	34.863	34.851	34.788	34.669	34.195	30.243
90	0.060	0.316	34.864	34.851	34.777	34.629	33.972	27.129

Temperature Variation with Flow Rate for a Fixed blockage (Fig. 11)

10% Blockage

ΔT, K	Flow Rate (Q), m^3/D							
L_B, m	1000	2000	3000	4000	5000	6000	7000	8000
100	34.99928	34.86069	34.14981	32.87556	31.30514	29.64707	28.01809	26.47426
200	34.99928	34.86044	34.14875	32.87356	31.30235	29.64369	28.01430	26.47021
500	34.99927	34.85967	34.14557	32.86756	31.29396	29.63353	28.00291	26.45802
1,000	34.99926	34.85837	34.14024	32.85752	31.27993	29.61656	27.98390	26.43767
5,000	34.99915	34.84756	34.09640	32.77546	31.16581	29.47880	27.82990	26.27313
10,000	34.99898	34.83288	34.03845	32.66845	31.01822	29.30165	27.63265	26.06300
20,000	34.99855	34.79915	33.91115	32.43873	30.70578	28.93009	27.22170	25.62744
25,000	34.99826	34.77981	33.84132	32.31552	30.54048	28.73533	27.00772	25.40176
35,000	34.99753	34.73537	33.68792	32.05104	30.19055	28.32685	26.56192	24.93398
40,000	34.99705	34.70989	33.60377	31.90918	30.00542	28.11273	26.32978	24.69160
43,000	34.99672	34.69344	33.55071	31.82081	29.89094	27.98098	26.18744	24.54339

APPENDIX E

DEVELOPMENT OF THE DIMENSIONLESS HEAT-BALANCE MODEL FOR A PARTIALLY-BLOCKED PIPE

Recalling the original form of the heat model for a partially blocked pipe:

$$\frac{T_{amb}-T_{mo}}{T_{amb}-T_{mi}}=\exp\left\{-\left(\frac{2\pi r_o L_p}{Q_{flow}\rho C_p\left(\frac{r_o}{h_i r_i}+\frac{r_o}{k_p}\ln\frac{r_o}{r_i}+\frac{1}{h_o}\right)}+\frac{2\pi r_o L_B}{Q_{flow}\rho C_p}\left(\frac{1}{\frac{r_o}{h_i r_B}+\frac{r_o}{k_w}\ln\frac{r_i}{r_B}+\frac{r_o}{k_p}\ln\frac{r_o}{r_i}+\frac{1}{h_o}}-\frac{1}{\frac{r_o}{h_i r_i}+\frac{r_o}{k_p}\ln\frac{r_o}{r_i}+\frac{1}{h_o}}\right)\right)\right\}$$

(C-5)

Expressed as a temperature drop in Eq. E-1:

$$T_{mi}-T_{mo}=T_{amb}\left[\exp(-Y)-1\right]+T_{mi}\left[1-\exp(-Y)\right] \quad \text{.....(E-1)}$$

where $$Y=\frac{2\pi r_o L_p}{Q_{flow}\rho C_p\left(\frac{r_o}{h_i r_i}+\frac{r_o}{k_p}\ln\frac{r_o}{r_i}+\frac{1}{h_o}\right)}+\frac{2\pi r_o L_B}{Q_{flow}\rho C_p}\left(\frac{1}{\frac{r_o}{h_i r_B}+\frac{r_o}{k_w}\ln\frac{r_i}{r_B}+\frac{r_o}{k_p}\ln\frac{r_o}{r_i}+\frac{1}{h_o}}-\frac{1}{\frac{r_o}{h_i r_i}+\frac{r_o}{k_p}\ln\frac{r_o}{r_i}+\frac{1}{h_o}}\right)$$

(E-2)

We define the following dimensionless terms and substitute them in Eqs. E-3 and E-4;

$$L_{BD}=\frac{L_B}{L_p} \quad \text{.....(E-3)}$$

$$r_{BD}=\frac{r_B}{r_i} \quad \text{.....(E-4)}$$

$$T_D = \frac{T_{mi} - T_{mo}}{T_{amb}} \quad \text{.....(E-5)}$$

$$T_D = \frac{T_{mi} - T_{mo}}{T_{amb}} = [\exp(-Y) - 1] + \frac{T_{mi}}{T_{amb}}[1 - \exp(-Y)] \quad \text{.....(E-6)}$$

$$Y = \frac{2\pi r_o}{Q_{\text{flow}} \rho Cp}\left[\frac{L_p}{\frac{r_o}{h_i r_i} + \frac{r_o}{k_p}\ln\frac{r_o}{r_i} + \frac{1}{h_o}} + L_B\left(\frac{1}{\frac{r_o}{h_i r_B} + \frac{r_o}{k_w}\ln\frac{r_i}{r_B} + \frac{r_o}{k_p}\ln\frac{r_o}{r_i} + \frac{1}{h_o}} - \frac{1}{\frac{r_o}{h_i r_i} + \frac{r_o}{k_p}\ln\frac{r_o}{r_i} + \frac{1}{h_o}}\right)\right]$$

(E-7)

$$Y = \frac{2\pi}{Q_{\text{flow}} \rho Cp}\left[\frac{L_p}{\frac{1}{h_i r_i} + \frac{1}{k_p}\ln\frac{r_o}{r_i} + \frac{1}{h_o r_o}} + L_p L_{BD}\left(\frac{1}{\frac{1}{h_i r_i r_{BD}} + \frac{1}{k_w}\ln\frac{1}{r_{BD}} + \frac{1}{k_p}\ln\frac{r_o}{r_i} + \frac{1}{h_o r_o}} - \frac{1}{\frac{1}{h_i r_i} + \frac{1}{k_p}\ln\frac{r_o}{r_i} + \frac{1}{h_o r_o}}\right)\right]$$

(E-8)

$$Y = \frac{2\pi L_p}{Q_{\text{flow}} \rho C_p}\left[\frac{1}{\frac{1}{h_i r_i} + \frac{1}{k_p}\ln\frac{r_o}{r_i} + \frac{1}{h_o r_o}} + L_{BD}\left(\frac{1}{\frac{1}{h_i r_i r_{BD}} + \frac{1}{k_w}\ln\frac{1}{r_{BD}} + \frac{1}{k_p}\ln\frac{r_o}{r_i} + \frac{1}{h_o r_o}} - \frac{1}{\frac{1}{h_i r_i} + \frac{1}{k_p}\ln\frac{r_o}{r_i} + \frac{1}{h_o r_o}}\right)\right]$$

(E-9)

We now define the dimensionless temperature drop factor (F_{TB}) as the square bracketed term.

$$F_{TB}=\left[\frac{1}{\frac{1}{h_i r_i}+\frac{1}{k_p}\ln\frac{r_o}{r_i}+\frac{1}{h_o r_o}}+L_{BD}\left(\frac{1}{\frac{1}{h_i r_i r_{BD}}+\frac{1}{k_w}\ln\frac{1}{r_{BD}}+\frac{1}{k_p}\ln\frac{r_o}{r_i}+\frac{1}{h_o r_o}}-\frac{1}{\frac{1}{h_i r_i}+\frac{1}{k_p}\ln\frac{r_o}{r_i}+\frac{1}{h_o r_o}}\right)\right] \quad \text{(E-10)}$$

$$F_{TB}=\left[\frac{L_{BD}}{\frac{1}{h_i r_i r_{BD}}+\frac{1}{k_w}\ln\frac{1}{r_{BD}}+\frac{1}{k_p}\ln\frac{r_o}{r_i}+\frac{1}{h_o r_o}}+\frac{1}{\frac{1}{h_i r_i}+\frac{1}{k_p}\ln\frac{r_o}{r_i}+\frac{1}{h_o r_o}}-\frac{L_{BD}}{\frac{1}{h_i r_i}+\frac{1}{k_p}\ln\frac{r_o}{r_i}+\frac{1}{h_o r_o}}\right] \quad \text{(E-11)}$$

The term 'Y' can be simplified as Eq. 89,

$$Y=\frac{2\pi L_p}{Q_{\text{flow}}\rho C_p}F_{TB} \quad \text{.....(E-12)}$$

and the dimensionless heat model for a partially-blocked pipe can be expressed as Eq. 90.

$$T_D=\left[\exp(-\frac{2\pi L_p}{Q_{\text{flow}}\rho C_p}F_{TB})-1\right]+\frac{T_{mi}}{T_{amb}}\left[1-\exp(-\frac{2\pi L_p}{Q_{\text{flow}}\rho C_p}F_{TB})\right] \quad \text{.....(E-13)}$$

APPENDIX F

SAMPLE EXCEL SPREADSHEET FOR DIMENSIONLESS HEAT-BALANCE MODEL FOR A PARTIALLY- BLOCKED PIPELINE

(Q = 4000 m^3/d)

Heat Transfer Approach to Blockage Detection

Partially Blocked Pipe

Reference pipe-North Sea Field

$2\pi L_p/($ = 3.5276

Lp =	43000	m			
Di =	0.38	m			
Do =	0.405	m			
Δt =	0.013	m			
r_i =	0.19	m			
r_o =	0.203	m			
kp =	43.25	W/mK			
As =	54765	m2			
T_s =	32	°C	305	K	
Inlet T T_{m1} =	35	°C	308	K	

Crude Oil Properties

ρ =	0.8753	g/cm^3	875.32	kg/m^3
μ =	1.0603	cp	0.0011	kg/ms
C_p =	1890	J/kgK		
k_w =	0.25	W/mK		
k_f =	0.1312	W/mK		

Air properties

ρ =	1.271	kg/m3		
T_{amb} =	0	°C	273	K
k_{air} =	0.026	W/mK		
v_{air} =	0.0305	m/s		
C_p =	1005	J/kgK		
μ_{air} =	0.0175	cp		
h_o =	4	W/m^{2}K		

B, %	Re	Pr	Nu_D	h_i
10	121488	15	609	222
25	110903	15	566	226
50	90552	15	481	235
75	64030	15	365	252
90	40496	15	253	276

$$T_D = \left[\exp\left(-\frac{2\pi L_p}{Q_{\text{flow}}\rho C_p}F_{TB}\right)-1\right]+\frac{T_{mi}}{T_{amb}}\left[1-\exp\left(-\frac{2\pi L_p}{Q_{\text{flow}}\rho C_p}F_{TB}\right)\right]$$

$$T_D = \frac{T_{mi}-T_{mo}}{T_{amb}}$$

$$F_{TB} = \left[\frac{\frac{L_{BD}}{\frac{1}{h_i r_i r_{BD}}+\frac{1}{k_w}\ln\frac{1}{r_{BD}}+\frac{1}{k_p}\ln\frac{r_o}{r_i}+\frac{1}{h_o r_o}}+\frac{1}{\frac{1}{h_i r_i}+\frac{1}{k_p}\ln\frac{r_o}{r_i}+\frac{1}{h_o r_o}}-\frac{L_{BD}}{\frac{1}{h_i r_i}+\frac{1}{k_p}\ln\frac{r_o}{r_i}+\frac{1}{h_o r_o}}\right]$$

														F_{TB}				T_D		
Di	B, %	r_{BD}	L_B, m	L_{BD}	r_B	v, m/s	Q, m^3/d	Q, m^3/s	R					1st Term	2nd Term	3rd Term	F_{TB}	1st Term	2nd Term	T_D	T_{B1} - T_{B3},
0.36	10	0.949	0	0.000	0.1802	0.408	4000	0.046	0.025	0.211	0.001	1.233	0.024	0.000	0.795	0.000	0.795	-0.939	1.060	0.120	32.878
			100	0.002										0.002		0.002	0.798	-0.940	1.061	0.121	32.903
			200	0.005										0.003		0.004	0.801	-0.941	1.061	0.121	32.928
			500	0.012										0.008		0.009	0.812	-0.943	1.064	0.121	33.002
			1,000	0.023										0.016		0.018	0.829	-0.946	1.068	0.121	33.119
			5,000	0.116										0.079		0.092	0.966	-0.967	1.091	0.124	33.841
			10,000	0.233										0.158		0.185	1.137	-0.982	1.108	0.126	34.367
			15,000	0.349										0.237		0.277	1.309	-0.990	1.117	0.127	34.654
			20,000	0.465										0.316		0.370	1.480	-0.995	1.122	0.128	34.811
			25,000	0.581										0.395		0.462	1.652	-0.997	1.125	0.128	34.897
			35,000	0.814										0.553		0.647	1.995	-0.999	1.127	0.128	34.969
			40,000	0.930										0.633		0.739	2.166	-1.000	1.128	0.128	34.983
			43,000	1.000										0.680		0.795	2.269	-1.000	1.128	0.128	34.988
Di	B, %	r_{BD}	L_B, m	L_{BD}	r_B	v, m/s	Q, m^3/d	Q, m^3/s	R					1st Term	2nd Term	3rd Term	F_{TB}	1st Term	2nd Term	T_D	T_{B1} - T_{B3},
0.33	25	0.866	0	0.000	0.1645	0.408	4000	0.046	0.027	0.575	0.001	1.233	0.023	0.000	0.795	0.000	0.795	-0.939	1.060	0.120	32.880
			100	0.002										0.001		0.002	0.798	-0.940	1.061	0.121	32.903
			200	0.005										0.003		0.004	0.801	-0.941	1.061	0.121	32.926
			500	0.012										0.006		0.009	0.810	-0.943	1.064	0.121	32.993
			1,000	0.023										0.013		0.018	0.826	-0.946	1.067	0.121	33.100
			5,000	0.116										0.063		0.092	0.951	-0.965	1.089	0.124	33.776
			10,000	0.233										0.127		0.185	1.106	-0.980	1.105	0.126	34.293
			15,000	0.349										0.190		0.277	1.262	-0.988	1.115	0.127	34.592
			20,000	0.465										0.253		0.370	1.418	-0.993	1.121	0.127	34.764
			25,000	0.581										0.316		0.462	1.573	-0.996	1.124	0.128	34.864
			35,000	0.814										0.443		0.647	1.885	-0.999	1.127	0.128	34.955
			40,000	0.930										0.506		0.739	2.041	-0.999	1.127	0.128	34.974
			43,000	1.000										0.544		0.795	2.134	-0.999	1.128	0.128	34.981

Di	B, %	r_{BD}	L_B, m	L_{BD}	r_B	v, m/s	Q, m^3/d	Q, m^3/s	R					1st Term	2nd Term	3rd Term	F_{TB}	1st Term	2nd Term	T_D	T_{B1} - T_{B3},
0.27	50	0.707	0	0.000	0.1344	0.408	4000	0.046	0.032	1.386	0.001	1.233	0.022	0.000	0.795	0.000	0.795	-0.940	1.060	0.120	32.884
			100	0.002										0.001		0.002	0.798	-0.940	1.061	0.121	32.904
			200	0.005										0.002		0.004	0.801	-0.941	1.061	0.121	32.924
			500	0.012										0.004		0.009	0.809	-0.942	1.063	0.121	32.983
			1,000	0.023										0.009		0.018	0.823	-0.945	1.066	0.121	33.078
			5,000	0.116										0.044		0.092	0.932	-0.963	1.086	0.123	33.692
			10,000	0.233										0.088		0.185	1.068	-0.977	1.102	0.125	34.191
			15,000	0.349										0.131		0.277	1.204	-0.986	1.112	0.126	34.500
			20,000	0.465										0.175		0.370	1.341	-0.991	1.118	0.127	34.691
			25,000	0.581										0.219		0.462	1.477	-0.995	1.122	0.128	34.809
			35,000	0.814										0.307		0.647	1.750	-0.998	1.126	0.128	34.927
			40,000	0.930										0.351		0.740	1.886	-0.999	1.127	0.128	34.955
			43,000	1.000										0.377		0.795	1.968	-0.999	1.127	0.128	34.966
Di	B, %	r_{BD}	L_B, m	L_{BD}	r_B	v, m/s	Q, m^3/d	Q, m^3/s	R					1st Term	2nd Term	3rd Term	F_{TB}	1st Term	2nd Term	T_D	T_{B1} - T_{B3},
0.19	75	0.5	0	0.000	0.095	0.408	4000	0.046	0.042	2.773	0.001	1.233	0.021	0.000	0.796	0.000	0.796	-0.940	1.060	0.120	32.891
			100	0.002										0.001		0.002	0.799	-0.940	1.061	0.121	32.909
			200	0.005										0.001		0.004	0.801	-0.941	1.061	0.121	32.927
			500	0.012										0.003		0.009	0.808	-0.942	1.063	0.121	32.979
			1,000	0.023										0.006		0.019	0.821	-0.945	1.066	0.121	33.064
			5,000	0.116										0.029		0.093	0.918	-0.961	1.084	0.123	33.625
			10,000	0.233										0.057		0.185	1.039	-0.974	1.099	0.125	34.104
			15,000	0.349										0.086		0.278	1.160	-0.983	1.109	0.126	34.416
			20,000	0.465										0.115		0.370	1.282	-0.989	1.116	0.127	34.619
			25,000	0.581										0.144		0.463	1.403	-0.993	1.120	0.127	34.752
			35,000	0.814										0.201		0.648	1.646	-0.997	1.125	0.128	34.895
			40,000	0.930										0.230		0.741	1.767	-0.998	1.126	0.128	34.931
			43,000	1.000										0.247		0.796	1.840	-0.998	1.126	0.128	34.947
Di	B, %	r_{BD}	L_B, m	L_{BD}	r_B	v, m/s	Q, m^3/d	Q, m^3/s	R					1st Term	2nd Term	3rd Term	F_{TB}	1st Term	2nd Term	T_D	T_{B1} - T_{B3},
0.12	90	0.316	0	0.000	0.0601	0.408	4000	0.046	0.060	4.605	0.001	1.233	0.019	0.000	0.798	0.000	0.798	-0.940	1.061	0.121	32.900
			100	0.002										0.000		0.002	0.800	-0.940	1.061	0.121	32.916
			200	0.005										0.001		0.004	0.802	-0.941	1.062	0.121	32.933
			500	0.012										0.002		0.009	0.809	-0.942	1.063	0.121	32.981
			1,000	0.023										0.004		0.019	0.820	-0.945	1.066	0.121	33.060
			5,000	0.116										0.020		0.093	0.910	-0.960	1.083	0.123	33.587
			10,000	0.233										0.039		0.185	1.022	-0.973	1.098	0.125	34.050
			15,000	0.349										0.059		0.278	1.135	-0.982	1.108	0.126	34.361
			20,000	0.465										0.079		0.371	1.247	-0.988	1.114	0.127	34.570
			25,000	0.581										0.099		0.464	1.360	-0.992	1.119	0.127	34.711
			35,000	0.814										0.138		0.649	1.585	-0.996	1.124	0.128	34.869
			40,000	0.930										0.158		0.742	1.697	-0.997	1.125	0.128	34.912
			43,000	1.000										0.169		0.798	1.764	-0.998	1.126	0.128	34.931

APPENDIX G

DATA FOR FIGS. 19, 26, 27, 28 AND 29

Data for Graphical Solution of Heat- and Volume-Balance Models (Fig. 19)

F_{VB} = 0.75 F_{TB} = 0.2

$r_{BD}=D_{BD}$	L_{BD}	L_{BD}
0.05	1.00278	0.08574
0.13	1.01600	0.12163
0.20	1.04097	0.15603
0.27	1.07942	0.19339
0.34	1.13433	0.23644
0.42	1.21050	0.28820
0.49	1.31576	0.35300
0.56	1.46347	0.43778
0.64	1.67792	0.55484
0.71	2.00793	0.72871
0.78	2.56772	1.01645
0.85	3.70021	
0.93	7.12056	

Blockage Map Data for Arbitrary Values of F_{TB} = 2.2 and F_{VB} = 0.75 (Fig. 26)

F_{TB} = 2.2

F_{VB} = 0.75

Uncertainty,	F_{TB}	F_{VB}
0	2.2	0.75
5	2.09	0.7125
10	1.98	0.675
15	1.87	0.6375
20	1.76	0.6
25	1.65	0.5625
30	1.54	0.525
35	1.43	0.4875
40	1.32	0.45
45	1.21	0.4125
50	1.1	0.375
55	0.99	0.3375

Data for Graphical Solution of Heat- and Volume-Balance Models Incorporating Varying Uncertainty (Figs. 27-29)

	10% Uncertainty		25% Uncertainty		50% Uncertainty	
	F_{TB} = 1.98	F_{VB} = 0.675	F_{TB} = 1.65	F_{VB} = 0.5625	F_{TB} = 1.1	F_{VB} = 0.375
$r_{BD}=D_{BD}$	L_{BD}	L_{BD}	L_{BD}	L_{BD}	L_{BD}	L_{BD}
0.05	0.23687	0.32590	0.20885	0.43872	0.16215	0.62674
0.13	0.33604	0.33020	0.29629	0.44450	0.23004	0.63500
0.20	0.43110	0.33831	0.38010	0.45542	0.29511	0.65060
0.27	0.53439	0.35081	0.47117	0.47225	0.36581	0.67464
0.34	0.65344	0.36866	0.57613	0.49627	0.44728	0.70896
0.49	0.97612	0.42762	0.86060	0.57564	0.66806	0.82235
0.56	1.21100	0.47563	1.06765	0.64027	0.82873	0.91467
0.64					1.05071	1.04870

APPENDIX H

PIPESIM OUTPUT DATA (COMPARISON OF PIPESIM AND MODEL TEMPERATURE DROP PREDICTIONS FOR A FULLY-BLOCKED PIPELINE)

Input Data to PIPESIM

Pipe Data			Fluid Data		
Inlet P	P_i =	5000 psia	Black Oil		
Inlet T	T_i =	35 °C	GOR =	300	scf/STB
Hor. Dist.	L_p =	43000 m	API =	30	
Inner D	D_i =	0.38 m			
Thickness	Δt =	0.0127 m	Wax		
Inner D	D_o =	0.4054 m	kw =	0.25	W/mK
Ambient T	T_{amb} =	0 °C			
	T_s =	32 °C	Air		
	k_p =	43.25 W/mK	v_{air} =	0.03048	m/s

Q, m^3/D	r_B, m	Wax thick., m	T_o, °C	PIPESIM ΔT	Model ΔT
1000	0.19	0	2.4415	32.5585	34.9993
	0.18	0.01	2.6763	32.3237	34.9967
	0.17	0.02	2.9228	32.0772	34.9892
	0.16	0.03	3.1854	31.8146	34.9713
	0.15	0.04	3.461	31.5390	34.9356
	0.14	0.05	3.756	31.2440	34.8724
	0.13	0.06	4.0614	30.9386	34.7706
	0.12	0.07	4.387	30.6130	34.6180
	0.11	0.08	4.7314	30.2686	34.4015
	0.1	0.09	4.6551	30.3449	34.1074
	0.09	0.1	4.1658	30.8342	33.7211
	0.08	0.11	4.0305	30.9695	33.2264
	0.07	0.12	4.3514	30.6486	32.6043
	0.06	0.13	5.4594	29.5406	31.8310
	0.05	0.14	7.8251	27.1749	30.8737
	0.04	0.15			
	0.03	0.16			
	0.02	0.17			
	0.01	0.18			

Q, m^3/D	r_B, m	Wax thick., m	T_o, °C	PIPESIM ΔT	Model ΔT
2000	0.19	0	5.3761	29.624	34.861
	0.18	0.01	5.431	29.569	34.692
	0.17	0.02	4.8188	30.181	34.424
	0.16	0.03	4.7166	30.283	34.046
	0.15	0.04	4.7435	30.257	33.552
	0.14	0.05	4.9113	30.089	32.944
	0.13	0.06	5.2344	29.766	32.224
	0.12	0.07	5.7289	29.271	31.400
	0.11	0.08	6.423	28.577	30.477
	0.1	0.09	7.3468	27.653	29.460
	0.09	0.1	8.5736	26.426	28.354
	0.08	0.11	10.2777	24.722	27.160
	0.07	0.12	12.8529	22.147	25.876
	0.06	0.13	16.8789	18.121	24.495
	0.05	0.14			
	0.04	0.15			
	0.03	0.16			
	0.02	0.17			
	0.01	0.18			

Q, m^3/D	r_B, m	Wax thick., m	T_o, °C	PIPESIM ΔT	Model ΔT
3000	0.19	0	3.6195	31.381	34.150
	0.18	0.01	4.0766	30.923	33.541
	0.17	0.02	4.6429	30.357	32.773
	0.16	0.03	5.3256	29.674	31.868
	0.15	0.04	6.1287	28.871	30.852
	0.14	0.05	7.0546	27.945	29.747
	0.13	0.06	8.1117	26.888	28.573
	0.12	0.07	9.3151	25.685	27.347
	0.11	0.08	10.7033	24.297	26.080
	0.1	0.09	12.3926	22.607	24.782
	0.09	0.1	14.4825	20.518	23.456
	0.08	0.11	17.2646	17.735	22.106
	0.07	0.12			
	0.06	0.13			
	0.05	0.14			
	0.04	0.15			
	0.03	0.16			
	0.02	0.17			
	0.01	0.18			
Q, m^3/D	r_B, m	Wax thick., m	T_o, °C	PIPESIM ΔT	Model ΔT
4000	0.19	0	4.1352	30.865	32.876
	0.18	0.01	5.096	29.904	31.803
	0.17	0.02	6.1694	28.831	30.597
	0.16	0.03	7.3445	27.656	29.303
	0.15	0.04	8.6114	26.389	27.956
	0.14	0.05	9.9757	25.024	26.584
	0.13	0.06	11.4663	23.534	25.203
	0.12	0.07	13.0674	21.933	23.826
	0.11	0.08	14.8539	20.146	22.461
	0.1	0.09	16.9601	18.040	21.111
	0.09	0.1	19.6061	15.394	19.778
	0.08	0.11	23.1015	11.899	18.458
	0.07	0.12	21.1743	13.826	17.148
	0.06	0.13			
	0.05	0.14			
	0.04	0.15			
	0.03	0.16			
	0.02	0.17			
	0.01	0.18			
Q, m^3/D	r_B, m	Wax thick., m	T_o, °C	PIPESIM ΔT	Model ΔT
5000	0.19	0	5.2838	29.716	31.307
	0.18	0.01	6.651	28.349	29.865
	0.17	0.02	8.1291	26.871	28.358
	0.16	0.03	9.6754	25.325	26.830
	0.15	0.04	11.2475	23.753	25.312
	0.14	0.05	12.8559	22.144	23.824
	0.13	0.06	14.5328	20.467	22.375
	0.12	0.07	16.3405	18.660	20.971
	0.11	0.08	18.3849	16.615	19.613
	0.1	0.09	20.8263	14.174	18.299
	0.09	0.1	23.9235	11.077	17.026
	0.08	0.11	28.5113	6.489	15.788
	0.07	0.12			
	0.06	0.13			
	0.05	0.14			
	0.04	0.15			
	0.03	0.16			
	0.02	0.17			
	0.01	0.18			

Q, m^3/D	r_B, m	Wax thick., m	T_o, °C	PIPESIM ΔT	Model ΔT
6000	0.19	0	6.7854	28.215	29.649
	0.18	0.01	8.4717	26.528	27.950
	0.17	0.02	10.1954	24.805	26.256
	0.16	0.03	11.9121	23.088	24.603
	0.15	0.04	13.6271	21.373	23.013
	0.14	0.05	15.3668	19.633	21.493
	0.13	0.06	17.1827	17.817	20.046
	0.12	0.07	19.1579	15.842	18.669
	0.11	0.08	21.4136	13.586	17.360
	0.1	0.09	24.1663	10.834	16.112
	0.09	0.1	27.7814	7.219	14.918
	0.08	0.11			
	0.07	0.12			
	0.06	0.13			
	0.05	0.14			
	0.04	0.15			
	0.03	0.16			
	0.02	0.17			
	0.01	0.18			
Q, m^3/D	r_B, m	Wax thick., m	T_o, °C	PIPESIM ΔT	Model ΔT
7000	0.19	0	8.2886	26.711	28.020
	0.18	0.01	10.203	24.797	26.152
	0.17	0.02	12.0797	22.920	24.353
	0.16	0.03	13.9155	21.085	22.646
	0.15	0.04	15.7309	19.269	21.040
	0.14	0.05	17.569	17.431	19.533
	0.13	0.06	19.4976	15.502	18.121
	0.12	0.07	21.6123	13.388	16.796
	0.11	0.08	24.0867	10.913	15.550
	0.1	0.09	27.1913	7.809	14.375
	0.09	0.1	31.7845	3.216	13.262
	0.08	0.11			
	0.07	0.12			
	0.06	0.13			
	0.05	0.14			
	0.04	0.15			
	0.03	0.16			
	0.02	0.17			
	0.01	0.18			
Q, m^3/D	r_B, m	Wax thick., m	T_o, °C	PIPESIM ΔT	Model ΔT
8000	0.19	0	9.7351	25.2649	26.477
	0.18	0.01	11.8035	23.1965	24.506
	0.17	0.02	13.7918	21.2082	22.656
	0.16	0.03	15.7127	19.2873	20.938
	0.15	0.04	17.6028	17.3972	19.347
	0.14	0.05	19.52	15.48	17.877
	0.13	0.06	21.5428	13.4572	16.514
	0.12	0.07	23.8091	11.1909	15.250
	0.11	0.08	26.5256	8.4744	14.071
	0.1	0.09	29.9906	5.0094	12.968
	0.09	0.1			
	0.08	0.11			
	0.07	0.12			
	0.06	0.13			
	0.05	0.14			
	0.04	0.15			
	0.03	0.16			
	0.02	0.17			
	0.01	0.18			

Wax Thickness, m	Q, m^3/d	Pipesim ΔT, K	Model ΔT, K	Wax Thickness, m	Q, m^3/d	Pipesim ΔT, K	Model ΔT, K
0.01	1000	32.324	34.997	0.08	1000	30.269	34.402
	2000	29.569	34.692		2000	28.577	30.477
	3000	30.923	33.541		3000	24.297	26.080
	4000	29.904	31.803		4000	20.146	22.461
	5000	28.349	29.865		5000	16.615	19.613
	6000	26.528	27.950		6000	13.586	17.360
	7000	24.797	26.152		7000	10.913	15.550
	8000	23.197	24.506		8000	8.474	14.071
0.03	1000	31.815	34.971	0.09	1000	30.345	34.107
	2000	30.283	34.046		2000	27.653	29.460
	3000	29.674	31.868		3000	22.607	24.782
	4000	27.656	29.303		4000	18.040	21.111
	5000	25.325	26.830		5000	14.174	18.299
	6000	23.088	24.603		6000	10.834	16.112
	7000	21.085	22.646		7000	7.809	14.375
	8000	19.287	20.938		8000	5.009	12.968
0.05	1000	31.244	34.872				
	2000	30.089	32.944				
	3000	27.945	29.747				
	4000	25.024	26.584				
	5000	22.144	23.824				
	6000	19.633	21.493				
	7000	17.431	19.533				
	8000	15.480	17.877				
0.06	1000	30.939	34.771				
	2000	29.766	32.224				
	3000	26.888	28.573				
	4000	23.534	25.203				
	5000	20.467	22.375				
	6000	17.817	20.046				
	7000	15.502	18.121				
	8000	13.457	16.514				
0.07	1000	30.613	34.618				
	2000	29.271	31.400				
	3000	25.685	27.347				
	4000	21.933	23.826				
	5000	18.660	20.971				
	6000	15.842	18.669				
	7000	13.388	16.796				
	8000	11.191	15.250				

VITA

Ebiaye Valerie Ombu was born in Edo, Nigeria on November 15, 1979, the daughter of Emmanuel Inatimi Ombu and Viola Kehinde Ombu. She attended Kwame Nkrumah University of Science and Technology, Kumasi, Ghana where she received a Bachelor of Science degree in chemical engineering in July 2001. In September 2002, she started work on a Master of Science degree in petroleum engineering at Texas A&M University, where she joined the Multiphase Research Group led by Dr. Stuart Scott. During that time, she was a 1st place sectional winner (Masters division) at the 2002 Texas A&M SPE Student Paper Contest for her paper titled, "Alternative Energy Sources for the Future, Fuel Cells?" She also completed an internship with Elf Petroleum Nigeria Limited as a member of the Well Performance Optimization team. She hopes to begin work with Halliburton in January 2005.

Permanent Address

PO Box 73365

Victoria Island

Lagos, Nigeria

Email

ebiaye@yahoo.com